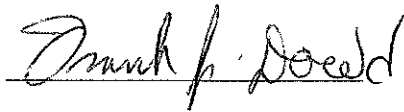


Dissertation Approved

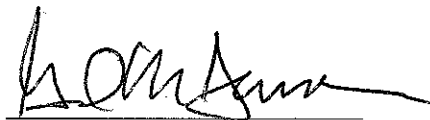
by



Major Advisor



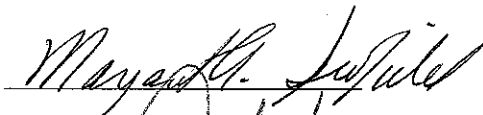
Co-Advisor



Dean

Committee Members:

Margaret A. Scofield, Ph.D.



Laura A. Hansen, Ph.D.



UPREGULATION OF PIP3-DEPENDENT RAC EXCHANGER 1 (P-REX1) PROMOTES
PROSTATE CANCER METASTASIS

BY

JIANBING QIN

A DISSERTATION

Submitted to the Faculty of the Graduate School of the Creighton University in Partial
Fulfillment of the Requirements for the Degree of Doctor of Philosophy in the
Department of Pharmacology

Omaha, Nebraska

(August 18, 2008)

ABSTRACT

Activation of Rac by guanine-nucleotide exchange factors (GEFs) at the leading edge of the cell plays an important role in directional cell migration, a critical step of tumor metastasis cascades. We investigated the role of P-Rex1, a novel specific GEF for Rac, in human prostate cancer metastasis. P-Rex1 expression (mRNA and/or protein) was almost undetectable in normal prostate epithelial cells (PrEC) and two nonmetastatic prostate cancer cell lines (LNCaP and CWR22Rv1), but was clearly detectable in highly metastatic prostate cancer cell lines (PC3-LN4 and PC-3). Studies of human prostate tumor specimens revealed a 1.6-fold increase in P-Rex1 protein expression in localized cancer cells and a 3.7-fold increase in lymph node prostate metastasis when compared to noncancerous prostate tissues. Migration abilities of various prostate cancer cell lines determined by transwell chamber assays were directly correlated with their P-Rex1 expression levels. Silencing endogenous P-Rex1 expression significantly reduced cell migration ability in metastatic PC-3 cells. Stable expression of wild-type P-Rex1 but not its "GEF-dead" mutant increased CWR22Rv1 cell migration and invasion by 3-fold. Further study indicated that P-Rex1 promotes prostate cancer cell migration and invasion via Rac activation. Finally, *in vivo* studies revealed that expression of wild-type P-Rex1 but not its "GEF-dead" mutant significantly promoted spontaneous metastasis of CWR22Rv1 cancer cells to mouse lymph nodes without effects on primary tumor growth. Altogether, our results identify P-Rex1 as an important regulator of prostate cancer metastatic progression and suggest that it may be targeted for prevention and treatment of prostate cancer metastasis.

PREFACE

Publications

J Qin, Y Xie, B Wang, M Hoshino, D Wolff, M Scofield, F Dowd, M Lin, Y Tu. (2008) Upregulation of PIP3-Dependent Rac Exchanger 1 (P-Rex1) promotes prostate cancer metastasis. (Submitted)

X Cao, ***J Qin**, Y Xie, O Khan, F Dowd, M Scofield, M-F Lin, Y Tu. (2006) Regulator of G-protein Signaling 2 (RGS2) inhibits androgen-independent activation of androgen receptor in prostate cancer cell. *Oncogene* 25:3719-34. (*co-first author)

Y Xie, D Wolff, B Wang, J Kirui, H Jiang, **J Qin**, P Abel, Y Tu. (2008) Breast Cancer Metastasis Depends on Proteasome Degradation of Regulator of G protein Signaling 4. (Submitted)

Published Abstracts

J Qin, Y Xie, B Wang, D Wolff, M Scofield, F Dowd, M Hoshino, Y Tu. (2008) "Upregulation of PIP3-Dependent Rac Exchanger 1 (P-Rex1) promotes prostate cancer metastasis" *The FASEB Journal* 22: 907.12.

J Qin, M Scofield, F Dowd, M Hoshino, Y Tu. (2007) "PIP3-Dependent Rac Exchanger 1 (P-Rex1) promotes prostate cancer cell migration" *The FASEB Journal* 21: 554.23.

DEDICATION

To:

My Parents, Wife and Daughter

With Love and Appreciation

ACKNOWLEDGEMENTS

Cancer research today is more complex and this complexity requires cooperative efforts. During my doctoral study, I have received support and assistance from many people to whom I would like to express my heartfelt gratitude and acknowledge their important contributions.

First, I would like to thank all of my committee members: Dr. Yaping Tu, Dr. Frank Dowd, Dr. Margaret Scofield, and Dr. Laura Hansen for their advice and guidance throughout my study. Dr. Tu has supervised all the aspects of my research. He taught me and was involved in the design of all the experiments presented in this dissertation. I also learned from him problem-solving skills and how to analyze and present data. Dr. Tu even demonstrated to me how to do some difficult experiments including Rac pull-down assays. More importantly, without Dr. Tu's provision of equipment and supplies I would not have been able to complete this study. Dr. Dowd has always been available when help is needed. He taught me statistics and how to think like a pharmacologist. Also, Dr. Dowd gave me a lot of warm encouragements and significant help with my writing. Without generous help from Dr. Scofield, I would not have been able to start my molecular pharmacology career quickly. She taught me many fundamental things about molecular biology and gave me the opportunity to practice my molecular skills in her laboratory. Dr. Scofield was also involved in the design of the plasmids used for the establishment of the CWR22Rv1 stable cell lines described in this dissertation. Dr. Hansen taught me important knowledge about cancer biology in the Advanced Cell Biology class. Her comments on my research work have always been insightful. In particular, the discussions with Dr. Hansen on RNAi experiments were very helpful. In

addition, I would like to thank all the committee members for reviewing the P-Rex1 paper manuscript. Due to their involvements, I have received thorough training on cancer molecular pharmacology. I am sure this training will serve me well and my appreciation will grow over the course of my career.

I would also like to thank Dr. Dennis Wolff for teaching me how to do animal studies and helping me with a lot of other things like manuscript preparation. I deeply appreciate the help and support I received from other members in Dr. Tu laboratory. In particular, the CWR22Rv1 stable cell lines have been established by them together with Dr. Scofield. Dr. Yan Xie created and provided me the Cortactin staining protocol, helped me with western blotting (Figure 8A) and CWR22Rv1 stable cell lines, and assisted in other experiments including RNAi experiments and animal studies. Also, I thank Dr. Haihong Jiang and Lyudmila Bataalkina for their expert technical assistance in many experiments like CWR22Rv1 stable cell lines, cell migration assays and routine PCRs. The discussions with Dr. Da Ha about molecular mechanisms of P-Rex1 upregulation have been helpful. I thank Joseph Kirui for the friendship, and most of all, fun.

I also wish to thank Dr. Bo Wang and Lisa Linder-Stephenson (Department of Pathology, Creighton University Medical Center) for the great help and technical assistance with the immunohistochemical analysis; Dr. Greg Perry (The Creighton Flow Cytometry Core Facility) for flow cytometry cell sorting; Dr. Mikio Hoshino (National Institute of Neuroscience, Kyoto, Japan) for providing the P-Rex1 antibodies; and the National Cancer Institute for providing the compound M119 (NSC119910).

Finally, I would like to thank Dr. Thomas Murray, Dr. Peter Abel and other members in the Department of Pharmacology for their insightful comments and discussions during my presentations and for their encouragement as well. I also thank all of my fellow graduate students and all the other people who have helped and supported me during my study. Thank you all.

TABLE OF CONTENTS

ABSTRACT	iii
PREFACE	iv
DEDICATION	v
ACKNOWLEDGEMENTS	vi
TABLE OF CONTENTS	viii
LIST OF FIGURES	x
CHAPTER I. BACKGROUNDS AND OVERALL OBJECTIVES OF THE STUDY	1
CHAPTER II. THE BIOLOGICAL IMPORTANCE OF P-REX1 IN PROSTATE CANCER CELL MIGRATION AND INVASION	13
A. INTRODUCTION	13
B. MATERIALS AND METHODS	16
C. RESULTS	28
D. DISCUSSION	35
E. FIGURES	44
CHAPTER III. EFFECTS OF P-REX1 IN PROSTATE TUMOR GROWTH AND METASTASIS IN VIVO	66
A. INTRODUCTION	66
B. MATERIALS AND METHODS	68

C.	RESULTS	69
D.	DISCUSSION	71
E.	FIGURES	74
CHAPTER IV. SUMMARY AND CONCLUSIONS		78
REFERENCES		83
APPENDIX		93

LIST OF FIGURES

CHAPTER I:

Figure 1: A schematic of the metastatic process

Figure 2: Regulation of cell migration by small GTPases via reorganization of the actin cytoskeleton

Figure 3: Activation and deactivation cycle of Rac

Figure 4: Schematic representation of the domain structure of P-Rex1

CHAPTER II

Figure 5: Transwell assay principle

Figure 6: (A) The mechanism of RNA interference (RNAi)

(B) P-Rex1 siRNA sequences

Figure 7: Analysis of P-Rex1 mRNA expression in human prostate cell lines

Figure 8: Analyses of P-Rex1 protein expression in prostate cancer cells

Figure 9: Transwell cell migration assays of prostate cancer cells toward NIH-3T3 CM

Figure 10: Immunohistochemical staining of human specimens for P-Rex1 protein

Figure 11: RNA interference for P-Rex1 expression in PC-3 cells using double transfection

Figure 12: (A) Treatment of PC-3 cells with P-Rex1 siRNA blocks the translocation of cortactin to the membrane

(B) RNA interference for P-Rex1 results in suppression of transwell migration of PC-3 cells

Figure 13: (A) Schematic structures of wild-type P-Rex1 and DH-deleted P-Rex1 mutant
(B) Transwell migration assay of CWR22Rv1 cells after transient transfection

Figure 14: (A) Expression of P-Rex1 and P-Rex1(-DH) protein
(B) Transwell migration assay of PC3-LN4 cells after transient transfection and cell sorting

Figure 15: (A) Scheme of regulation of prostate cancer cell migration by small GTPases
(B) Transwell migration assay of PC-3 cells using Rac, Rho, and Rho kinase inhibitors

Figure 16: Transwell migration assays of PC-3 or PC3-LN4 cells without or with G_i protein inhibitor pertussis toxin

Figure 17: Transwell migration assays of PC-3 cells in the presence of Gβγ specific inhibitor M119

Figure 18: (A) Representative western blot showing effective inhibition of activated Akt (pAkt), a downstream effector of PI3K, by 10μM LY or 100nM Wort
(B) Transwell migration assays of PC-3 cells in the presence of PI3K inhibitors LY294002 (LY, 10 μM), wortmannin (Wort, 100 nM) or vehicle control

Figure 19: (A) Schematic structures of full-length P-Rex1 and P-Rex1 “GEF-dead” mutant.
(B) Expression levels of P-Rex1 and its mutant in CWR22Rv1 cells

Figure 20: Transwell migration assay of CWR22Rv1 stable cells

Figure 21: Transwell invasion assay of CWR22Rv1 stable cells

Figure 22: P-Rex1 promotes the formation of lamellipodia and the translocation of cortactin

Figure 23: P-Rex1 activates Rac in prostate cancer cells (Rac pull down assay)

Figure 24: Analysis of GEF mRNA expression in human prostate cell lines

CHAPTER III

Figure 25: Representative tumor formation and growth that results from subcutaneous injection of CWR22Rv1 cells into nude mice

Figure 26: P-Rex1 does not affect prostate tumor growth

Figure 27: P-Rex1 induces spontaneous lymph node metastasis in mouse models

Figure 28: Representative histopathology (H&E staining) of primary tumors and lymph node metastases of CWR22Rv1 P-Rex1 cells and PC3-LN4 cells

CHAPTER IV

Figure 29: A proposed model for the regulation of P-Rex1-mediated prostate cancer metastasis

CHAPTER I

BACKGROUNDS AND OVERALL OBJECTIVES OF THE STUDY

Prostate cancer and metastasis

Prostate cancer is a major public health problem affecting men worldwide. In the United States, it is the most common form of cancer and the second leading cause of cancer death in men. It has been predicted that in 2008, approximately 186,320 (25% of total in males) new cases of prostate cancer will be diagnosed and over 28,660 (10% of total in males) men will die from this disease in the United States [Jemal et al. 2008]. Prostate cancer progresses on a continuum through localized, locally advanced, advanced and hormone-refractory stages. Choice of treatments for prostate cancer patients includes watchful waiting, surgeries (radical prostatectomy or pelvic lymphadenectomy), radiation therapy, hormone therapy and chemotherapy, which are dependent on the stage of disease. A tumor localized to the prostate itself is generally not deadly on its own, with 100% of patients living more than five years [Jemal et al. 2008]. However, as the prostate tumor grows, some of tumor cells may break off and spread to other parts of the body, a process known as metastasis. Distant metastases, most commonly to bone, are detected in about 5% of prostate cancer patients at the time of diagnosis. The development of such metastases leads to painful and untreatable consequences to which the vast majority of prostate cancer death (32% five-year survival rate) has been related [Jemal et al. 2008; Carroll and Grossfeld 2002].

Metastasis is a complex pathophysiological process which consists of a long series of sequential, interrelated steps (**Figure 1**). Tumor cells detach from the primary tumor site and invade local host stroma by breaking down the basement membrane and then, enter via the lymph system or directly into the bloodstream circulation. Some remaining tumor cells become trapped in the capillary beds of distant organs. Extravasation occurs next, probably with similar mechanisms operating during invasion. After being exposed to factors of the microenvironment that support proliferation and angiogenesis, metastasis occurs eventually at the target organ [Steeg 2002; Mundy 2002]. Prostate cancer metastasis is highly organ selective and involves numerous interactions between metastatic tumor cells and the host. Several general theories on the pathogenesis of cancer metastasis, including the “seed and soil” hypothesis and the homing theory, have been proposed [Fidler 2003; Murphy 2001]. There are also some putative prostate cancer metastasis-suppressor genes that have been identified over the years [Karayi and Markham 2004]. Despite extensive studies, the precise molecular mechanisms responsible for prostate cancer metastasis remain largely unknown [Gupta and Massague 2006], which presents a major hurdle for the treatment of metastatic prostate cancer. Thus, a better understanding of the molecular events underlying the prostate cancer metastasis becomes an important goal of prostate cancer research and holds the promise of effective therapeutic approaches for treating this disease.

Rac, a key regulator of directional cell migration

Tumor cells move toward targets by their own motility during metastasis, therefore the acquisition of directional migration is a critical and fundamental step for tumor cells to

invade and metastasize. Contributing to both pathological and physiological (e.g. development, immunity) processes, cell migration has been explored extensively over the past few years. In general, to migrate, cells must operate in cycles of a highly integrated multistep process in which a chemotactic signaling cascade(s) is triggered by the binding of chemoattractants to cell surface receptors (e.g. GPCRs) [Karnoub et al. 2004]. The cycle starts with formation of a membrane protrusion at a polarized cell leading edge which pushes the membrane forward (**Figure 2**). These extensions can be large, broad lamellipodia or spike-like filopodia. Then new cell-substrate adhesions form at sites close to the leading edge. Next, the cell body is translocated by actomyosin-mediated contractile forces. Finally, at the cell rear, adhesions disassemble as the tail of the cell retracts. It has been well established that reorganization of the actin cytoskeleton plays a pivotal role in these processes of cell migration cycle and is regulated by Rho family small GTPases such as Rac, Cdc42 and Rho [Yamazaki 2005; Nobes and Hall 1995; Hall 1998]. During cell movement, Rac is crucial for generating the actin-rich lamellipodial protrusions at the leading edge that are thought to be a major part of the driving force for directional movement [Ridley et al. 2003]. Moreover, Rac is also required in the second step of cell migration, formation of new contacts to stabilize the protrusion. Because of its importance in cell migration due to its ability to initiate and maintain protrusion, the study of Rac pathway in human cancer malignant transformation has been attractive to some research groups. Ever-increasing evidence, including RNA interference data [Chan et al. 2005], shows that Rac supports a central role in human tumor invasion and metastasis. Interestingly, Knight-Krajewski et al. demonstrated that Rac activity was significantly higher in more metastatic prostate cancer cells compared

to that in less aggressive prostate cancer cells [Knight-Krajewski et al 2004]. It was also reported that NSC23766, a Rac-specific small molecule inhibitor, was able to inhibit prostate cancer cell migration and invasion that requires endogenous Rac activity [Gao et al. 2004]. The finding that Rac is involved in prostate cancer metastasis is not surprising since it is one of the key regulators of cell migration. However, little is known regarding the molecular mechanisms underlying the hyperactivity of Rac in metastatic prostate cancer.

Like other members of Rho family GTPases, Rac acts as a molecular switch and can cycle between an inactive GDP-bound form and an active GTP-bound form (**Figure 3**). The GTP/GDP cycle is regulated by two distinct families of proteins. Guanine nucleotide exchange factors (GEFs) activate Rac GTPase by catalyzing the release of GDP, thereby facilitating GTP binding. Conversely, GTPase-accelerating proteins (GAPs) negatively regulate Rac function by increasing the GTP hydrolysis rate, therefore promoting formation of the GDP-bound state and leading to inactivation of the GTPase cycle [Karnoub 2004]. Once activated, Rac GTPase can interact with a spectrum of downstream effectors, stimulating cellular responses that control actin organization and other activities.

P-Rex1, a novel Rac-GEF

Interactions between chemoattractants and their corresponding receptors trigger a series of coordinated cellular events including the stimulation of Rho GEFs and eventually the activation of Rho GTPases. Since the discovery of the first Rho GEF Dbl (from diffuse B-cell-lymphoma cells) proto-oncogene [Hart et al. 1991], a large family of

Rho GEFs has been identified [Karnoub et al. 2004 and Rossman et al. 2005]. For example, T lymphoma invasion and metastasis 1 (Tiam1) is a Rac specific GEF in vivo and has been extensively explored. It was originally identified in 1994 as an invasion & metastasis-inducing gene in T lymphoma cells [Habets et al. 1994]. Tiam1 is highly expressed in the brain and testis and at relatively low levels in other tissues [habets et al. 1994 & 1995]. Interestingly, the role of Tiam1 in cellular migration, invasion, and metastasis is not limited to T lymphoma cells in which it was first discovered. To date, studies have demonstrated that Tiam1 is important in promoting tumor progression in a variety of cancers, such as breast cancer [Minard et al. 2004], colorectal cancer [Minard et al. 2004 & 2006; Liu et al. 2006] and Ras-induced skin tumors [Malliri et al. 2002]. Preliminary studies assessing Tiam1 expression in human specimens suggest that Tiam1 may be a prognostic marker for breast cancer [Adam et al. 2001], prostate cancer [Engers et al. 2006], though more tests are needed to confirm this. Despite the notable role of Tiam1 in cancer, it shares the phosphorylation-based mechanisms of activation with many other Rac-GEFs [Schiller 2006]. Phosphorylation is the major pathway by which GEFs are activated and is primarily regulated by phosphoinositide 3-kinases (PI3Ks) involved in extracellular stimulation of cell surface receptors such as tyrosine kinase receptors and tyrosine kinase-associated cytokine receptors [Karnoub et al. 2004]. Cancer is a complicated and heterogeneous disease. It's reasonable that multiple signal transduction pathways contribute to tumor cell migration, invasion and metastasis. As a matter of fact, silencing of Tiam1 can only reduce, but not eliminate, colorectal metastasis [Liu et al. 2006]. Existence of various Rac-GEFs is probably due to the fact that Rac takes part in different biological activities under different conditions or at

different sites. Therefore, identification of major GEF-mediated signal transduction pathways in specific diseases is of great interest.

In 2002, Welch H.C.E. et al. purified and identified a novel Rac activator, P-Rex1 [Welch et al. 2002]. It is a 185-kDa specific GEF for Rac initially identified in neutrophil cytosol based on its activity. The protein contains a tandem DH (Dbl-homology) / PH (pleckstrin homology) domain typical of Rho-GEFs, two DEP (disheveled, EGL-10, pleckstrin homology) and two PDZ (post-synaptic density disc-large zo-1 homology) domains and an IP4P (inositol polyphosphate 4-phosphatase) domain (**Figure 4**) [Weiner 2002]. P-Rex1 is a very unique Rac-GEF since it is directly, substantially, and synergistically activated by PIP3 produced by PI3Ks and the $\beta\gamma$ subunits of heterotrimeric G proteins both in vitro and vivo. P-Rex1 is the first well-confirmed example of Rho family GEFs that is directly activated by $G\beta\gamma$. It is a very efficient signal network, representing about 65% of the total Rac GEF activity in neutrophil lysates [Welch et al. 2002]. Data also showed the degree of GEF activation by PIP3 was much higher for P-Rex1 (20-fold) than for some other PIP3-inducible Rac-GEFs (e.g. less than 2.5-fold for Val1 and Pix) [Weiner 2002]. More interestingly, like Tiam1, P-Rex1 is expressed in brain and has been shown to be involved in the central nervous system development by enhancing migration of neurons. In addition to the uniqueness of P-Rex1 mentioned above, P-Rex1 is structurally and functionally similar to Tiam1 which was initially identified as a cancer metastasis promoter. It is unclear whether P-Rex1 is also involved in tumor cell migration, invasion and metastasis. To answer this question, I first analyzed the expression profile of P-Rex1 in my study system, prostate cancer, and then investigated its potential role and mechanisms.

Objectives of the study

The overall goal of my study was to investigate the biological importance of P-Rex1 and its signal transduction pathways in prostate cancer. I proposed that P-Rex1 promotes prostate cancer metastasis. In order to accomplish the goal and test my hypothesis, I used various prostate cell lines and clinical human samples to identify P-Rex1 as a target. In vivo studies were also performed to validate this target. In summary, the following objectives were pursued in my studies.

1. Assess the biological importance of P-Rex1 in prostate cancer.
 - a) Characterize the expression profile of P-Rex1 in prostate cell lines of different metastatic abilities and in human prostate cancer specimens.
 - b) Determine the effect of knock-down of endogenous P-Rex1 using siRNA on prostate cancer cell migration.
 - c) Determine the effect of exogenous expression of P-Rex1 by transient transfection on prostate cancer cell migration.
2. Investigate the mechanism by which P-Rex1 promotes prostate cancer cell migration and invasion.
 - a) Involvement of small GTPases Rac and Rho in prostate cancer cell migration.
 - b) Involvement of G_i protein in prostate cancer cell migration.
 - c) Involvement of $G\beta\gamma$ protein in prostate cancer cell migration.
 - d) Involvement of PI3K in prostate cancer cell migration.
 - e) Determine whether P-Rex1 promotes prostate cancer cell migration and

invasion via Rac activation.

3. In vivo studies using mouse models.

- a) Determine effect of P-Rex on tumor growth: subcutaneous injection in a mouse model.
- b) Determine effect of P-Rex on prostate spontaneous metastasis to lymph nodes: intraprostatic injection in a mouse model.

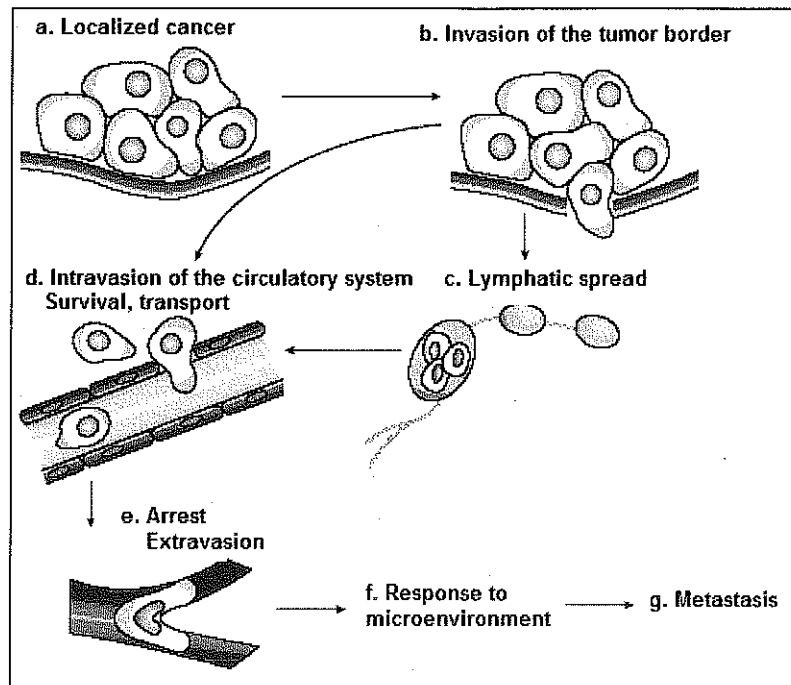


Figure 1. A schematic of the metastatic process [adapted from Steeg 2002; Mundy 2002]. Metastasis proceeds through the migration and invasion of cancer cells into surrounding vasculature following by extravasation from the circulation and proliferation at sites distant from the primary tumor.

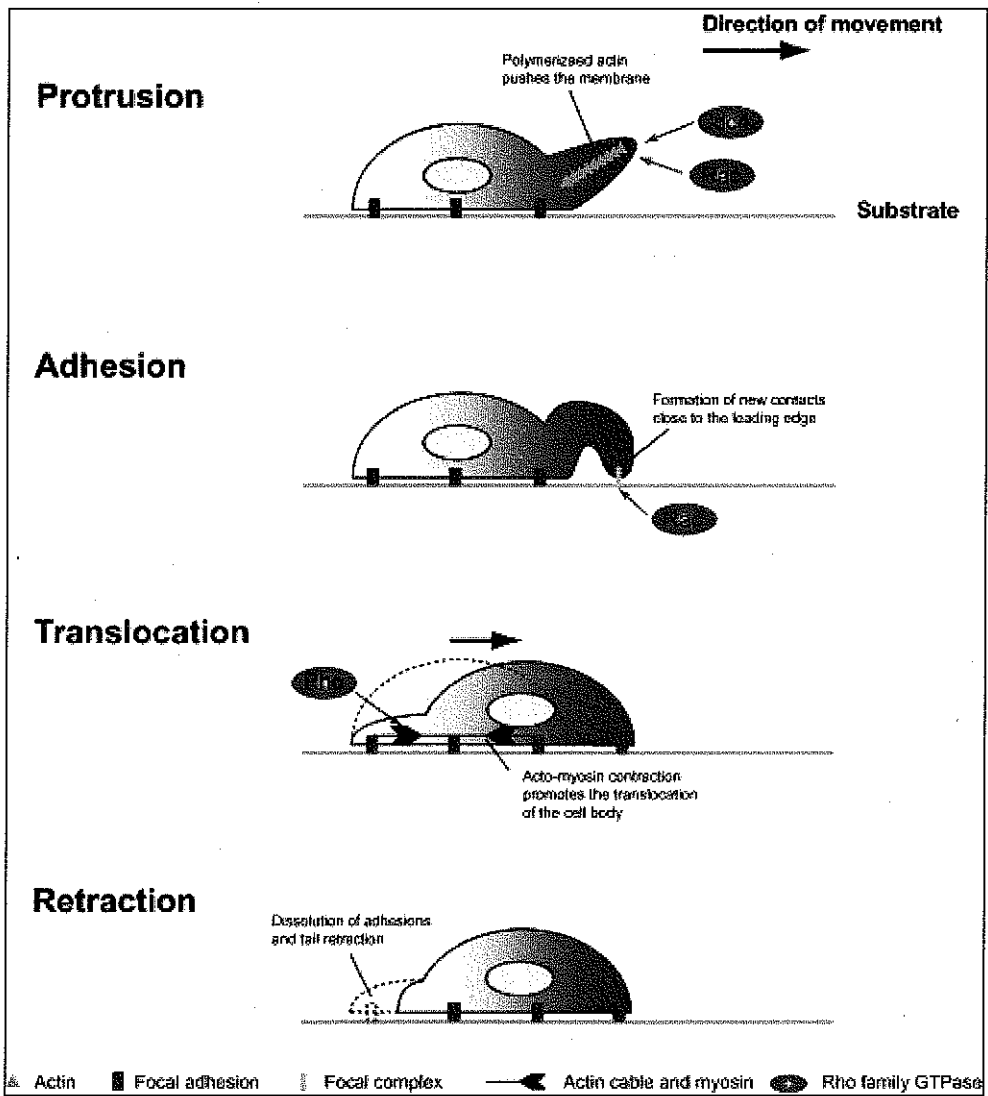


Figure 2. Regulation of cell migration by small GTPases via reorganization of the actin cytoskeleton. [Yamazaki 2005]

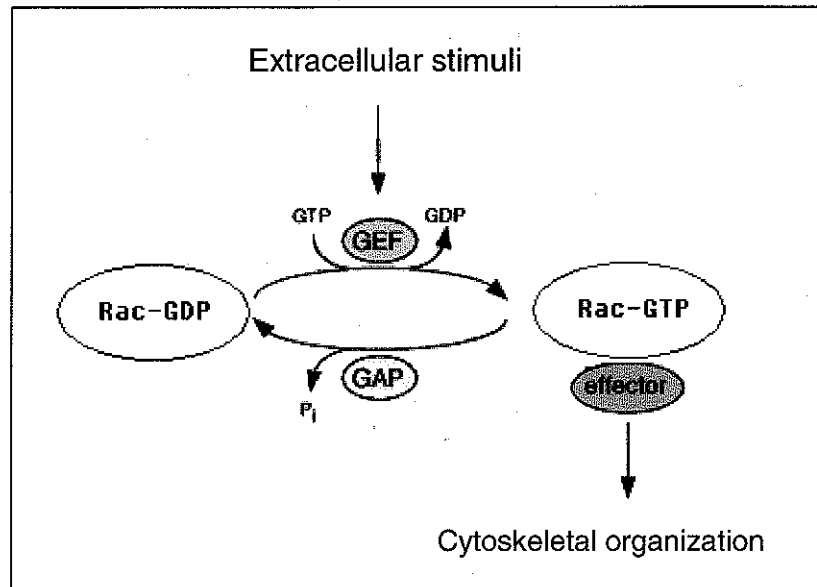


Figure 3. Activation and deactivation cycle of Rac. Diverse activation signals through cell surface receptors like G protein-coupled receptors, receptor tyrosine kinases and integrins stimulate Rac-GEFs, resulting in activation of Rac and thus its downstream effectors. This leads to a number of cellular responses including cytoskeletal organization. Rac GAPs accelerate the GTP hydrolysis terminating the signal.



Figure 4. Schematic representation of the domain structure of P-Rex1 (total 1659 amino acids)

CHAPTER II

THE BIOLOGICAL IMPORTANCE OF P-REX1 IN PROSTATE CANCER CELL MIGRATION AND INVASION

A. INTRODUCTION

As mentioned above, prostate cancer is the most commonly diagnosed cancer in American men and the second leading cause of cancer mortality. Prostate tumor metastases account for the majority of deaths from prostate cancer. Therefore, a better understanding of the molecular mechanisms that regulate prostate cancer metastasis is of immediate importance, because this may lead to developments of new and safer treatments for prostate cancer metastasis in patients. Metastasis is an orderly, multistep process involving the migration and invasion of cancer cells from the primary tumor to specific organs. Past studies have clearly established that Rho small GTPases play a critical role in cell migration and invasion via cytoskeleton rearrangements. The Rho GTPase family is a branch of the Ras superfamily of small GTPases [Sahai and Marshall, 2002]. So far, more than 20 different members of the Rho family have been identified [Hall 2005]. Three subgroups of them, Rac, Rho and Cdc42, have been well characterized. All of them are involved in the regulation of coordinated cell movement, while Rac induces actin polymerization at the cell periphery to produce protrusions driving cells move toward chemoattractants. Rac is activated when bound to GTP, which is catalyzed by guanine nucleotide exchange factors (GEFs) in response to membrane

receptor-mediated stimulations. Previous studies have discovered a large family of GEFs (more than 80 in mammals). The majority (about 69) of known GEFs belong to the Dbl subgroup that contains a DH (Dbl homology) / PH (pleckstrin homology) tandem domain. Others were identified more recently and are related to the member of DOCK (dedicator of cytokinesis). Some Dbl-GEFs have been studied in great detail and several GEFs for Rac have been suggested to play roles in tumor cell migration, invasion and metastasis. Among them, Tiam1 is a typical example. Ever-increasing evidence shows Tiam1-Rac signaling is involved in metastasis of different types of cancers including prostate cancer. Nevertheless, signal transduction pathways involved in prostate cancer metastasis are still far from being understood. It is most likely that multiple pathways play roles in this pathological process. Identifying new potential targets (e.g. GEFs) and defining their signaling may help to develop novel strategies for prostate cancer metastasis therapies.

We therefore performed a small screening to identify the Rac-GEFs that may be differentially expressed in established prostate normal and cancer cell lines with various metastatic abilities. Five cell lines were used in our study as in vitro models, including a representative normal prostate epithelial cell line (PrEC) and four commonly used prostate cancer cell lines (LNCaP, CWR22Rv1, PC3-LN4 and PC-3). These in vitro cell models have been established from different sources and vary in characteristics [Arun and Figg, 2005]. LNCaP cells were isolated from a needle aspiration biopsy of a human prostate cancer lymph node metastatic lesion, while CWR22Rv1 is a human prostate carcinoma epithelial cell line. Both LNCaP and CWR22Rv1 cell lines express androgen

receptor and prostate specific antigen (PSA). Injecting either of these two cell lines into athymic mouse prostates did not result in metastases [Arun and Figg, 2005; Kovar et al. 2006]. PC-3 cells were derived from a bone metastasis from a white man and PC3-LN4 is a subline of PC-3. In contrast to LNCaP and CWR22Rv1 cells, PC3-LN4 and PC-3 cell lines express no androgen receptor and prostate specific antigen (PSA) and metastases have been detected in both PC3-LN4 and PC-3 orthotopic injection mouse models [Arun and Figg, 2005]. Interestingly, we found that P-Rex1, a novel Rac Dbl-GEF, was upregulated in metastatic PC3-LN and PC-3 cells. This finding was further confirmed in human clinical specimens. P-Rex1 is a recently identified unique Rac-GEF since so far it is the only example of Rho family GEFs that could be directly activated by G $\beta\gamma$ subunits, and also by the PIP3, a product of PI3Ks. They can function either independently of each other or in synergy. Because of the unique expression pattern of P-Rex1, we then extensively investigated its role in prostate cancer cell migration and invasion. Experiments using a small interfering RNA indicate that endogenous P-Rex1 is involved in Rac activation and prostate cancer cell migration. We also found that P-Rex1-mediated prostate cancer cell migration is blocked by the G $_i$ specific inhibitor pertussis toxin (PTx), consistent with the previous report that PTx treatment significantly reduces metastasis of human prostate cancer cell in nude mice. Inhibition studies also suggest G $\beta\gamma$ subunits are required for activating P-Rex1, and synergize with PIP3 through PI3Ks for P-Rex1 activation. Finally, GTPase pull-down assays show that P-Rex1 can activate Rac in prostate cancer cells, which is further demonstrated by cortactin staining. Collectively, our study presents the first evidence showing P-Rex1 plays important role in prostate cancer cell migration and invasion via activating small GTPase Rac.

B. MATERIALS AND METHODS

Materials and reagents. Pertussis toxin, wortmannin, LY294002, NSC23766 and anti-Green Fluorescent Protein (GFP) antibody were purchased from Calbiochem (San Diego, CA). C3 transferase and the F-actin visualization kit were purchased from Cytoskeleton, Inc (Denver, CO). The Rac activation assay kit was from Upstate (Charlottesville, VA). Rat monoclonal anti-P-Rex1 antibodies (4A3 and 3A11) and P-Rex1 "GEF-dead" mutant were generated as described previously, respectively [Yoshizawa et al. 2005 and Hill et al. 2005]. Rabbit anti-HA and anti- β -actin antibodies were purchased from Santa Cruz Biotechnology (Santa Cruz, CA). The IRDye-labeled secondary antibodies were purchased from LI-COR Biosciences (Lincoln, NE). Fetal bovine serum (FBS) was from Hyclone (Logan, UT). Trizol, LipofectamineTM 2000, RPMI-1640 and DMEM media were purchased from Invitrogen (Carlsbad, CA). Matrigel was obtained from BD Biosciences (Bedford, MA).

Cells and cell culture. PC-3 cell line (ATCC) was cultured in RPMI-1640 medium supplemented with 10% FBS. PC3-LN4 cell line (a gift from Dr. Melanie A. Simpson, University of Nebraska at Lincoln) was cultured in DMEM supplemented with 10% FBS, non-essential amino acids and 1.0 mM sodium pyruvate. LNCaP and CWR22Rv1 cell lines (ATCC) were grown in RPMI-1640 medium supplemented with 10% FBS, 10 mM HEPES and 1.0 mM sodium pyruvate. The human prostate epithelial cell line (PrEC) was a gift from Dr. Zafar Nawaz (University of Miami). All cell lines were routinely maintained at 37°C in a humidified atmosphere of 5% CO₂ in air.

Conventional RT-PCR and quantitative real-time RT-PCR.

(a) Total RNA isolation and reverse transcription (RT)

Total RNA was isolated from cells using Trizol Reagent according to the manufacturer's protocol. The quality of the RNA was confirmed by visualization of the integrity of the 18S and 28S RNA bands on agarose gel. The concentration of the total RNA was determined by measuring the absorbance at 260nm with an ultraviolet spectrophotometer.

All the RNA samples used for assay were treated with DNase I to remove contaminating genomic DNA prior to experiments. To do that, 1 µg of RNA was added into a 0.2 ml RNase-free PCR tube on ice which contained the following: 1 µl 10X DNase I reaction buffer, 1 µl DNase I (1U/µl, Invitrogen #18068-015), 0.25 µl RNase inhibitor (40U/µl, Promega #2611), and diethylpyrocarbonate (DEPC)-treated water to a final volume of 10 µl. After incubating the tube for 15 min at room temperature, the DNase I was inactivated by the addition of 1 µl of 25 mM ethylenediaminetetraacetic acid (EDTA) solution to the reaction mixture (now 11 µl in total) followed by heating at 75°C for 10 min with a thermocycler. If needed, the reaction was scaled up linearly for larger amounts of RNA.

Following DNase treatment, the RNA was reverse transcribed into complementary DNA (cDNA). The RT reaction was performed by incubating a reaction mixture containing 2 µl of 10X PCR buffer, 2 µl of 50mM MgCl₂, 2 µl of 10mM dNTP Mix (Invitrogen #18427-088), 1 µl of 50uM random hexamer primer (Applied Biosystems #N808 0127), 1 µl of 50U/µl MuLV reverse transcriptase (Applied Biosystems #N808

0018), 0.5 μ l of 40U/ μ l RNase inhibitor (Promega #2611), 11 μ l DNase reaction solution (from the above step, equivalent to 1.0 μ g RNA), and DEPC-treated water in a total volume of 20 μ l at room temperature for 10 min, then at 42°C for 50 min, followed by 95°C for 5 min. No-reverse transcriptase negative controls were also prepared containing DEPC water in place of reverse transcriptase. The cDNA samples were then stored at -20°C until use.

(b) Conventional PCR and real-time PCR

For PCR reactions, specific primers were designed and synthesized by IDT (Integrated DNA Technologies, Inc.). Human primers were as following. P-Rex1 (predicted PCR product size: 163-bp): forward 5'-CCTTCTTCCTCTTCGACAAC -3' and reverse 5'-CCATCTTCCACATTCTCCAC -3'; P-Rex2 (228-bp): forward 5'-ACCAAAGTCCACATCCAAAGCTGCC -3' and reverse 5'-CGATGCACACCGCTGCTGCAC -3'; P-Rex2b (223-bp): forward 5'-GGTTTTACAATTTACAGCACGGC -3' and reverse 5'-CCAAAGGGTAAGAATCAGACAGGGG -3'; Tiam1 (253-bp): forward 5'-AAGACGTAAGTCCAGGCCATGTCC -3' and reverse 5'-GACCCAAATGTGCGAGTCAG -3'; Vav1 (323-bp): forward 5'-CGACATGGGCAAGATTTCCAG -3' and reverse 5'-GCGTACCAGAGATGAACAGACAG -3'; Vav2 (314-bp): forward 5'-ACAAAGCCAATGCCAACCACC -3' and reverse 5'-CCTCAGCAGCTCAAGCACGTC -3'; Vav3 (273-bp): forward 5'-GGGACACTCAAACCTACCAGAGAAAC -3' and reverse 5'-CACACATGGGCAAGGCTTGAC -3'. The house keeping gene β -actin (forward primer: 5'-AGCACGGCATCGTCACCAACT-3'; reverse primer: 5'-

TGGCTGGGGTGTGAAGGTCT-3') was used as a control gene. The predicted size of the PCR product was 180-bp for β -actin. The conventional PCR was performed in a 100 μ l reaction volume. The following was added to each PCR tube: 10 μ l of 10X PCR buffer, 3 μ l of 50mM $MgCl_2$, 2 μ l of 10mM dNTP Mix, 2 μ l of 25uM forward and reverse primers, 0.5 μ l of 5U/ μ l Taq DNA polymerase (Invitrogen #18038-018), 10 μ l of cDNA from RT, and DEPC-treated water. The PCR cycling conditions were 1 cycle at 94°C for 3 min, 35 (figure 7A) or 25 (figure 24) cycles of 94°C for 30 seconds, 55°C for 30 seconds, 72°C for 30 seconds, followed by 1 cycle at 72°C for 7 min. The PCR products were separated by 3% agarose gel electrophoresis, stained with ethidium bromide, and then digitally photographed under UV light. P-Rex1 PCR product was confirmed by DNA sequencing analysis.

To do quantitative Real-Time PCR, human P-Rex1 and β -actin plasmids were prepared by using the Qiagen Spin Mini-Prep Kit. Quantification of plasmid was performed by using a UV/visible spectrophotometer. To create a standard curve with either of these plasmid DNA templates, the mass of a single plasmid molecule was first calculated using the following formulation: mass (g) = plasmid size (bp) X 1.096×10^{-21} g/bp [Applied Biosystems Reference 2003]. Next, mass of plasmid DNA needed was calculated by multiplying mass of single plasmid with copy number of interest. Finally, the mass needed was divided by the plasmid concentration to calculate the volumes for the preparation of a dilution series of each plasmid from 10^8 to 10^2 copy number. The same human P-Rex1 primers were used as in conventional PCR. New β -actin primers (forward primer: 5'-AATGTGGCCGAGGACTTTGATTGC-3'; reverse primer: 5'-

AGGATGGCAAGGGACTTCCTGTAA-3') were designed and synthesized for real-time PCR and the predicted PCR size is 93-bp. A 96-well optical plate was prepared in triplicate with each well containing 12.5 μ l of 2X SYBR Green PCR Master Mix (Applied Biosystems), 0.3 μ l of 25 μ M forward and reverse primers, 2 μ l template DNA (either cDNA or plasmid DNA dilutions), and DEPC-treated water to a final volume of 25 μ l. The real-time PCR was performed using an ABI Prism 7000 Sequence Detection System (Applied Biosystems) under default condition as follows: 10 min at 95°C, then 40 cycles of 15 seconds at 95°C, and 1 min at 60°C. Standard curves were drawn by plotting the threshold cycle (CT) against the natural log of the copy number of plasmid molecules. The CT value is defined as the cycle at which a statistically significant increase in the magnitude of the signal generated by the PCR reaction was first detected. The equations drawn from the graphs were used to calculate the copy numbers of cDNA molecules present in the unknown samples based on the corresponding CT values. Finally the expression of specific RNA levels was calculated relative to the control of β -actin RNA.

Protein extraction, electrophoresis and western blot analysis. Cells were seeded onto 6-well or 12-well plates. At the confluence of about 80%, culture medium was carefully removed from adherent cells, followed by washing twice with cold PBS. Cells were then lysed in cold RIPA (RadiolImmunoPrecipitation) buffer (100 μ l / well for 6-well plates, 50 μ l/well for 12-well plates) containing Tris HCl 50 mM, NaCl 150 mM, EDTA 1 mM, ethylene glycol tetraacetic acid (EGTA) 1 mM, Triton X-100 0.1% and sodium dodecyl sulfate (SDS) 0.1%. Protease inhibitors were added to RIPA buffer

immediately before use: 10 µg/ml leupeptin, 10 µg/ml aprotinin and 1 mM phenylmethylsulfonyl fluoride (PMSF). The cell lysate was gathered using a cell scraper, collected and transferred to a microcentrifuge tube which was then kept on ice for 30 min and sonicated 3 times for 5 seconds each. To pellet the cell debris, the sample was centrifuged at 12,000 X g for 10 min. The supernatant was transferred to a new tube and the protein content was quantitated by Bradford assay (Bio-Rad). Protein samples (40 µg) and prestained protein standards were loaded on 10% SDS polyacrylamide gels, electrophoresed (120 V for 1 hr at room temperature) and transferred to a polyvinylidene fluoride (PVDF) membrane (200 mA for 2 hr at 4°C) (Millipore, Immobilon-FL#IPFL10100). The membrane was blocked in Odyssey Blocking Buffer (LI-COR #927-40000) for 1 hr at room temperature. Primary antibodies were used to determine the specific protein. β-Actin was also measured as a loading control. For the detection of endogenous P-Rex1, the 3A11 rat monoclonal antibody was used (1:1000). The blot was incubated with these primary antibodies diluted in Odyssey blocking buffer overnight at 4°C, respectively. After a thorough washing, the blot was incubated with a species-appropriate secondary antibody labeled with either IRDye700 or IRDye800 (50 min at room temperature, protect from light), and then imaged with a Li-Cor Odyssey (LI-COR Biosciences, Lincoln, NE) at wavelengths of 700 or 800 nm.

For the Akt phosphorylation detection, 24 hr post serum-starvation, PC-3 cells were treated with DMSO or inhibitors as indicated for 1 hr, followed by 10 min treatment of 3T3 CM plus corresponding DMSO or inhibitors. In this case, a different lysis buffer was prepared, which contained Tris HCl 20 mM, NaCl 137 mM, CaCl₂ 1 mM, MgCl₂ 1 mM, and

Nonidet P-40 0.5%. Protease inhibitors were added to this buffer immediately before use: 10 µg/ml leupeptin, 10 µg/ml aprotinin and 1 mM phenylmethylsulfonyl fluoride (PMSF). In addition, a phosphatase inhibitor cocktail (Pierce #78420) was also added. Phospho-Akt (Ser473) (Cell Signaling Technology #9271, 1:1000) antibody was used for p-Akt detection and Akt antibody (Cell Signaling Technology #9272, 1:1000) for the total Akt as a loading control. All the other steps for western blot were followed as described above.

Fluorescence Microscopy. Human prostate cancer cells were cultured in 6-well plates containing coverslips. They were washed three times in ice-cold PBS and fixed and permeabilized in 100% methanol at -20°C for 10 min. After fixation, cells were washed three times for 5 min increments in PBS, blocked for 40 min with 10% horse serum & 1% BSA in PBS, and washed once for 5 min with PBS. They were then incubated overnight at 4°C in 100% humidity, together with the primary antibodies for P-Rex1 (1:40 in 1% BSA in PBS, rat monoclonal P-Rex1 4A3 antibody). Second antibody-only controls were also prepared for P-Rex1 (1:400 in 1% BSA in PBS, Alex Fluor® 488-conjugated donkey anti-rat IgG second antibody, Molecular Probes). After washing off the primary antibodies with PBS three times for 5 min increments, the slips were incubated at room temperature in the dark for 30 min with the secondary antibodies, then washed in PBS and mounted in a Vectorshield® mounting medium with 4,6-diamidino-2-phenylindole hydrochloride (DAPI), which stains the nuclei. Images were captured by fluorescent microscopy.

For cortactin and F-actin double staining, cells seeded on coverslips were grown in full growth media to 30% to 50% confluency. Media were changed to serum-free DMEM for 24 hr then to DMEM or NIH-3T3 CM for additional 5 hr. The F-actin visualization Biochem kit (Cytoskeleton #BK005) was used for the staining procedure as follows. Coverslips were carefully removed from media using tweezers and placed with cell side up on the filter paper in the Dark Box. Next, samples were washed once with 200 μ l of Wash Buffer (contained in the kit) for 30 seconds at room temperature. Wash Buffer was removed using kimwipes by touching the side of coverslips. 200 μ l of Fixative Working Solution was added to coverslips which were then incubated for 10 min at room temperature. Coverslips were washed and dried once again following the same procedures described above. Cells were permeabilized by adding 200 μ l of Permeabilization Buffer to coverslips and incubating for 5 min at room temperature. After washing, they were then incubated with the primary antibody for cortactin (Millipore mouse anti-cortactin p80/85, clone 4F11, 1:200) overnight at 4°C in 100% humidity. After washing off the primary antibody with Washing Buffer, coverslips were incubated at 37°C in the dark for 1 hr with the secondary antibody, anti-mouse IgG Flu (1:200), then washed in Washing Buffer again. Next, F-actin was stained with rhodamine-labeled phalloidin by incubating the samples with 200 μ l of working stock Rhodamine Phalloidin for 30 min at room temperature. Finally, coverslips were mounted onto microscope slides with mounting media. Images were captured by CoolSNAP CF camera attached to a Nikon Ti-80 microscope and processed by Image-Pro® Plus software (v6.1). Lamellipodia were identified as a smooth convex stretch of perpendicular actin stain at the peripheral edge of the cell as apparent in the rhodamine-labeled phalloidin stain.

Conditioned medium preparation and cell migration and invasion assays. NIH-3T3 fibroblast cells were cultured in complete growth medium to 50% confluence. The medium was then changed to serum-free medium. After incubating for an additional 48 hr, the conditioned medium (CM) was collected with cellular debris removed by centrifugation. Prostate cancer cell migration was determined using a 24-well transwell apparatus (8- μ m pore size with polycarbonate membrane; Corning Costar) according to the manufacturer's instructions (**Figure 5**). In brief, cells (50,000) suspended in 200 μ l serum-free medium were seeded to the upper chamber. 600 μ l CM was added to the lower chamber to serve as a chemoattractant. After incubation at 37°C, migrated cells were fixed and stained using the Diff-Quik kit (Andwin Scientific, Addison, IL). These cells were quantified by counting seven randomly selected and non-overlapping microscope fields at 40X magnification. For inhibition experiments, cell suspensions were incubated with various concentrations of inhibitors for 15 min and then added to the transwell chambers, while CM was supplemented with inhibitors in parallel. Transwell invasion assays were similar to the migration assays except that Matrigel (40 μ g/100 μ l in serum-free medium) was polymerized in the upper chamber at 37°C for 5 hr before cells were added. All experiments were performed at least three times; bars, mean \pm S.E.

Immunohistochemistry analysis. Formalin-fixed, paraffin-embedded blocks of cancerous prostate tissue were collected with informed consent for research purposes by the Department of Pathology of the Creighton University Medical Center. The use of sections from these tissue blocks for immunohistochemistry analysis was approved by the Institutional Review Board at Creighton University. Immunohistochemistry was performed using standard techniques. Tissue sections were cut from the tissue blocks

and deparaffinized. Antigen was retrieved by boiling the slides in an antigen unmasking solution (Vector Laboratories, Burlingame, CA). Any residual endogenous peroxidase activity was quenched with hydrogen peroxide and nonspecific binding was blocked with normal goat serum before incubating the sections with a rat monoclonal anti-P-Rex1 4A3 antibody (1:200). For detection of the immunoreactivity, the sections were then incubated with biotinylated anti-rat antibody and developed with 3,3'-diaminobenzidine (DAB substrate kit; Vector Laboratories). The sections were counterstained with hematoxylin. The levels of cellular expression of P-Rex1 protein were measured on immunohistochemically stained tissue slides using the Automated Cellular Imaging System (ACIS, ChromaVision Medical Systems, Inc., San Juan Capistrano, CA) as described previously [Gao et al. 2005]. This system combines color-based imaging technology with automated microscopy to provide quantitative information on intensity of staining. A "histo-score" (H score) was calculated for each case to estimate the P-Rex1 protein expression level and was obtained by multiplying the percentage (P) of staining positive cells with the average intensity (I), *i.e.* $H = P \times I$.

RNA Interference (RNAi). RNAi is a post-transcriptional process triggered by the introduction of small double-stranded RNA (referred as small interfering RNA or siRNA) which leads to gene silencing in a sequence-specific manner. The siRNAs are incorporated in the RNA Induced Silencing Complex (RISC), which contains several protein components including a ribonuclease which degrades the targeted mRNA, and then knocks down the synthesis of its corresponding protein (**Figure 6**). The antisense strand of the siRNA duplex directs target specificity of the RISC RNase activity while the

sense strand functions mainly to stabilize the RNA prior to entry into RISC and is degraded after entering RISC.

To knock down P-Rex1 at specific target sequence 5'-GCAACGACTTCAAGCTAGTGGAGAA-3' (gene accession number NM_020820.2), a 21-nt siRNA duplex with 3'-UU overhangs, antisense 5'-ACGACUUCAAGCUGGUGGAUU-3' and sense 5'-UCCACCAGCUUGAAGUCGUUU-3', was designed and ordered from IDT. PC-3 cells were initially transfected with 50 nM of scramble siRNA (negative control #1 siRNA, Ambion) or synthesized P-Rex1 siRNA in suspensions using Lipofectamine™ 2000 according to the manufacturer's instructions. After 5 hr of incubation, 90% of the transfection medium volume was replaced with fresh culture medium. One day later, adherent PC-3 cells were re-transfected with 50 nM of siRNAs. After an additional 2 days of incubation, cells were harvested and subjected to real-time RT-PCR, western blot analysis of P-Rex1 protein expression using the anti-P-Rex1 antibody 3A11 (1:1000), cortactin staining and the transwell migration assay.

Establishing stable cell lines. Stable wild-type P-Rex1, P-Rex1 “GEF-dead” E56A/N238A mutant or pcDNA3.1 vector expressing CWR22Rv1 cell lines were established according to a standard protocol. In brief, CWR22Rv1 cells were transfected with 20 µg of DNA for each 100 mm tissue culture dish using Lipofectamine™ 2000. After 48 hr of incubation, cells were selected with G-418 (400 µg/ml) for two weeks. Positive clones were selected, amplified and verified by Western blotting for P-Rex1 expression.

Rac Activation Assay. Activated Rac was assayed in an *in vitro* pull-down assay using the Rac Activation Assay Kit. Cells at 70% - 90% confluency were washed with ice-cold Tris-Buffered Saline (TBS), lysed using lysis buffer by scraping, and transferred to microfuge tubes on ice. The cell lysates were then pre-cleared by incubating with glutathione agarose and centrifuge. The supernatant aliquots were collected for immediate use. PAK-1-PBD (10 μ g) coupled to agarose beads was added to the supernatant and the mixture incubated at 4 °C for 60 min with gentle agitation. Beads were washed three times and samples were subjected to 10% SDS-polyacrylamide gel electrophoresis (SDS-PAGE) followed by immunoblot with anti-Rac antibody (clone 23A8, Upstate). The secondary antibody was tagged with IRDye800, and membrane imaging was carried out using a Li-Cor Odyssey at a wavelength of 800 nm. The corresponding 10% of the lysate was also assayed for total Rac.

Statistical analysis. Results are expressed as the mean \pm S.E. of at least three determinations and statistical comparisons are based on the Student's t-test. A probability (P) value of < 0.05 was considered to be significant.

C. RESULTS

P-Rex1, a Rac specific activator, is upregulated in highly metastatic human prostate cancer cell lines. Total RNA was isolated and both real-time RT-PCR and conventional RT-PCR were performed (**Figure 7**). As shown in **Figure 7B**, quantitative real-time RT-PCR analysis indicated that expression levels of P-Rex1 mRNA were significantly higher in the metastatic PC3-LN4 and PC-3 cells but was low or undetectable in normal primary human prostate epithelial cells (PrEC) as well as in nonmetastatic prostate cancer LNCaP and CWR22Rv1 cells. Consistent with this result, the conventional RT-PCR showed product of P-Rex1 was clearly detected in more aggressive prostate cancer cell lines but almost undetectable in normal and less aggressive prostate cancer cell lines (**Figure 7A**). In supporting of this finding, western blot analysis indicated that P-Rex1 protein was significantly higher in PC-3 cells than in LNCaP and CWR22Rv1 cells (**Figure 8A**). These results were further confirmed by immunofluorescent staining using a P-Rex1 specific antibody. Interestingly, the majority of the P-Rex1 is located in the cytosol, with a small fraction found on the leading edge of the plasma membrane of PC-3 cells, but not in LNCaP or CWR22Rv1 cells (**Figure 8B**). More importantly, migration abilities of those prostate cancer cells in response to the NIH-3T3 CM, as measured by transwell chamber assays, were directly correlated with their P-Rex1 expression levels (**Figure 9**). Taken together, these results indicated that P-Rex1 expression was significantly elevated in metastatic prostate cancer cells and provided the initial evidence that upregulation of P-Rex1 may be associated with increased metastatic abilities of prostate cancer cells.

P-Rex1 protein is upregulated in human prostate adenocarcinoma and lymph node metastasis. We further performed immunohistochemical analysis of P-Rex1 protein expression in neoplastic cells of formalin-fixed, paraffin-embedded prostate tissue blocks. **Figure 10A** shows the representative immunostaining of P-Rex1 protein as indicated by brown color in prostate carcinoma with adjacent noncancerous tissue (A1 and A2) as well as their metastases in lymph nodes (A3 and A4) of two prostate cancer cases. Compared with the noncancerous tissue (green arrows), the immunostaining intensity of P-Rex1 is greatly increased in metastases in lymph nodes (red arrows), but only slightly increased in the localized prostate carcinoma (black arrows). Prostate tissue sections from eight prostate cancer patients were immunohistochemically stained for P-Rex1 protein and then analyzed by an Automated Cellular Imaging System (Gao et al. 2005). From each patient, noncancerous prostate tissue; adjacent localized cancer; and a lymph node metastasis were examined. The average H-score, an indication of the expression levels of P-Rex1 in these tissues, is shown in **Figure 10B**. All cancer samples exhibited increased immunostaining intensity compared with the noncancerous tissue. Although not quantified, the staining tends to be more homogeneous in the metastatic prostate cancer than localized cancer. On average, there was an approximately 3.7-fold increase in the mean H-score in the lymph node metastases and about a 1.6-fold increase in localized prostate tumors when compared to nearby noncancerous prostate tissues, differences that were statistically significant ($P = 0.0004$ and $P = 0.016$, respectively) by Student's paired *t* test analysis. Furthermore, the H-score was significantly higher in prostate cancer lymph node metastases than in the localized tumor from the same patient ($P = 0.0055$), raising the

possibility that heterogeneous upregulation of P-Rex1 in the primary tumor is associated with progression to the invasive phenotype.

Knock-down of endogenous P-Rex1 reduces Rac-dependent prostate cancer cell migration. To examine the biological function of P-Rex1 in prostate cancer, we used a P-Rex1-specific siRNA to silence endogenous P-Rex1 expression in PC-3 cells which have the highest P-Rex1 expression among all the prostate cell lines used in our study. Delivery of this synthesized P-Rex1 siRNA into PC-3 cells suppressed expression of P-Rex1 mRNA level by over 60% (**Figure 11A**) and effectively decreased P-Rex1 protein level as compared to cells transfected with the scramble siRNA (**Figure 11B**). We further studied the subcellular localization of cortactin. Cortactin is a cytosolic protein and is translocated by activated Rac to the lamellipodia (Li et al. 2004). As shown in **Figure 12A**, knock-down of P-Rex1 blocks the translocation of cortactin to the lamellipodia in PC-3 cells. This finding of altered cortactin subcellular localization is consistent with the notion that the P-Rex1 stimulates Rac activation. Consequently, the cell migration was decreased by about 45% (**Figure 12B**). These data suggest that endogenous P-Rex1 functions as a regulator of prostate cancer cell migration, and further demonstrate that the elevated P-Rex1 level in metastatic prostate cancer cells contributes to the increased cell migration.

Expression of P-Rex1 increases prostate cancer cell migration. Since CWR22Rv1 cells express very low endogenous P-Rex1 protein, we first used this cell line as an *in vitro* model to investigate the effect of transient expression of exogenous P-Rex1 protein on the prostate cancer cell migration in response to NIH-3T3 CM. As shown in **Figure 13**, under 40-50% of transfection efficiency, exogenous expression of

P-Rex1 increased CWR22Rv1 cell migration by about two-fold. Deletion of the DH domain, the Rac-GEF functional domain of P-Rex1 protein, completely abolished its ability to enhance the CWR22Rv1 cell migration. This result suggests that P-Rex1-promoted CWR22Rv1 cell migration is dependent on the Rac-GEF function of P-Rex1. To determine if the stimulatory effect of P-Rex1 on CWR22Rv1 cell migration was applicable to other prostate cancer cells, we transiently expressed GFP-tagged P-Rex1 protein in PC3-LN4 cells which express modest level of endogenous P-Rex1 protein (see Figure 7). Since the transfection efficiency of PC3-LN4 cells was only about 25%, we enriched the transfected cells by flow cytometry sorting based on the GFP fluorescence (Singh et al. 2005) and then performed transwell migration assays. As expected, despite a similar expression level (**Figure 14A**), exogenous expression of wild-type P-Rex1 but not the P-Rex1 (-DH) mutant resulted in a four-fold increase in PC3-LN4 cell migration (**Figure 14B**).

Rac activation plays an important role in directed migration of prostate cancer cells. PC-3 adenocarcinoma cell line, originally established from bone metastases of prostate cancer, has been widely used as a model for studying prostate cancer metastasis (Sobel and Sadar 2005). To investigate the molecular mechanisms underlying P-Rex1-mediated prostate cancer migration, we examined the effects of inhibitors selective for Rac, Rho or Rho-kinase, a downstream effector of Rho, on the directional migration of PC-3 cells (**Figure 15**). As shown in **Figure 15B**, the basal migration of PC-3 cells in response to the DMEM is very low, demonstrating that the migration observed is dependent on factors present in the NIH-3T3 CM. NSC23766, a

Rac-specific inhibitor (Gao et al. 2004), significantly inhibited the PC-3 cell migration in a dose-dependent manner, causing about a 70% inhibition at 100 μ M without a significant effect on cell viability. In contrast, C3 transferase (2 μ g/ml), a cell permeable Rho inhibitor or 15 μ M Y-27632, a selective inhibitor of Rho-kinase, only reduced the cell mobility by about 35%. Taken together, our results indicated that Rho family GTPases, particularly Rac, play an important role in directed migration of prostate cancer cells.

G β γ subunits and PI3K activation contribute to GPCR-stimulated migration of prostate cancer cells. Rac is activated by GEFs upon external stimuli from surface ligand-receptor systems such as GPCRs and receptor tyrosine kinases (Ellenbroek and Collard 2007). We found that pre-treatment of PC-3 cells with PTx (500 ng/ml, 6 hr), a G_i specific inhibitor, blocked cell migration by over 80% (**Figure 16, left**). Interestingly, PTx treatment also inhibited cell migration of another highly metastatic prostate cancer cell line PC3-LN4 by over 90% (**Figure 16, right**). Therefore, our data suggest that activation of G_i-coupled receptors is required for directed prostate cancer cell migration, which is consistent with a previous report showing a role of the G_i family of G proteins in prostate cancer metastasis *in vivo* (Bex et al. 1999).

The binding of ligand (such as chemokines) to a GPCR promotes its interaction with G proteins, resulting in dissociation of the G α -GTP from G β γ subunits. As shown in **Figure 17**, M119, a recently identified specific inhibitor of G β γ (Bonacci et al. 2006), reduced PC-3 cell migration in a dose-dependent manner, with over 85% inhibition observed at 25 μ M without a significant effect on cell viability (over 95% of the cells were

trypan blue impermeable), suggesting an important role of $G\beta\gamma$ in prostate cancer migration.

$G\beta\gamma$ subunits released from G_i proteins can trigger a number of downstream events, including activation of the PI3K signaling cascade (Brock et al. 2003). PI3Ks have been implicated as major regulators of Rac-GEFs (Vivanco and Sawyers 2002) and PI3K-dependent stimulation of Rac plays a critical role in regulating the migration of many cell types (Barber and Welch 2006). However, blocking PI3K activity by the specific inhibitor LY294002 (10 μ M) or wortmannin (100 nM) only resulted in less than 50% inhibition of PC-3 cell migration (**Figure 18B**). This partial inhibitory effect was not due to inefficient inhibition of PI3K activity because LY294002 (10 μ M) or wortmannin (100 nM) can block more than 85% of the activity of Akt, a down-stream effector of PI3Ks (**Figure 18A**). Therefore, our data suggest that directed migration of prostate cancer cells is dependent on $G\beta\gamma$ subunits, and may be regulated by both PI3K-dependent and -independent mechanisms.

P-Rex1 promotes prostate cancer cell migration and invasion via Rac activation. To further determine whether the effect of P-Rex1 was specifically dependent on its ability to activate Rac via its GEF activity, we generated stable CWR22Rv1 cells expressing either wild-type P-Rex1 or a P-Rex1(E56A/N238A) “GEF-dead” mutant (**Figure 19A**). Although P-Rex1 “GEF-dead” mutant expression was similar to wild-type P-Rex1 (**Figure 19B**), cells expressing wild-type P-Rex1 but not its mutant showed an approximate 3-fold increase in both cell migration (**Figure 20**) as compared to control cells stably transfected with vector. More importantly, cell invasion

(**Figure 21**), another critical step in cancer metastatic cascades, was also increased about 3-fold upon expression of wild-type P-Rex1.

Cell migration is a sequential, interrelated multistep process (Yamazaki et al. 2005). It involves the formation of lamellipodia at the front edge (Hall 2005), cycles of adhesion and detachment, cell body contraction, and tail retraction. As shown in the **Figure 22 (A)**, Lamellipodia (white arrows) form in metastatic PC-3 cells, but not in nonmetastatic CWR22Rv1 cells. Stable expression of P-Rex1, but not its “GEF-dead” mutant, significantly increased the lamellipodia formation (**Figure 22 (B)**). Because Rac controls lamellipodia formation and P-Rex1 is a Rac-specific activator, we used a GST-PAK1 fusion protein containing the Rac-binding domain as an affinity reagent to analyze the activated GTP-bound Rac levels in prostate cancer cells. As shown in **Figure 23**, Rac activities were much higher in PC3 cells than in CWR22Rv1 cells. This result correlates with the level of endogenous P-Rex1 in those cells (Figure 7). Interestingly, CWR22Rv1 cells expressing wild-type P-Rex1 had significantly higher Rac activity as compared to the control cells or cells expressing the “GEF-dead” P-Rex1 mutant.

To confirm this finding, we further studied the subcellular localization of cortactin. As shown in Figure 22A&B, similar to F-actin polymer staining, the translocation of cortactin to the lamellipodia is detected in PC-3 cells or CWR22Rv1 cells expressing wild-type P-Rex1 protein but not control CWR22Rv1 cells or cells expressing the “GEF-dead” P-Rex1 mutant. These findings of altered cortactin subcellular localization are consistent with the notion that the P-Rex1 stimulates Rac activation. Altogether, our data provide a molecular mechanism by which P-Rex1 promotes prostate tumor metastasis through stimulation of Rac activity and, thus, the enhancement of lamellipodia formation.

D. DISCUSSION

Metastasis is the spread of primary tumor cells to other sites elsewhere in the body by way of the blood vessels or lymphatic systems. It plays the major contributing role in cancer mortality and has attracted more and more interests of tumor biology researchers. The process of metastasis heavily depends on the acquisition of increased motility and invasiveness of cancer cells. In another words, the ability of a cell to metastasize requires changes that allow it to escape the normal boundaries of the tumor in which it originated, and to migrate to and invade sites distinct from the primary tumor. It is therefore important to define the signaling pathway(s) involved in the activation and promotion of cancer cell migration and invasion. Extensive studies have revealed that the small GTPase Rac significantly contributes to these signaling transductions. It is reasonable to investigate how Rac is involved in cell migration and invasion by studying its activators, GEFs. Although some important Rac-GEFs, like Tiam1, have been identified, the whole or major network remains to be elucidated. In this study, we report that an increase of P-Rex1 protein, a novel Rac specific GEF that normally helps regulate neutrophil chemotaxis (Welch et al. 2002 & 2005), is markedly upregulated in metastatic prostate cancer and may be another GEF that contributes to prostate cancer cell migration and invasion.

In the present study we measured and compared gene expressions of some typical GEFs, Tiam1 (GEF for Rac), Vav1/2/3 (GEF for Rac, Rho and Cdc42), and P-Rex1, in the four different prostate cancer cell lines with varying degrees of metastatic activity. As indicated by white arrows in **Figure 24**, we were surprised to find that P-Rex1 showed a similar expression pattern as Tiam1: significantly elevated in metastatic

prostate cancer cells, while Vav1/2/3 had a random expression (**Figure 24**). As mentioned earlier, involvement of Tiam1 in cancer cell migration and invasion has been well established. Therefore, we proposed that P-Rex1 may be another molecular contributor of prostate cancer metastasis and focused our research on the role of P-Rex1 in prostate cancer cell movement. In this dissertation, after demonstrating that the endogenous levels of P-Rex1 directly correlated with the degree of *in vitro* migration of prostate cancer cells, we carried out a series of experiments to test our hypothesis. Silencing the endogenous expression of P-Rex1 protein in highly metastatic prostate cancer PC-3 cells significantly reduced their ability to migrate. Conversely, when P-Rex1 was transiently expressed in CWR22Rv1 cells that express low levels of endogenous P-Rex1, the cells exhibited increased migratory activity. Similarly, PC3-LN4 cells that possess a modest level of P-Rex1 also gained increased migratory activity upon transient expression of P-Rex1. We also investigated archived specimens from human prostate cancer. The P-Rex1 protein expression level is higher in metastatic tumors when compared to non-cancerous prostate tissue and localized prostate cancer. All our results suggest an important functional role for the P-Rex1 in contributing to prostate cancer cell motility.

P-Rex1 is a GEF that was discovered based on its ability to specifically activate Rac in migrating cells (Welch et al. 2002; Yoshizawa et al. 2005). It is a member of the P-Rex family which consists of P-Rex1, P-Rex2 and P-Rex2b (a splice variant of P-Rex2). They are homologous but differ in tissue distributions. P-Rex1 is mainly found in neutrophils and in brain, whereas P-Rex2 has a wide tissue distribution except in neutrophils. The heart is the major site where P-Rex2b is expressed (Donald et al. 2004;

Rosenfeldt et al. 2004). It is worth noting that our PCR experiments showed both P-Rex2 and P-Rex2b were almost undetectable in the prostate cancer cells for which parallel PCRs were also carried out for P-Rex1 and other GEFs described above (**Figure 24**). Therefore, it is not likely that P-Rex2 or P-Rex2b is involved in prostate cancer metastasis. In cells, P-Rex1 can only activate Rac, though it becomes less specific in the test tube, where it also can activate cdc42. There are three Rac subfamilies: Rac1, 2 and 3. They are highly homologous in sequence but have distinct tissue distribution. Rac2 is specifically found in hematopoietic cells, whereas Rac3 is highly expressed in the brain and detected at lower levels in a wide range of tissues. In contrast, Rac1 is ubiquitously expressed and has been well characterized [Chan 2005]. In our Rac pull-down assay, only Rac1, but not Rac2 (not shown), was detected by using specific antibodies. It is most likely that P-Rex1 activates Rac1 subfamily in prostate cancer cells, though we did not measure Rac3. In normal stationary epithelial cells, Rac appears to be of greatest importance during initial cell-cell contacts when new epithelial monolayers form, and immediately thereafter when there is assembly of tight junctions and the underlying cytoskeleton between adjacent cells (Braga 2000). Pathologically, Rac hyperactivation has been reported to play a critical role in cancer metastasis (Sun et al. 2006). In 2004, Gao et al. designed and developed a specific inhibitor of Rac, NSC23766 (Gao et al. 2004). This small molecule compound can effectively inhibit Rac1-mediated cellular functions by interfering Rac1 interaction with the Rac-GEFs, without affecting Cdc42 or RhoA activation. In NIH 3T3 cells, the effective dose of NSC23766 for blocking Rac1 is 50 to 100 μ M (Gao et al. 2004). In our study, NSC23766 reduced metastatic prostate cancer PC-3 cell migration *in vitro* by about 50% at 50 μ M

and up to 70% at 100 μ M, indicating a significant role of Rac in regulating prostate cancer cell migration.

P-Rex1 has been shown to be activated by PIP3 and G β γ (Welch et al. 2002). Interestingly, G β γ not only interacts with P-Rex1 but also stimulates PIP3 production by activation of PI3Ks. Therefore, both co-activators of P-Rex1 are naturally produced upon activation of G-protein coupled receptors (GPCRs). GPCRs play a critical role in physiological and pathological processes. Dysfunction of GPCRs is responsible for many human diseases and more than 50% of current pharmaceutical products target GPCR-mediated signal cascades [Edwards et al. 2000]. Recent studies have demonstrated that many GPCRs and their ligands are also involved in cancer progression and metastasis [Daaka 2004; Dorsam and Gutkind 2007], and the list of overexpression of GPCRs in different types of cancer cells is huge [Li et al. 2005]. In malignant prostate cancer, several metastasis-promoting ligands/GPCRs are excessively up-regulated and convey signals that control the mobility and invasive potential of cancer cells, for example chemokine ligand/GPCR axes (stromal-derived factor-1(SDF-1)/CXCR4, CCL5/CCR5) [Sun et al. 2005; Cooper et al. 2003; Vaday et al. 2005], protease-activated receptor (PAR1) [Chay et al. 2002] and matrix metalloproteinases [Cao et al. 2005; Daja et al. 2003]. These ligands/GPCRs play important roles in prostate cancer invasion and metastasis, particularly skeletal metastasis, the most common metastasis of prostate cancer. Although over-stimulated GPCR signaling pathways are implicated in cancer metastasis, molecules linking hyperactivated GPCRs with cancer cell migration remain to be elucidated. Classically, G β γ released from G proteins upon activation of GPCR activates GEFs such as Tiam1 and Vav3 only by stimulating PI3Ks to produce PIP3.

However, a unique feature of P-Rex1 is that it can be synergistically activated by both G β γ and PIP3. It is possible that selective upregulation of P-Rex1 contributes to the hyperactivation of Rac in metastatic prostate cancer cells (Knight-Krajewski et al. 2004). As we have shown, there is a correlation between the P-Rex1 expression level and metastasis in both cell lines and human prostate cancer tissues. GPCRs have been shown to be involved in the prostate cancer migration and metastasis both in vitro (our data) and in vivo (Bex et al. 1999). In particular, the newly identified G β γ inhibitor, M119 compound, dramatically reduced the migration of high P-Rex1 expressing PC-3 cells at 10 - 25 μ M. This is well consistent with the published data in which the same concentration range is required to block the interactions between G β γ and its downstream targets (Bonacci et al. 2006). Taken together, these studies suggest that hyperactivation of Rac may be due to, at least in part, elevated P-Rex1, which contributes to the progression of prostate cancer to the metastatic stage.

Like Tiam1, P-Rex1 is a multi-domain Dbp-like GEF, which means it has a DH domain and other domains. It is well known that the GEF DH domain is an essential region and has nucleotide exchange activity. Structurally, DH domains consist of three conserved regions (CR1 – CR3) and poorly conserved “seat-back” regions. These regions can extensively interact with the switch domains of small GTPases, causing the remodeling of the switch regions. Eventually, these interactions at the Rho-GEF/GTPase interface will alter nucleotide-binding pockets of GTPases, resulting in GDP/GTP exchange (Rossmann et al. 2005). Two P-Rex1 mutants were used in our studies. One is the DH-deleted mutant and another is the “GEF-dead” DH-E56A/N238A dual-point mutant. Regulating accessibility of the substrate GTPase to the GEF DH domain is

important for GEF activation. The design of the P-Rex1 DH-E56A/N238A mutant has been based on the alignment of the Tiam1 DH domain. Glu⁵⁶ in P-Rex1 is equivalent to Glu¹⁰⁴⁷ in Tiam1 and Asn²³⁸ in P-Rex1 to Asn¹²³² in Tiam1 (Hill et al. 2005). Studies suggested that these two residues in Tiam1 are involved in building the interface with Rac. Both DH-deleted and DH-dual point mutants lack Rac-GEF activity and failed to activate Rac activity, resulting in a loss of its ability to promote prostate cancer cell migration and invasion in the present study. These experiments demonstrated the importance of the classical action of P-Rex1 as a GEF in prostate cancer cells.

A major function of Rac is its control of actin polymerization in the cytoskeleton to form lamellipodia, the thinned-out leading edge that is a crucial invasive characteristic of metastatic cancer cells. Indeed, we found that expression of wild-type P-Rex1, but not its “GEF-dead” mutant, promotes lamellipodia formation in prostate cancer cells. These data indicated that the cellular basis for the action of P-Rex1 on prostate cancer metastasis involves the activation of Rac with subsequent formation of lamellipodia and the DH is the catalytic domain for P-Rex1 GEF function. Importantly, it has been reported that the DH domain is the region by which G β γ regulates P-Rex1 GEF activity (Hill et al. 2005). This finding is supportive of our G β γ inhibition results as mentioned above. In Dbl-like GEFs, the DH domain is usually followed by a PH motif. There is no exception for P-Rex1. P-Rex1 also possesses two tandem PDZ domains, two tandem DEP domains and a carboxyl-terminal IP4P domain. We did not examine the potential roles of these motifs in regulating prostate cancer cell migration. Generally, the DH-associated PH domains regulate GEF activity by binding to phosphoinositides, which has been confirmed for P-Rex1 (Hill et al. 2005). PDZ and DEP domains are known as

protein-interaction domain serving adaptor-type functions to target their proteins to specific positions like membranes. The IP4P has a primary structure similar to inositol polyphosphate-4-phosphatase. However, the detailed roles of PDZ, DEP and IP4P domains are unknown in the P-Rex1 protein, though there is evidence showing the presence of these domains affects both basal and stimulated P-Rex1 Rac-GEF activity, which is likely due to their autoinhibition effect (Hill et al. 2005).

The reason for the upregulation of P-Rex1 in metastatic prostate cancer cells is unclear. The gene for P-Rex1 is found at chromosome 20q13.13. Most of the prostate cancer cell lines studied frequently have excess copies of chromosome 20 (Aurich-Costa et al. 2001 and Strefford et al. 2001). In addition, histone deacetylation and methylation seems to contribute to the silencing of endogenous P-Rex1 expression in CWR22Rv1 cells (Dr Tu lab, unpublished observations). This suggests that there could be both genetic and epigenetic alterations in the regulation of P-Rex1 expression, which is a focus of on-going research in our lab.

Although our work has only focused on the small GTPase Rac, it is always important to take into account all the major subfamilies of Rho small GTPases. It has been well established that Rac, Rho and Cdc42 are all involved in the assembly and organization of the actin cytoskeleton (Hall 1998). Generally, Rac activation leads to formation of lamellipodia, while as Cdc42 and Rho induce filopodia and stress fibers, respectively. During the cell movement, Rac and Cdc42 work together promoting formation of protrusions at the leading edge, and Rho induces retraction at the tailing portion. It is this coordinated reorganization of cell skeleton that permits cells to move toward a target. Thus, it was not surprising that Rho also played a role in prostate cancer

cell migration as shown in our Rho inhibition experiments. In our study model, Rac and Rho demonstrated differential effects on prostate cancer cell migration. We are not sure if this applies to other disease models, because the difference may vary due to cell and tissue types.

In the present study, we used the simple and classic transwell cell migration assay, a modified Boyden chamber assay. This is a very reliable approach for the analysis of chemotaxis, directed cell migration (Guan 2005). In general, cells placed on the top compartment are allowed to migrate through the pores of the membrane into the lower compartment. This process is driven by the chemotactic agents present in the lower chamber. In our study, NIH 3T3 conditioned media has been used as the source of chemotactic agents. We have so far not been able to identify individual components contained in this media and what stimulating factors are involved in the P-Rex1-mediated signal transduction pathways. However, evidence suggests that NIH 3T3 conditioned media is a rich source of chemoattractants. In addition, matrix proteins in this media like fibronectin and vitronectin can form a supportive coat at the underside of the membrane and this coat may provide a matrix substrate used by the migrated cells to adhere (Guan 2005). Thus, NIH 3T3 conditioned media has been widely used in the cell migration and invasion assays. Cell invasion is a defining step in tumor progression and one of the hallmarks of the metastatic phenotype. The same transwell device was applied for invasion assays, but with a basement membrane matrix preparation coated on the top of the filter membrane. The matrix preparation used in our study is Matrigel which is a soluble matrix extracted from the Engelbreth-Holm-Swarm (EHS) mouse sarcoma, a tumor rich in extracellular matrix proteins. Although Matrigel is not likely to be

able to represent all the aspects of an actual basement membrane, it is an effective membrane barrier to mimic it. Albini et al. (1987) demonstrated that there was an ideal correlation between the invasive behavior of tumor cells in vivo and their ability to invade in vitro using this approach. Cell migration and invasion have become the focus of much research because of their importance. Therefore, more and more new testing methods have emerged. It is important to note that although our transwell assays provided useful basic knowledge of P-Rex1-mediated prostate cancer cell migration and invasion pathways, further understanding of the signaling by using complicated assay systems is still desired. For example, using the Dunn chemotaxis chamber with time-lapse microscopy (video) will allow us to observe directly the morphological changes of cells in response to chemoattractants in real time. Tumor cells can move either in single-cell model or monolayer cell migration model. It is not clear whether prostate cancer cells adopt one of modes or the combination. Performing a scatter assay or wound-healing assay will help us obtain more detailed information (Guan 2005).

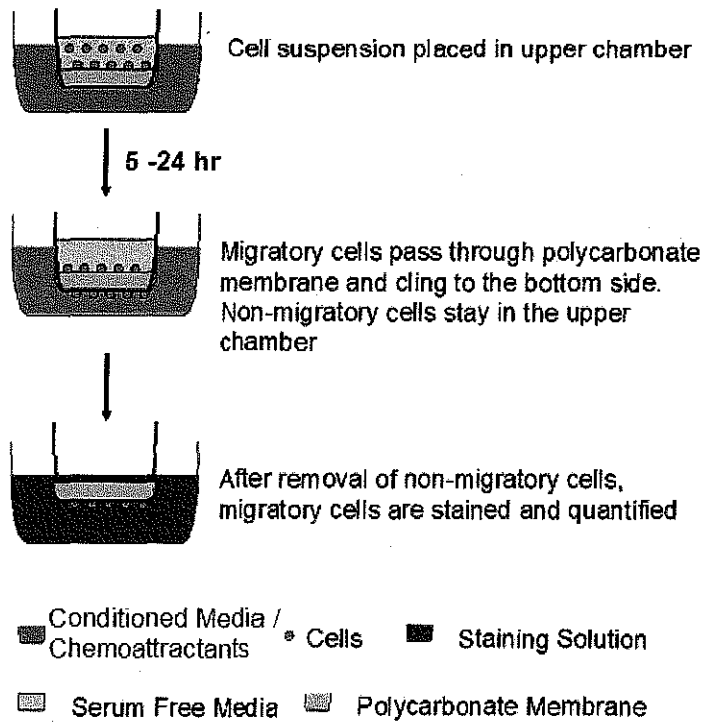
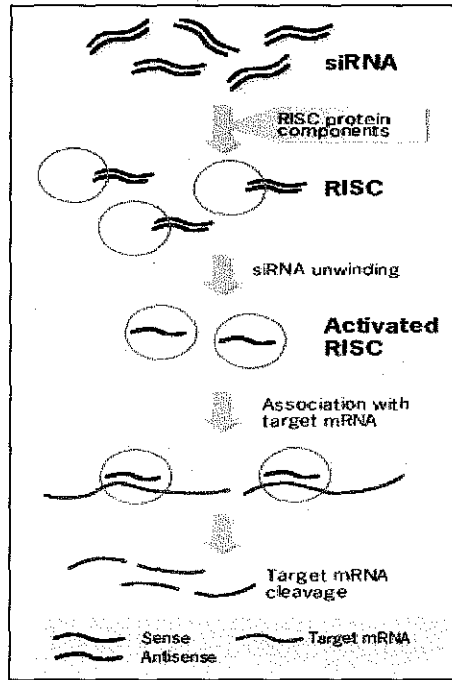


Figure 5. Transwell assay principle (adapted from www.cellbiolabs.com).

A.



B.

Sense : 5'-rArCrGrArCrUrUrCrArArGrCrUrGrGrUrGrGrATT-3'

Anti-sense: 5'-rUrCrCrArCrCrArGrCrUrUrGrArArGrUrCrGrUTT-3'

Figure 6. (A) The mechanism of RNA interference (RNAi) (adapted from http://www.ambion.com/techlib/append/RNAi_mechanism.html). (B) P-Rex1 siRNA sequences.

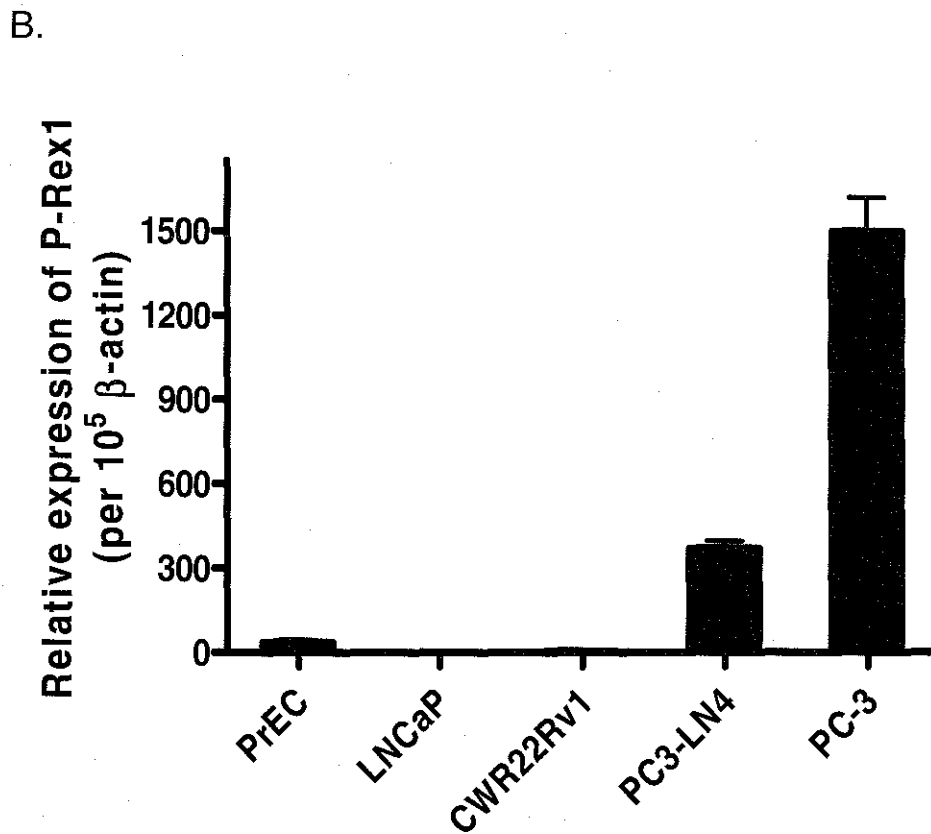
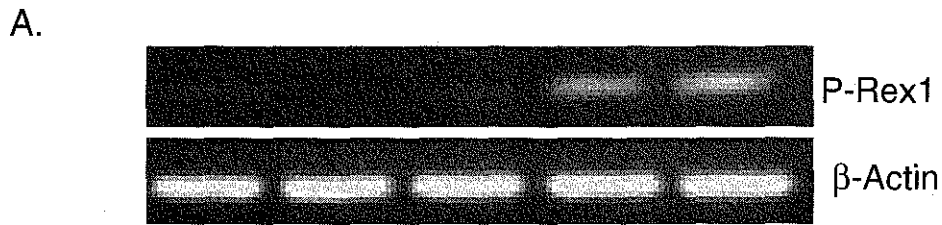
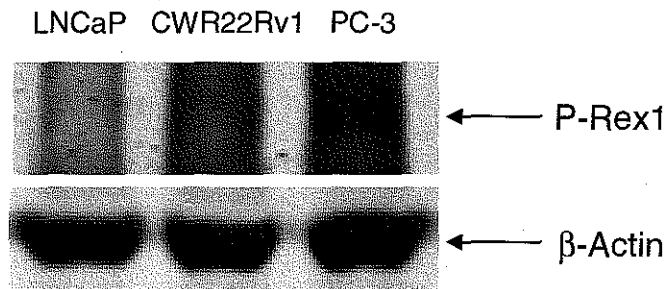


Figure 7. Analysis of P-Rex1 mRNA expression in human prostate cell lines. Total RNA was isolated from cultures of normal prostate epithelial cells (PrEC) and four prostate cancer cell lines (LNCaP, CWR22Rv1, PC3-LN4 and PC-3). (A) Conventional RT-PCR (35 cycles of 94°C for 30 seconds, 55°C for 30 seconds, 72°C for 30 seconds). PCR products were subjected to 3% agarose gel electrophoresis and visualized by staining with ethidium bromide. House-keeping gene β -actin was used as an internal control. (B) Quantitative real-time RT-PCR. Bars represent the mean \pm S.E. values of P-Rex1 mRNA levels normalized to β -actin levels (n=5).

A.



B.

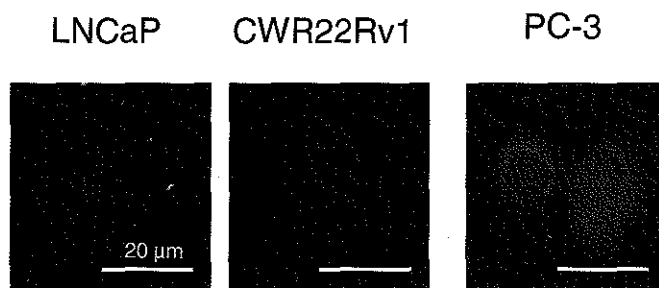


Figure 8. Analysis of P-Rex1 protein expression in prostate cancer cells. A: Western blot analysis of P-Rex1 protein using the anti-P-Rex1 antibody 3A11. B: Representative immunofluorescence staining of prostate cancer cells for P-Rex1 protein with the anti-P-Rex1 antibody 4A3, followed with Alexa-F488 (green)-linked secondary antibody. DAPI staining (blue) indicates the nuclei.

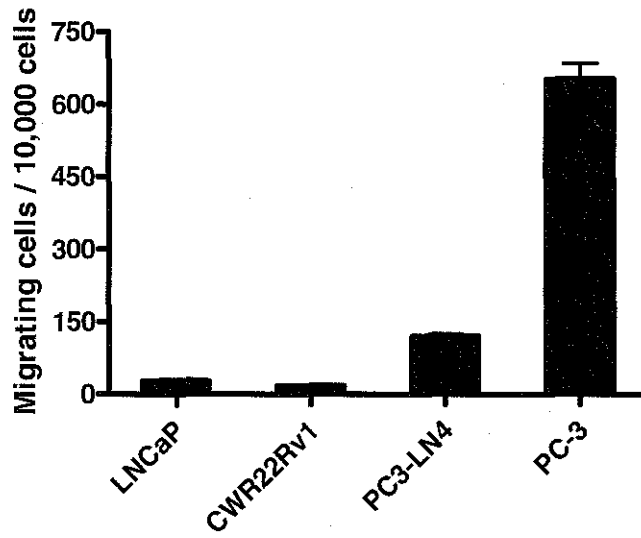


Figure 9. Transwell cell migration assays of prostate cancer cells toward NIH-3T3 CM. All results are represented as mean \pm S.E. of migrated cells per 10,000 loaded cells (n=3).

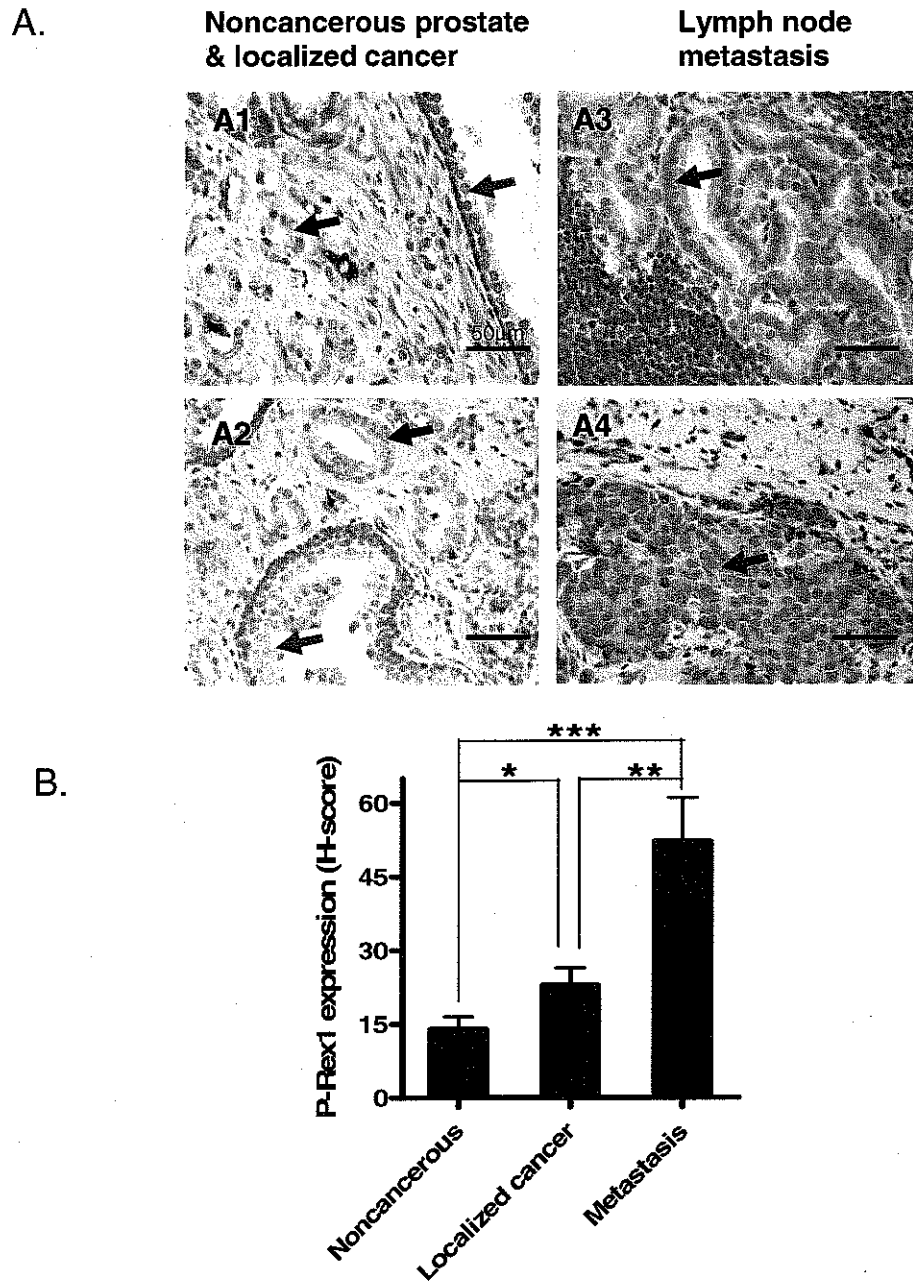
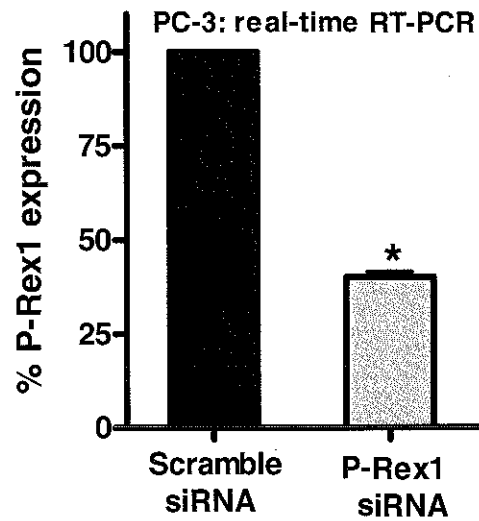


Figure 10. Immunohistochemical staining of human specimens for P-Rex1 protein using the antibody 4A3 as indicated by brown color. The top panel shows representative staining. A1 and A2 show noncancerous prostate epithelial cells (green arrow) and localized prostate cancer (black arrow). Prostate metastases (red arrow) into lymph nodes are illustrated in A3 and A4. The average H-score was used to grade P-Rex1 expression levels. The bottom panel shows the mean \pm S.E of eight cases. * $p=0.016$, ** $p=0.0055$, *** $p=0.0004$.

A.



B.

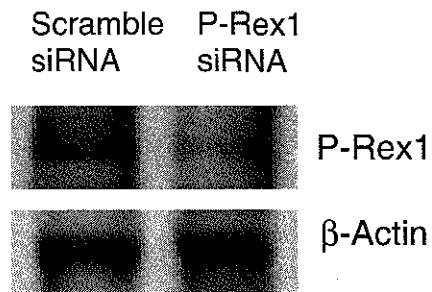


Figure 11. RNA interference for P-Rex1 expression in PC-3 cells using double transfection as described in the Materials and Methods. Cells were then harvested for real-time RT-PCR (A) and Western blot analysis (B) to detect P-Rex1 expression. Bars show mean \pm S.E. with * $p < 0.05$ compared to control ($n=3$).

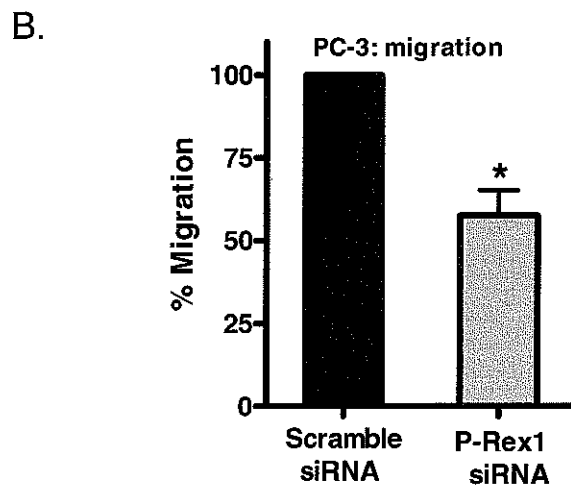
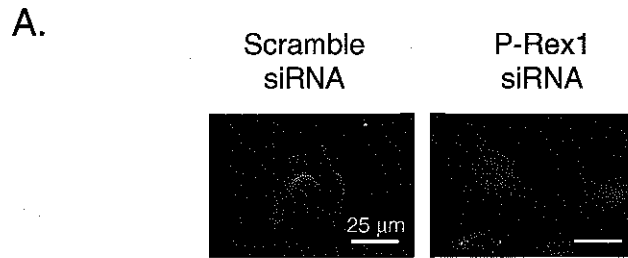


Figure 12. (A) Treatment of PC-3 cells with P-Rex1 siRNA blocks the translocation of cortactin (green) to the membrane. DAPI staining (blue) indicates the nuclei. (B) RNA interference for P-Rex1 results in suppression of transwell migration of PC-3 cells.

A.



B.

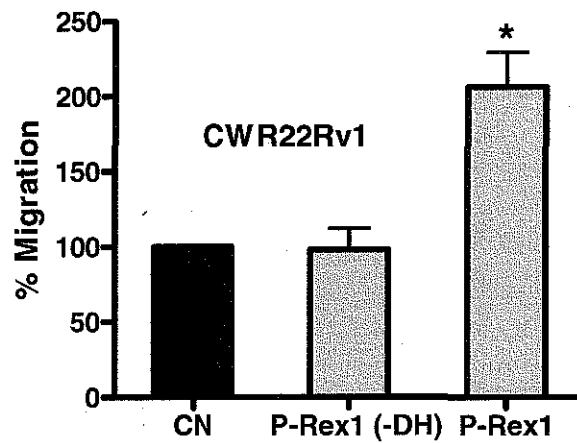


Figure 13. (A) Schematic structures of wild-type P-Rex1 and DH-deleted P-Rex1 mutant. Numbers: amino acid positions. (B) CWR22Rv1 cells were transfected with control GFP, GFP-tagged P-Rex1 or P-Rex1(-DH) for 48 h, and then subjected to transwell migration assay for 8 h. Bars show mean \pm S.E. with $*p < 0.05$ compared to control set at 100% (n=3).

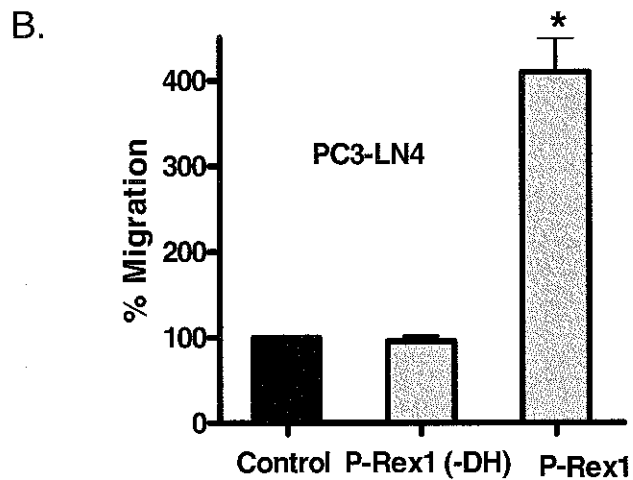
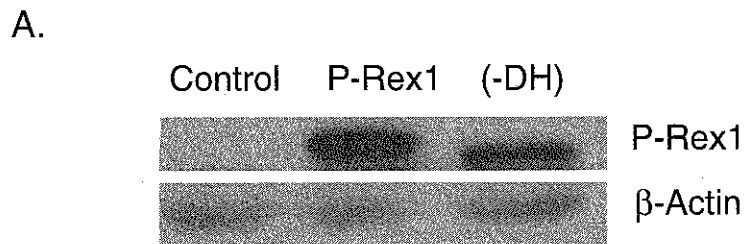


Figure 14. PC3-LN4 cells were transfected with the indicated plasmids. (A) Expression of P-Rex1 and P-Rex1(-DH) protein detected by western blot analysis using anti-GFP antibody. (B) Transfected cells were selected by flow cytometry cell sorting based on GFP fluorescence, followed by transwell migration assays. Bars show mean \pm S.E. with * $p < 0.05$ compared to control (n=3).

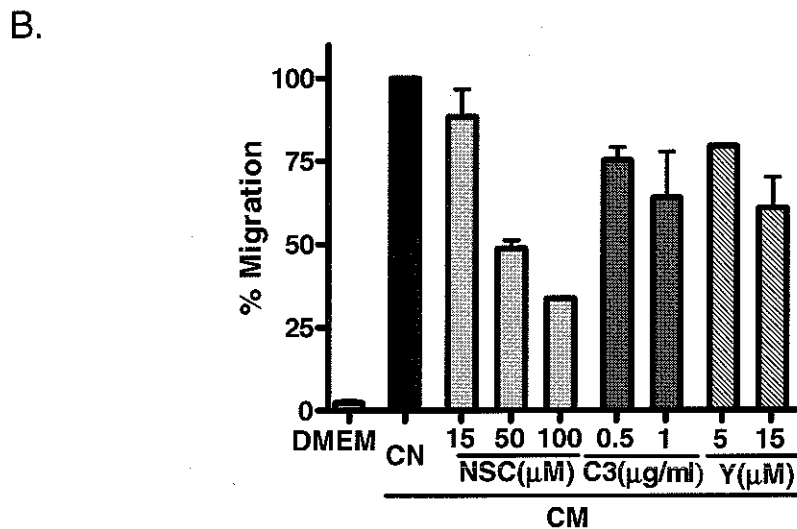
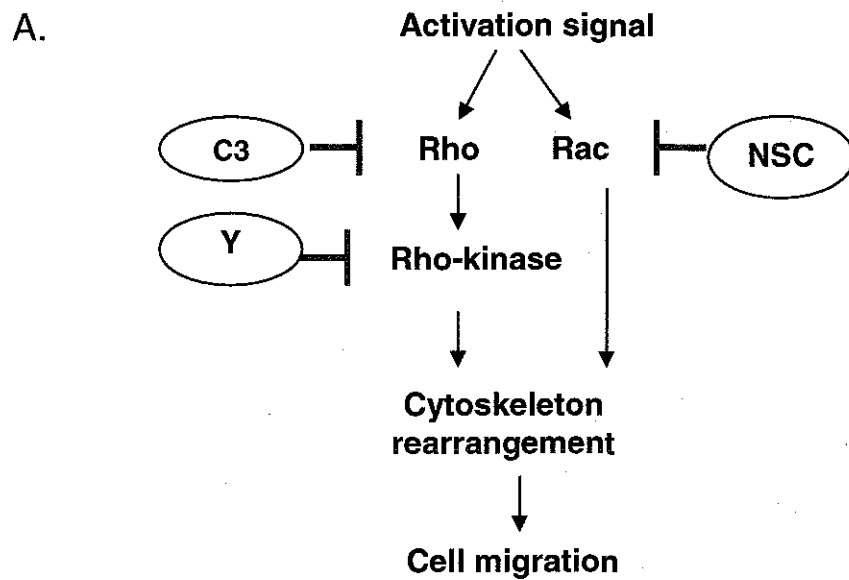


Figure 15. (A) Scheme of regulation of prostate cancer cell migration by small GTPases. (B) Prostate cancer cells were pretreated with different inhibitors and then added to the upper well (50,000 cells/well) of each chamber and allowed to migrate for 5 h toward DMEM medium or NIH-3T3 CM in the absence or presence of inhibitors. Migration toward CM in the absence of inhibitors was normalized to 100% (about 663 ± 95 per

10,000 loaded cells). PC-3 cell transwell migration assays without (control: CN) or with indicated concentrations of Rac inhibitor NSC23766 (NSC), Rho inhibitor C3 transferase (C3) or Rho-kinase inhibitor Y27632 (Y). Bars show the mean \pm S.E. (n=3) with *p<0.05.

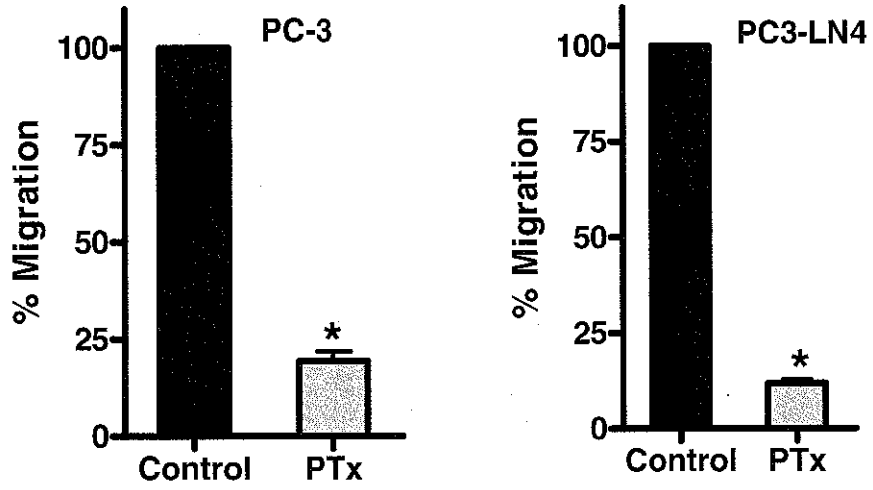


Figure 16. Transwell migration assays of PC-3 or PC3-LN4 cells without (CN) or with G_i-protein inhibitor pertussis toxin (PTx, 500 ng/ml) pretreatment for 6hr. Bars show the mean ± S.E. (n=3) with *p<0.01 compared to untreated cells (Control).

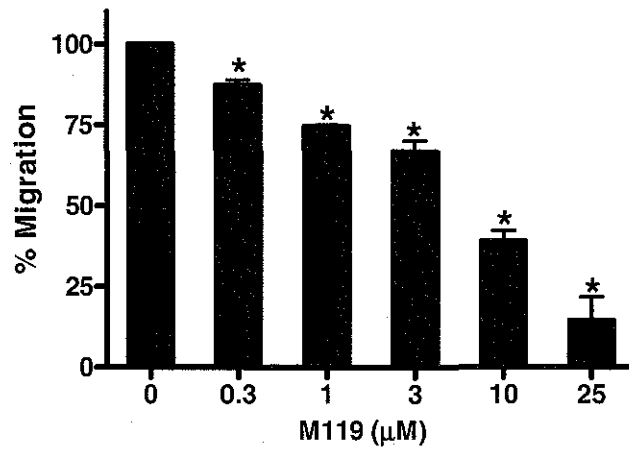


Figure 17. Transwell migration assays of PC-3 cells in the presence of Gβγ specific inhibitor M119 at the indicated concentrations. Bars show the mean ± S.E. (n=4) with *p<0.05 compared to control.

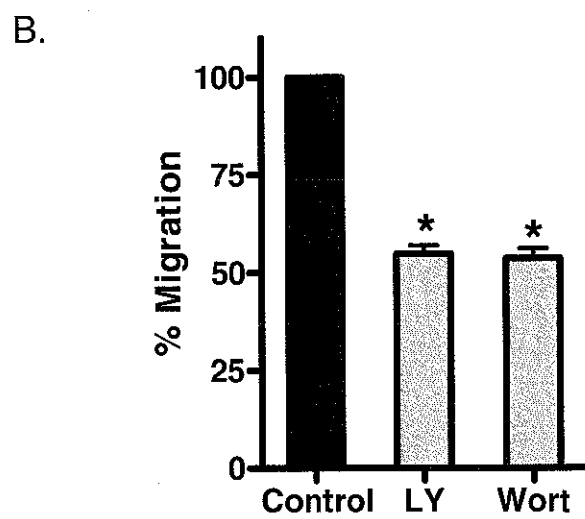
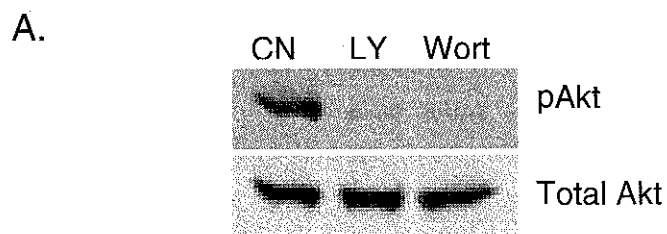


Figure 18. (A) Representative western blot showing effective inhibition (85%) of activated Akt (pAkt), a downstream effector of PI3K, by 10 μ M LY or 100nM Wort. Total Akt was used as a loading control. (B) Transwell migration assays of PC-3 cells in the presence of PI3K inhibitors LY294002 (LY, 10 μ M), wortmannin (Wort, 100 nM) or vehicle control (CN). Bars show the mean \pm S.E. (n=3) with *p<0.01 compared to control.

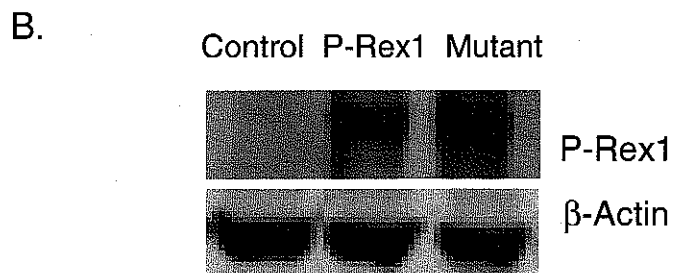
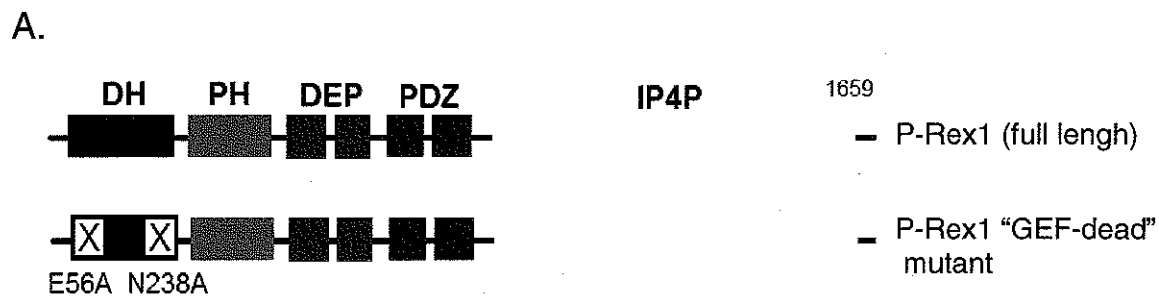


Figure 19. (A) Schematic structures of full-length P-Rex1 and P-Rex1 “GEF-dead” mutant. Numbers denote amino acid positions. E: glutamic acid; A: alanine; N: asparagines. (B) Expression levels of P-Rex1 and its mutant in CWR22Rv1 cells were determined by western blot analysis.

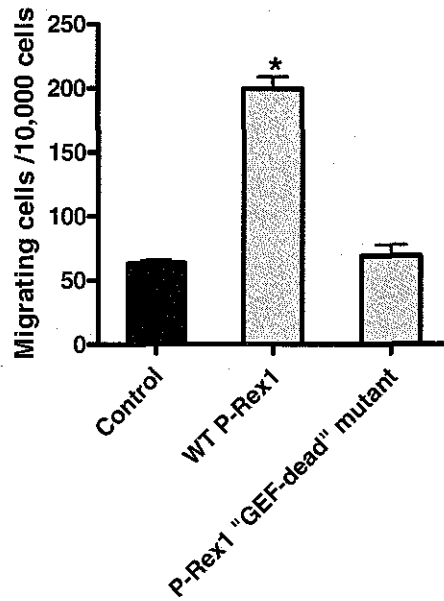


Figure 20. CWR22Rv1 cells stably expressing wild type P-Rex1, P-Rex1 "GEF-dead" mutant or control vector were subjected to migration assay for 24 h. Bars show mean \pm S.E. with * $p < 0.01$ compared to control ($n=3$).

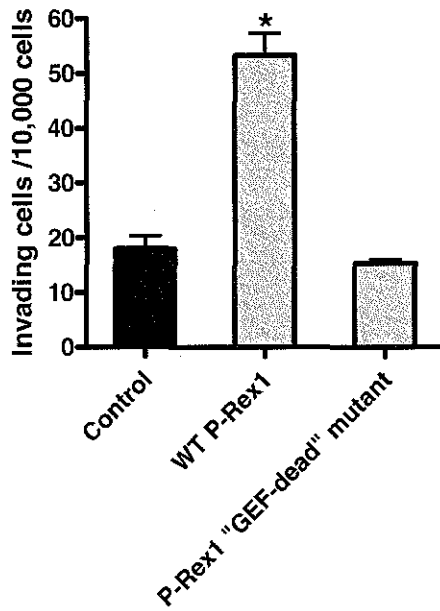


Figure 21. CWR22Rv1 cells stably expressing wild type P-Rex1, P-Rex1 "GEF-dead" mutant or control vector were subjected to invasion assay through Matrigel for 24 hr. Bars show mean \pm S.E. with * $p < 0.01$ compared to control (n=3).

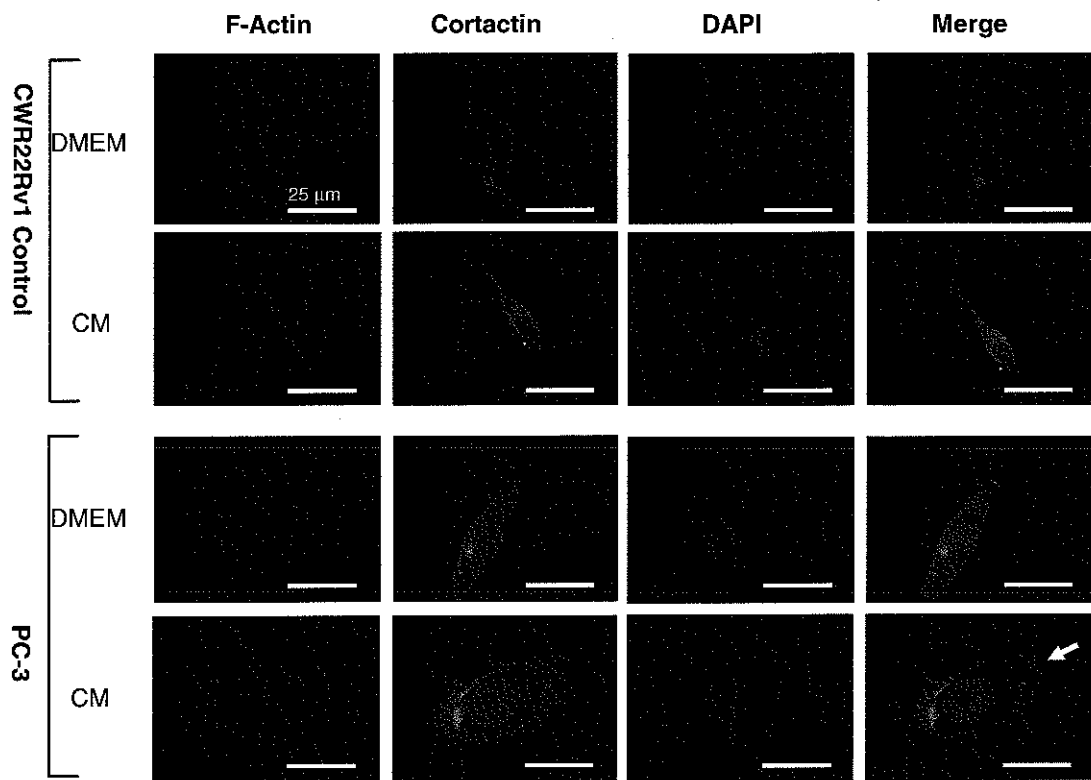


Figure 22 (A). P-Rex1 promotes the formation of lamellipodia and the translocation of cortactin. CWR22Rv1 cells stably expressing vector is used as negative control and PC-3 cells used as positive control. Serum-starved CWR22Rv1 or PC-3 cells were incubated with DMEM or NIH-3T3 CM for 5 hr and then stained with anti-cortactin antibody and FITC-conjugated secondary antibody (green) to detect cortactin in combination with rhodamine-conjugated phalloidin (red) for detection of F-actin. DAPI staining (blue) indicates the nuclei. Accumulation of cortactin and F-actin at the cell periphery is indicated by arrows.

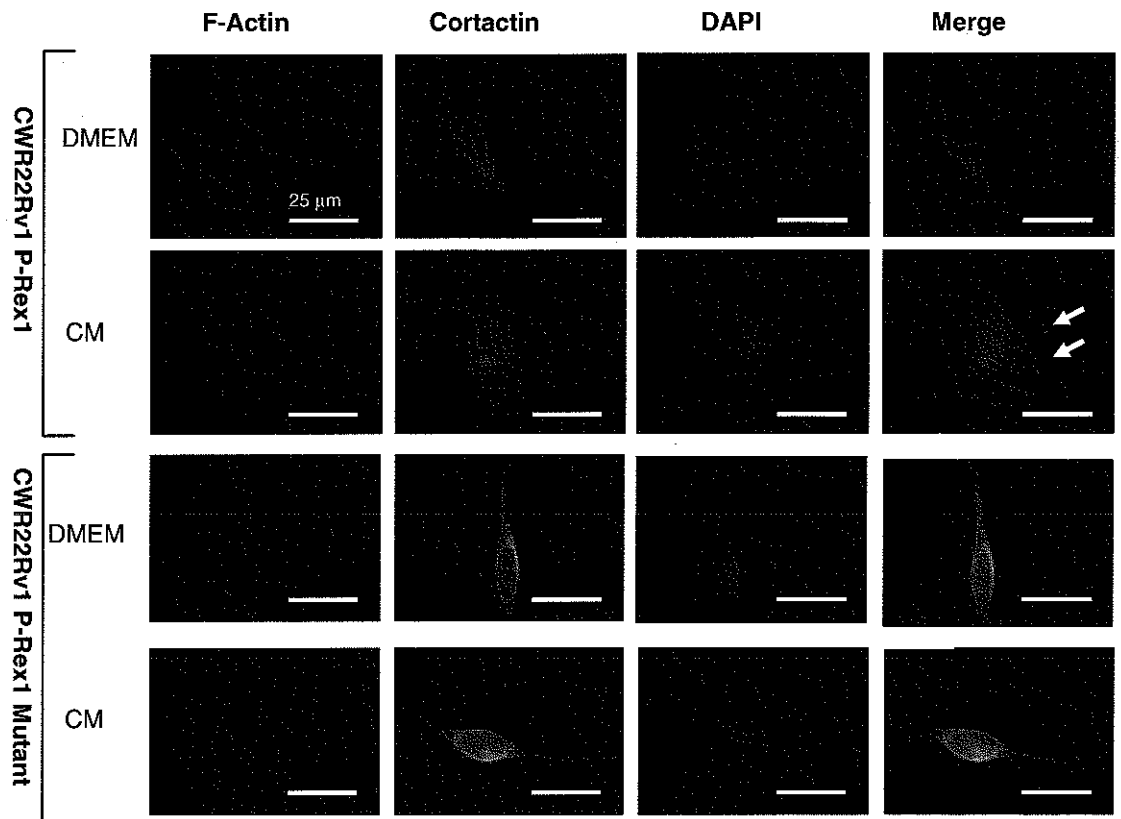


Figure 22 (B). P-Rex1 promotes the formation of lamellipodia and the translocation of cortactin.

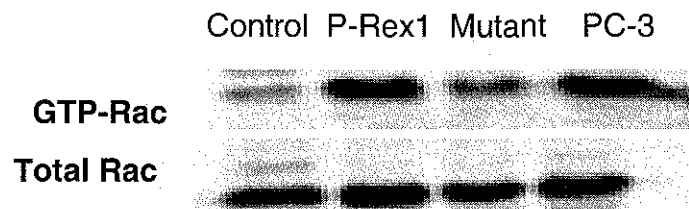


Figure 23. P-Rex1 activates Rac in prostate cancer cells. The amount of activated GTP-bound Rac was quantified by PAK-1-PBD-conjugated agarose pull-down assay as described in the Materials and Methods. The precipitated active Rac was analyzed by immunoblotting with anti-Rac antibody (top panel). The immunoblot of the cell lysates (bottom panel) was used as an index of the total Rac for the pull-down assay.

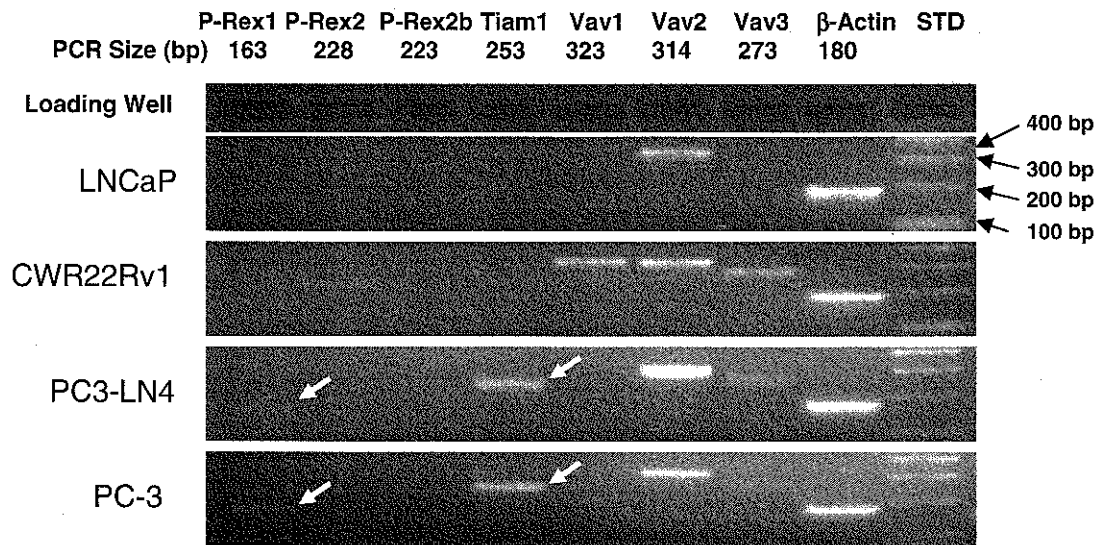


Figure 24. Analysis of GEF mRNA expression in human prostate cell lines. Total RNA was isolated from cultures of four prostate cancer cell lines (LNCaP, CWR22Rv1, PC3-LN4 and PC-3), followed by conventional RT-PCR (25 cycles of 94°C for 30 seconds, 55°C for 30 seconds, 72°C for 30 seconds). PCR products were subjected to 3% agarose gel electrophoresis and visualized by staining with ethidium bromide. House-keeping gene β -actin was used as an internal control. White arrow: bands of P-Rex1 and Tiam1. STD: standard.

CHAPTER III

EFFECTS OF P-REX1 IN PROSTATE TUMOR GROWTH AND METASTASIS IN VIVO

A. INTRODUCTION

We previously demonstrated that P-Rex1 was elevated in metastatic prostate cancer cells and human clinical tissues. Alteration of P-Rex1 expression was positively correlated with cell migration in prostate cancer cell models. Cell models are useful research tools for testing of genes of interest in vitro, but after all they are simplified systems and may not display real features of more complicated biological systems. Animal models have been widely used in the translational and preclinical research phases of new drug discovery and development. Therefore, we next performed in vivo studies to examine the role of P-Rex1 in prostate cancer growth and metastatic progression.

In order to carry out in vivo studies, CWR22Rv1 stable cell lines were established and PC3-LN4 has enhanced metastatic potential and then was chosen as positive cell model. Since P-Rex1 is a Rac GEF and Rac may have other functions than being a regulator of cell migration, we first examined the effect of P-Rex1 on prostate tumor growth by injecting prostate cancer cells with varying P-Rex1 expression subcutaneously into nude mice. For the in vivo metastasis testing, we used the orthotopic mouse model in which prostate cancer cell were injected directly into mouse prostates.

We compared tumor growth kinetics and prostate spontaneous lymph node metastases of stable CWR22Rv1 cell lines expressing empty vector, P-Rex1 or P-Rex1

mutant lacking GEF function. We provided the first evidence that P-Rex1 can promote prostate cancer metastasis in vivo.

B. MATERIALS AND METHODS

Subcutaneous injection of prostate tumor cells. These *in vivo* experiments were performed in accordance with protocols approved by the Creighton University Institutional Animal Care and Use Committee. A stable CWR22Rv1 cell suspension (1×10^6 cells in 200 μ l of 1:1 culture medium and Matrigel) was injected subcutaneously into the dorsal surfaces of male athymic Nu/Nu-Foxn1 mice (Charles River, Wilmington, MA, five mice per group). Tumor growth was monitored once a week and tumor volume (V) was estimated from the volume formula for an ellipsoid: $V = 0.5236 \times \text{length} \times \text{width} \times \text{height}$ (Fizazi et al. 2002).

Orthotopic injection of prostate tumor cells. Orthotopic injections of tumor cells were performed as described elsewhere (Kovar et al. 2006). Briefly, the left anterior prostate of male NOD/SCID mice (Charles River) was exteriorized through a small suprapubic abdominal incision and injected with 50,000 CWR22Rv1 cells or PC3-LN4 cells in 15 μ l growth media. After returning the abdominal contents, wounds were sutured and the mice were checked at least once per week for 9 weeks. At the endpoint, abdominal cavities of mice were opened to remove the primary prostate tumors and then dissected to examine tumor metastases into the para-aortic lymph nodes.

C. RESULTS

P-Rex1 does not affect prostate tumor growth We tested the effect of P-Rex1 expression on prostate tumor growth *in vivo*. CWR22Rv1 control cells or cells stably expressing wild-type P-Rex1 or the P-Rex1 “GEF dead” mutant were subcutaneously injected into nude mice, and tumor volumes were measured once a week. PC3-LN4 was used as a positive control. **Figure 25** showed representative CWR22Rv1 tumor formation and growth over the five-week experiment period. At week 1 no macroscopic tumor was found. Tumors were detected beginning week 2 and continued to grow in the rest of studies. However, there was no statistical difference in the growth rate of the subcutaneous tumors among the groups (**Figure 26**), suggesting that P-Rex1 does not have a direct impact on prostate tumor growth.

P-Rex1 induces spontaneous lymph node metastasis in mouse models. We therefore used a well-characterized orthotopic model to determine the role of P-Rex1 in the prostate cancer spontaneous metastasis to lymph nodes. The CWR22Rv1 stable transfectants were orthotopically implanted into prostate of immunodeficient male NOD/SCID mice. The highly metastatic PC3-LN4 cell line was used as a positive control. Animals were tracked through a 9-week period and then dissected to expose the primary tumors and lymph nodes at the endpoint. All mice bore primary prostate tumors and there were no significant difference in size of these tumors among three CWR22Rv1 groups. However, as shown in the **Figure 27**, all mice in the PC3-LN4 positive control group showed macroscopic lymph node metastases. There was no visible metastasis detected in any mice bearing tumors derived from CWR22Rv1 cancer cells expressing either vector or P-Rex1 “GEF-dead” mutant. In contrast, expression of wild-type P-Rex1 in CWR22Rv1 cells significantly increased the incidence of lymph node metastasis (3 out of 5 mice). To further evaluate and confirm tumor growth and metastasis, formalin-

fixed mouse prostate and lymph node tissues were routinely embedded, sectioned, and stained with hematoxylin and eosin using standard techniques for microscopic examination. As shown in **Figure 28**, histopathology of the prostates from both CWR22Rv1 P-Rex1 and PC3-LN4 groups showed the prostate glands were almost replaced by tumor cells (PC3-LN4 cells are larger than CWR22Rv1 cells) and few glandular structures of epithelial cells were observed. Interestingly, we found widespread infiltration of tumor cells in lymph node metastases. The majority area of lymph nodes analyzed was occupied by tumor cells. These findings clearly demonstrate that P-Rex1 promotes spontaneous prostate cancer metastasis in vivo.

D. DISCUSSION

There are some methods which may closely mimic that observed in vivo, such as three-dimensional matrices. However, understanding the process of metastasis in animals can provide tremendous insight into the mechanisms in real biological systems. Mice have provided a powerful model for cancer in a mammalian system. This has allowed us to define signal transduction pathways and identify potential molecular targets. In our work, traditional xenograft mouse models have been used to study potential roles of P-Rex1 in prostate cancer progression. In these models, primary or genetically cell lines derived from primary tumors were incorporated into immunodeficient mice. Nu/Nu-Foxn1 mouse model is athymic and T-cell deficient, whereas NOD/SCID mice have impaired T and B cell lymphocyte function as well as lacking NK function and the ability to stimulate complement activity. These features will allow the engraftment of human tumor cells in mice.

Subcutaneous and orthotopic mice models are two commonly used in vivo models. There has been a debate on the utility of subcutaneous tumor models versus orthotopic models. Generally speaking, subcutaneous models seem to be more suitable for tumor growth testing, because it is easier to monitor and measure formed tumors in a relatively shorter time after injection. On the other hand, orthotopic models show some advantages over subcutaneous models for tumor metastatic studies. This method preserves the relevant tumor microenvironment and may give rise of to spontaneous metastases, which mimics the whole process of metastasis event, including local invasion, survival and colony formation.

In our studies, CWR22Rv1 stable cell lines were compared for tumorigenic and grow potential in subcutaneous injections. No statistic differences were found in growth

rates of these tumor cells, although they vary in P-Rex1 or its mutant expressions. This result suggested that P-Rex1 did not influence prostate cancer cell growth. It is reported that Rho family proteins could play many roles in biological events, including migration, invasion, cell cycle, growth and survival [reviewed by Ridley, 2004]. P-Rex1 can activate Rac, a member of Rho family. We did not see an effect of P-Rex1 on prostate tumor growth and it may be because Rho-mediated events are cell or tissue specific.

In our *in vivo* metastasis testing, same cell lines used in subcutaneous models were implanted into mouse prostates respectively by doing surgery. None of mice injected with CWR22Rv1 control cells developed spontaneous lymph node metastases, whereas metastases were detected in all positive controls. Kovar et al. reported the same results as our control groups previously (Kovar et al. 2006). Consistent with *in vitro* observations, expression of P-Rex1, but not its “GEF-dead” mutant, significantly promoted CWR22Rv1 tumor metastases. Taken together, P-Rex1 not only enhanced prostate cancer cell migration and invasion *in vitro*, but also promoted prostate tumor metastasis *in vivo*.

While our data suggest a functional role of upregulated P-Rex1 in prostate cancer metastatic progression both *in vitro* and *in vivo*, further research is required to explore how P-Rex1 is involved in this process in greater detail. Metastasis is complex multiple-step cascade, including primary tumor growth, detachment/local invasion, survival in the circulation, arrest in organs, extravasation and progressive outgrowth within distant organs (Fidler 2002). Each of these major steps can be rate limiting. Based on our results, it is likely P-Rex1 is a motility-related gene and can facilitate some steps of metastasis such as local invasion of some tumor cells into the host stroma, intravasation and extravasation, because directed cell migration is required in these steps. It is interesting to note that directed cell migration is critical for both cancer metastasis and inflammation responses and P-Rex1 represents about 65% of the total Rac GEF activity

in neutrophils. Thus, in cancer cells P-Rex1 probably adapted mechanisms similar to those operated by inflammatory cells. As a multigene phenomenon, the outcome of metastasis largely depends on the context of the cancer cells and the particular extracellular milieu. P-Rex1 appears to be just one of factors that can influence the process. It is not clear if P-Rex1 plays roles other than enhancing directed cell migration. There are many other factors involved in the metastasis cascade. For example, loss or downregulation of metastasis suppressor genes such as KAI-1, CD44 and NM23 may contribute to the prostate cancer metastatic progression (Karayi and Markham 2004). Integrins-mediated tumor cell-extracellular matrix interactions are important for the development of metastasis (Steeg 2006). Moreover, the biological heterogeneity of tumor cells is one of main barriers to treatment of metastasis. Specific pathways may be limited to a subset of tumor cell types. Thus, further understanding of the P-Rex1-mediated pathway in cancer metastasis is still desired.

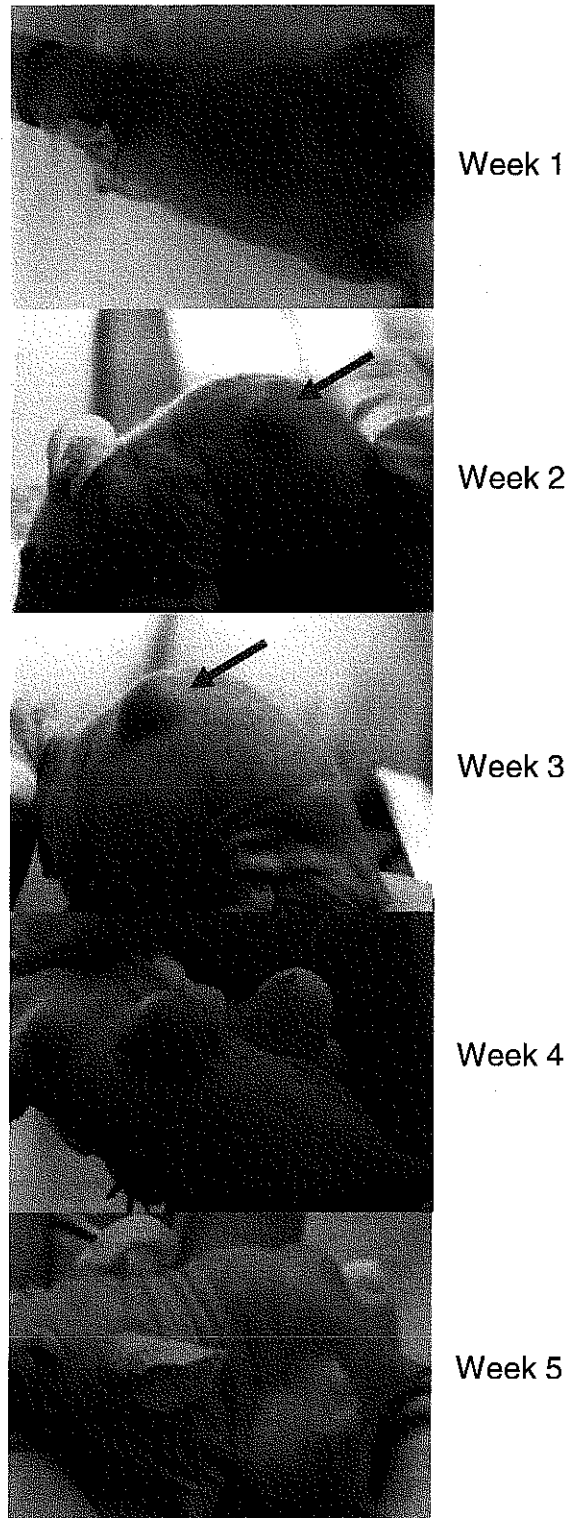


Figure 25. Representative tumor formation and growth (red arrow) that results from subcutaneous injection of CWR22Rv1 cells into nude mice.

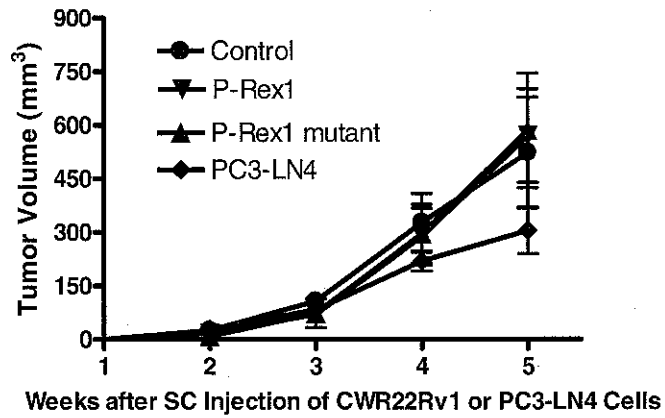
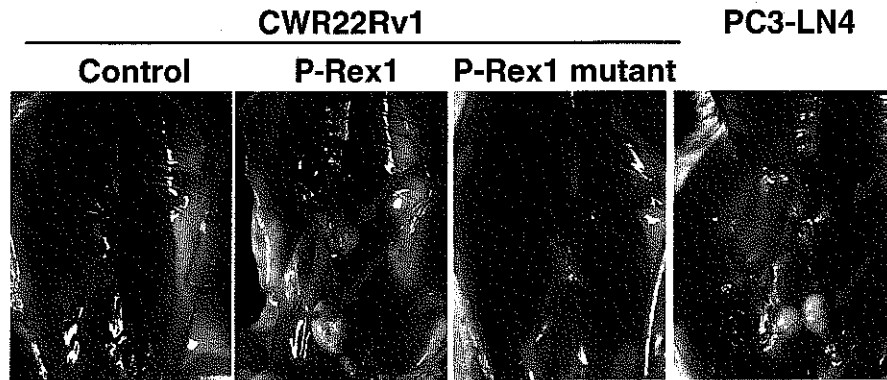


Figure 26. CWR22Rv1 cells (1×10^6) stably expressing either wild-type P-Rex1, P-Rex1 “GEF-dead” mutant, vector or positive control PC3-LN4 cells were injected subcutaneously (SC) into Nu/Nu mice (five mice per group). Tumor growth was monitored once per week for 5 weeks. One way ANOVA analysis indicates no statistical differences in tumor growth among the three groups.



Incidence of Metastasis	
CWR22Rv1 Control	0/5
CWR22Rv1 P-Rex1	3/5
CWR22Rv1 P-Rex1 mutant	0/5
PC3-LN4	5/5

Figure 27. Intraprostatic injection of CWR22Rv1 cells or PC3-LN4 cells into male NOD/SCID mice (50,000 cells in 15 μ l culture medium/mouse) as described in the Materials and Methods. Nine weeks post injection, mice were sacrificed to examine spontaneous metastases (green arrow) of prostate tumor into lymph nodes. The incidence of spontaneous metastasis in each group is shown in the table.

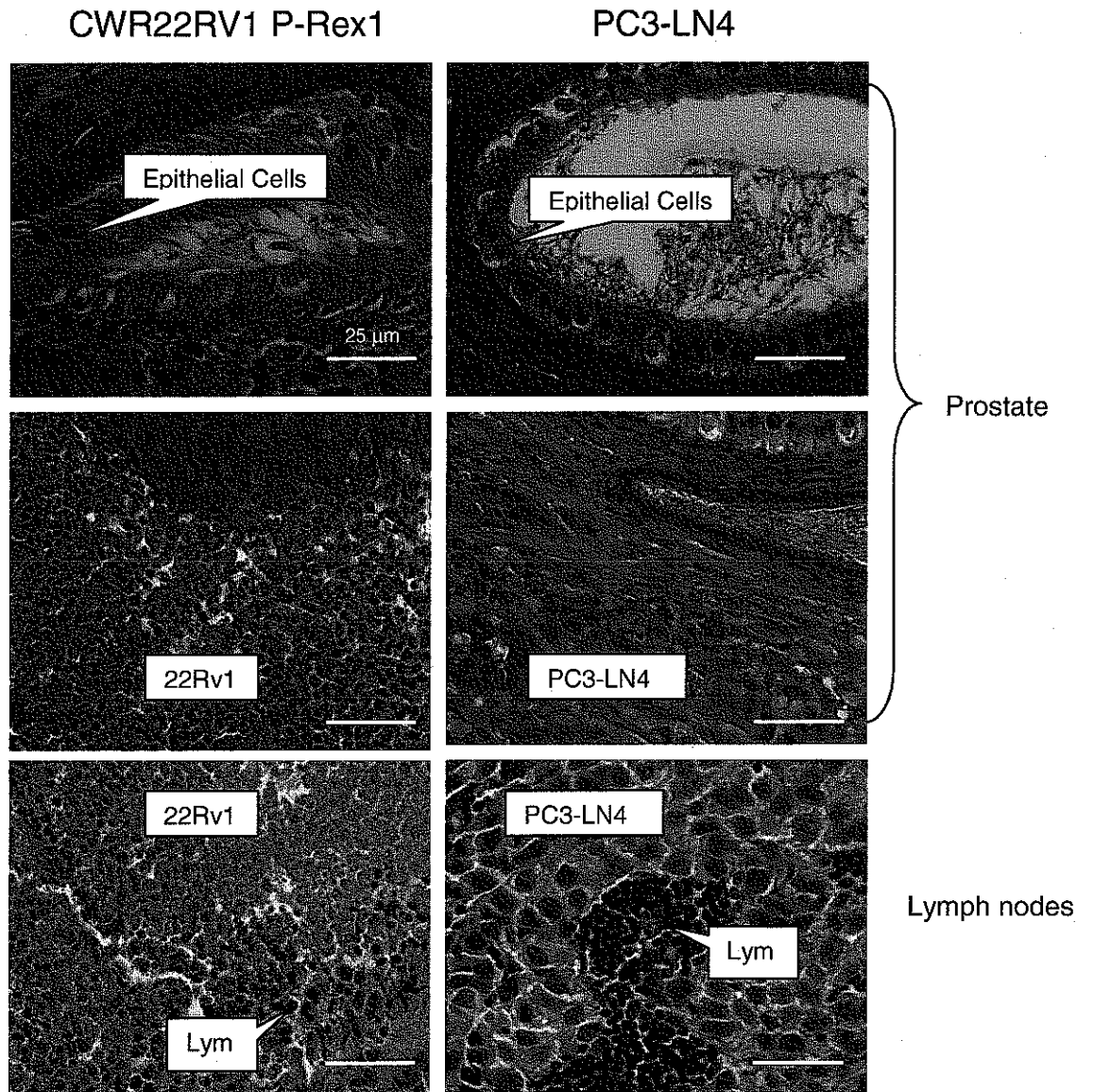


Figure 28. Representative histopathology (H&E staining) of primary tumors and lymph node metastases of CWR22Rv1 P-Rex1 cells and PC3-LN4 cells. Lym: lymphatic cells.

CHAPTER IV

SUMMARY AND CONCLUSIONS

The aim of our study was to investigate the role of P-Rex1 in prostate cancer migration, invasion and metastasis. The first major objective of our study was to assess the biological importance of P-Rex1 in prostate cancer. Different prostate cell lines were cultured, harvested and then RNA was extracted for both conventional RT-PCR and real-time PCR. It was found that P-Rex1 gene expression is significantly elevated in metastatic prostate cancer cells, but very low or undetectable in normal prostate cells or nonmetastatic prostate cancer cells. To see if P-Rex1 protein expression is consistent with its gene expression, we did both western blot and immunofluorescence staining and, as expected, there was higher P-Rex1 protein expression in more aggressive prostate cancer cells. More importantly, the transwell migration assay shows prostate cancer cell migration is positively correlated with its P-Rex1 expression. To determine whether the findings in cell lines that P-Rex1 expression is upregulated in metastatic prostate cancer cells extend to clinical human tissues, we collaborated with the Department of Pathology, Creighton University, to carry out immunohistochemical analysis of P-Rex1 protein expression in specimens from prostate cancer patients, including primary tumor and lymph node metastasis samples. Our data revealed that P-Rex1 level was slightly increased in noncancerous prostate tissues and much more significantly elevated in lymph node prostate metastases. These results suggested that P-Rex1 may be involved in and play an important role in prostate cancer metastasis, probably by promoting cell migration and invasion.

Next, we investigated what potential biological function P-Rex1 may have in prostate cancer cell migration. RNAi technology has been commonly used to knock down genes of interest. In our studies, knock-down of endogenous P-Rex1 using siRNA reduced prostate cancer cell migration. We also showed that this process was Rac-dependent. Transient expression of P-Rex1 by transfection in prostate cancer cells increased their migration. Taken together, manipulation of P-Rex1 expression positively affects prostate cancer cell migration. In addition, our data indicated the DH domain of P-Rex1 was critical for its GEF function.

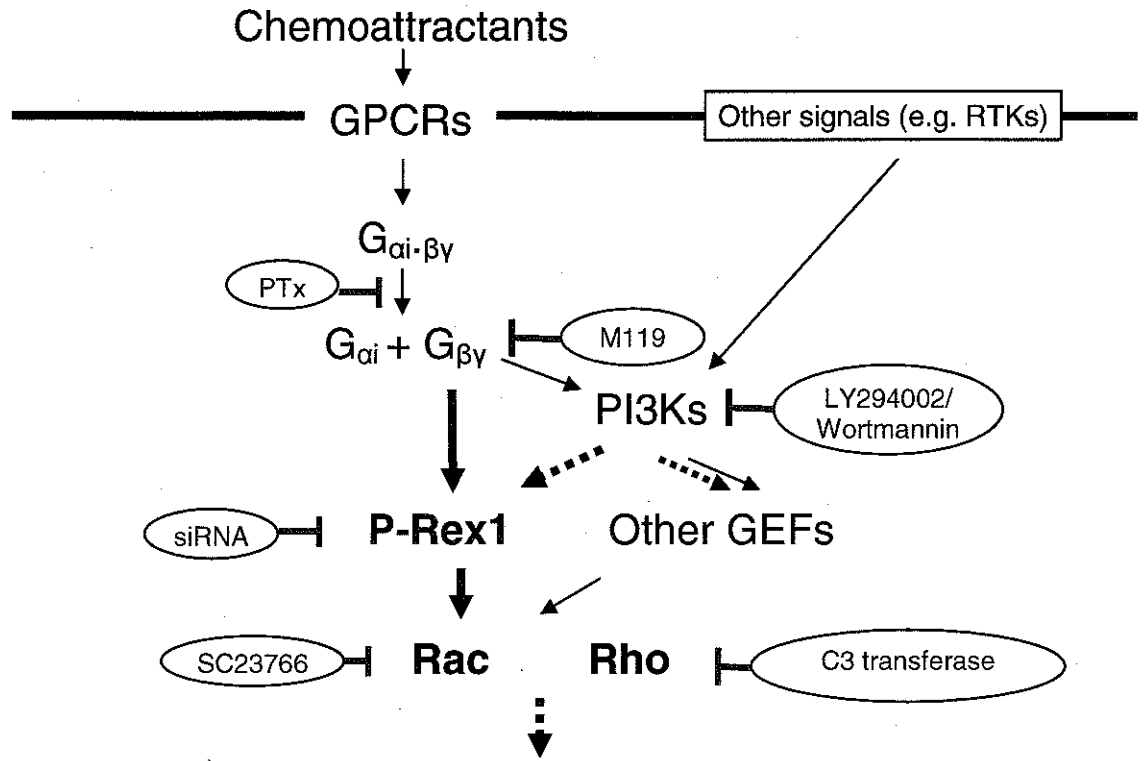
The second major objective of our study was to investigate the molecular mechanisms underlying P-Rex1-mediated prostate cancer cell migration and invasion. Sufficient evidence shows small Rho GTPases are important regulators of cell migration. Therefore, we first examined involvement of small GTPases Rac and Rho in prostate cancer cell migration. As expected, both Rac and Rho play a significant role in this important biological event. Our inhibition experiments also suggested that G_i protein, Gβγ subunits and PI3Ks are involved in prostate cancer cell migration. All these results obtained from prostate cancer cell models are consistent with data previously published by other research groups. P-Rex1 was discovered as a Rac specific activator. However, none of past P-Rex1-related studies has been performed on cancer cells. To determine whether P-Rex1 promotes prostate cancer cell migration and invasion via Rac activation, we established CWR22Rv1 cell lines stably expressing vector, full-length P-Rex1 or P-Rex1 “GEF-dead” mutant. Once again, expression of P-Rex1 enhanced prostate cancer cell migration. More importantly, P-Rex1 also promoted CWR22Rv1 cell invasion, which is another critical step in tumor metastasis. In our studies, Rac activation by P-Rex1 in

prostate cancer cell models were demonstrated either indirectly through observation of lamellipodia formation and cortactin subcellular translocation, or directly by the Rac pull-down assay which determines the amount of activated Rac. This series of in vitro experiments using prostate cell models suggested that P-Rex1 can activate Rac and promote prostate cancer cell migration and invasion.

Finally, in vivo studies using mouse models were performed to determine effect of P-Rex on tumor growth and spontaneous metastasis to lymph nodes. The subcutaneous injection mouse model showed P-Rex1 did not affect prostate tumor formation and growth rate. However, we found that expression of P-Rex significantly promoted prostate cancer spontaneous metastasis to lymph nodes in an intraprostatic injection mouse model. This in vivo metastasis study further verified our in vitro finding that P-Rex1 was involved in prostate cancer migration and invasion.

In summary, our data are consistent with the model depicted in **Figure 29** showing chemotactic factor-stimulated G_i -coupled GPCR induced dissociation of $G\beta\gamma$ from $G\alpha$. Free $G\beta\gamma$ (inhibited by M119) can activate P-Rex1 directly or indirectly through a PI3K-dependent pathway (inhibited by LY294002 and Wortmannin). Synergistic activation of P-Rex1 by $G\beta\gamma$ and PIP3 causes hyperactivation of Rac (inhibited by NSC23766), which drives prostate cancer cell migration. In addition, PTx can attenuate activation of G_i -protein, thus blocking prostate cancer cell migration. Evidence is presented that P-Rex1 plays an important role in prostate cancer metastasis in vivo. The pathway(s) leading to Rac activation in prostate cancer cells offer possible targets for intervention (Sun et al. 2006), and the important effects of P-Rex1 documented here make it one of those targets. P-Rex1 was postulated to function as a coincidence detector of signaling for cell migration (Welch et al. 2002). Also, the Rac GTPase acts as a node of signaling

convergence and divergence for outside-in signaling transmission. We have not been able to identify individual membrane receptor systems that play considerable roles in P-Rex1 activation signals. It is most likely that diverse extracellular stimuli that not only recognize GPCRs, but also other receptors like receptor tyrosine kinase (RTK), tyrosine kinase associated receptors, integrins ($\alpha\beta$ heterodimers), and other cell surface receptors contribute to prostate cancer progression (Mimeault et al. 2006, Karnoub et al. 2004). By functioning as a molecule that integrates separate inputs from GPCRs and receptor tyrosine kinases or adhesion molecules simultaneously activated in the local microenvironment, P-Rex1 could also help control the direction of prostate cancer cell movement.



Prostate cancer cell migration, invasion and metastasis

Figure 29. A proposed model for the regulation of P-Rex1-mediated prostate cancer metastasis through Gi-coupled receptor signaling pathway. Chemoattractants bind to G protein-coupled receptors (GPCRs) of prostate tumor cells and then trigger G proteins to activate a signaling cascade that causes chemotaxis (stimulated, directed cell migration). Up-regulated P-Rex1-mediated signal transduction plays an important role in prostate cancer cell migration, invasion and metastasis because P-Rex1 is a unique and efficient Rac activator. P-Rex1 can be activated not only by PI3Ks (like many other Rho family GEFs) but also by G $\beta\gamma$ subunit directly. PI3Ks can also be activated by other signals like receptor tyrosin kinases (RTKs) (solid line: direct interaction; dashed line: indirect interaction). Inhibitors of this signal pathways can attenuate directed prostate cancer cell migration.

REFERENCES

Adam, L., Vadlamudi, R.K., McCrea, P., and Kumar, R. Tiam1 overexpression potentiates heregulin-induced lymphoid enhancer factor-1/beta -catenin nuclear signaling in breast cancer cells by modulating the intercellular stability. *J Biol Chem.* 2001;276:28443-28450

Albini, A., Iwamoto, Y., Kleinman, H.K., Martin, G.R., Aaronson, S.A., Kozlowski, J.M., McEwan, R.N. A rapid in vitro assay for quantitating the invasive potential of tumor cells. *Cancer Res.* 1987 Jun 15;47(12):3239-45.

Applied Biosystems Reference. Creating Standard Curves with Genomic DNA or Plasmid DNA Templates for Use in Quantitative PCR. 2003; http://www.appliedbiosystems.com/support/tutorials/pdf/quant_pcr.pdf

Aurich-Costa, J., Vannier, A., Gregoire, E., Nowak, F., and Cherif, D. IPM-FISH, a new M-FISH approach using IRS-PCR painting probes: application to the analysis of seven human prostate cell lines. *Genes Chromosomes Cancer* 2001;30:143-160.

Barber, M. A. and Welch, H. C. PI3K and RAC signalling in leukocyte and cancer cell migration. *Bull Cancer* 2006;93:E44-E52.

Bex, A., Lummen, G., Rembrink, K., Otto, T., Metz, K., and Rubben, H. Influence of pertussis toxine on local progression and metastasis after orthotopic implantation of the

human prostate cancer cell line PC3 in nude mice. *Prostate Cancer Prostatic Dis* 1999;2:36-40.

Bonacci, T. M., Mathews, J. L., Yuan, C., Lehmann, D. M., Malik, S., Wu, D., Font, J. L., Bidlack, J. M., and Smrcka, A. V. Differential targeting of Gbetagamma-subunit signaling with small molecules. *Science* 2006;312:443-446.

Braga, V. Epithelial cell shape: cadherins and small GTPases. *Exp Cell Res* 2000;261:83-90.

Brock, C., Schaefer, M., Reusch, H. P., Czupalla, C., Michalke, M., Spicher, K., Schultz, G., and Nurnberg, B. Roles of G beta gamma in membrane recruitment and activation of p110 gamma/p101 phosphoinositide 3-kinase gamma. *J Cell Biol* 2003;160:89-99.

Cao, J., Chiarelli, C., Kozarekar, P. and Adler, H.L. Membrane type I-matrix metalloproteinase promotes human prostate cancer invasion and metastasis. *Thromb Haemost.* 2005;93:770-778.

Carroll, P.R. and Grossfeld, G.D. *Prostate Cancer*. BC Decker Inc. (London). 2002;Page 1 & 317.

Chan, A.Y., Coniglio, S.J., Chuang, Y.Y., Michaelson, D., Knaus, U.G., Philips, M.R. and Symons, M. Roles of the Rac1 and Rac3 GTPases in human tumor cell invasion. *Oncogene* 2005; 24:7821-7829.

Chay, C.H., Cooper, C.R., Gendernalik, J.D., Dhanasekaran, S.M., Chinnaiyan, A.M., Rubin, M.A., Schmaier, A.H. and Pienta, K.J. A functional thrombin receptor (APR1) is expressed on bone-derived prostate cancer cell lines. *Urology*. 2002;60:760-765.

Cooper, C.R., Chay, C.H., Gendernalik, J.D., Lee, H.L., Bhatia, J., Taichman, R.S., McCauley, L.K., Keller, E.T. and Pienta, K.J. Stromal factors involved in prostate carcinoma metastasis to bone. *Cancer Supplement*. 2003;97:739-747.

Daaka, Y. G proteins in cancer: the prostate cancer paradigm. *Sci. STKE* 2004, re2.

Daja, M.M., Xiu, X., Zhao, Z., Brown, J.M. and Russell, P.J. Characterization of expression of matrix metalloproteinases and tissue inhibitors of metalloproteinases in prostate cancer cell lines. *Prostate Cancer and Prostatic Diseases*. 2003;6:15-26.

Donald, S., Hill, K., Lecureuil, C., Barnouin, R., Krugmann, S., John Coadwell, W., Andrews, S.R., Walker, S.A., Hawkins, P.T., Stephens, L.R., and Welch, H.C. P-Rex2, a new guanine-nucleotide exchange factor for Rac. *FEBS Lett*. 2004;572:172-6.

Dorsam, R. T. and Gutkind, J. S. G-protein-coupled receptors and cancer. *Nat Rev Cancer* 2007;7:79-94.

Edwards, S.W., Tan, C.M. and Limbird, L.E. Localization of G protein-coupled receptors in health and disease. *Trends in Pharmacological Sciences*. 2000;21:304-308.

Ellenbroek, S. I. and Collard, J. G. Rho GTPases: functions and association with cancer. *Clin Exp Metastasis* 2007;24:657-672.

Engers, R., Mueller, M., Walter, A., Collard, J.G., Willers, R., and Gabbert, H.E. Prognostic relevance of Tiam1 protein expression in prostate carcinomas. *Br J Cancer* 2006;95:1081-1086

Fidler, I. The pathogenesis of cancer metastasis: the "seed and soil" hypothesis revisited. *Nature Reviews: cancer* 2002;3:1-6.

Fizazi, K., Martinez, L. A., Sikes, C. R., Johnston, D. A., Stephens, L. C., McDonnell, T. J., Logothetis, C. J., Trapman, J., Pisters, L. L., Ordonez, N. G., Troncoso, P., and Navone, N. M. The association of p21((WAF-1/CIP1)) with progression to androgen-independent prostate cancer. *Clin Cancer Res* 2002;8:775-781.

Gao, X., Mohsin, S. K., Gatalica, Z., Fu, G., Sharma, P., and Nawaz, Z. Decreased expression of e6-associated protein in breast and prostate carcinomas. *Endocrinology* 2005;146:1707-1712.

Gao, Y., Dickerson, J. B., Guo, F., Zheng, J., and Zheng, Y. Rational design and characterization of a Rac GTPase-specific small molecule inhibitor. *Proc Natl Acad Sci U S A* 2004;101:7618-7623.

Guan, J. *Cell migration: Development methods and protocols*. 2005;Humana Press, Totowa, New Jersey.

Gupta, G. P. and Massague, J. Cancer metastasis: building a framework. *Cell* 2006;127:679-695.

Habets, G.G., Scholtes, E.H., Zuydgeest, D., van der Kammen, R.A., Stam, J.C., Berns, A., and Collard. J.G. Identification of an invasion-inducing gene, Tiam-1, that encodes a protein with homology to GDP-GTP exchangers for Rho-like proteins. *Cell* 1994;77:537-549.

Habets, G.G., van der Kammen, R.A., Stam, J.C., Michiels, F., and Collard. J.G. Sequence of the human invasion-inducing TIAM1 gene, its conservation in evolution and its expression in tumor cell lines of different tissue origin. *Oncogene* 1995;10:1371-1376.

Hall, A. Rho GTPase and the actin cytoskeleton. *Science* 1998;279:509-514

Hall, A. Rho GTPases and the control of cell behaviour. *Biochem Soc Trans* 2005;33:891-895.

Hart, M.J., Eva, A., Evans, T., Aaronson, S.A., and Cerione, R.A. Catalysis of guanine nucleotide exchange on the CDC42Hs protein by the *dbl* oncogene product. *Nature* 1991;354:311-314.

Hill, K., Krugmann, S., Andrews, S. R., Coadwell, W. J., Finan, P., Welch, H. C., Hawkins, P. T., and Stephens, L. R. Regulation of P-Rex1 by phosphatidylinositol (3,4,5)-trisphosphate and Gbetagamma subunits. *J Biol Chem* 2005;280:4166-4173.

Jemal, A., Siegel, R., Ward, E., Hao, Y., Xu, J., Murray, T., and Thun, M. J. Cancer statistics, 2008. *CA Cancer J Clin* 2008;58:71-96.

Karayi, M.K., and Markham, A.F. Molecular biology of prostate cancer. *Prostate cancer and prostatic diseases* 2004;7:6-20.

Karnoub, A., Symons, M., Campbell, S.L. and Der, C.J. Molecular basis for Rho GTPase signaling specificity. *Breast Cancer research and Treatment* 2004;84:61-71.

Knight-Krajewski, S., Welsh, C. F., Liu, Y., Lyons, L. S., Faysal, J. M., Yang, E. S., and Burnstein, K. L. Deregulation of the Rho GTPase, Rac1, suppresses cyclin-dependent kinase inhibitor p21(CIP1) levels in androgen-independent human prostate cancer cells. *Oncogene* 2004;23:5513-5522.

Kovar, J. L., Johnson, M. A., Volcheck, W. M., Chen, J., and Simpson, M. A. Hyaluronidase expression induces prostate tumor metastasis in an orthotopic mouse model. *Am J Pathol* 2006;169:1415-1426.

Li, S.Y., Huang, S.G., and Peng, S.B. Overexpression of G protein-coupled receptors in cancer cells: Involvement in tumor progression. *International Journal of Oncology*. 2005;27:1329-1339.

Li, Y., Uruno, T., Haudenschild, C., Dudek, S. M., Garcia, J. G., and Zhan, X. Interaction of cortactin and Arp2/3 complex is required for sphingosine-1-phosphate-induced endothelial cell remodeling. *Exp Cell Res* 2004;298:107-121.

Liu, L., Zhang, Q., Zhang, Y., Wang, S., and Ding, Y. Lentivirus-mediated silencing of Tiam1 gene influences multiple functions of a human colorectal cancer cell line. *Neoplasia* 2006;8:917-24.

Malliri, A., van der Kammen, R.A., Clark, K., van der Valk, M., Michiels, F., and Collard, J.G. Mice deficient in the Rac activator Tiam1 are resistant to Ras-induced skin tumours. *Nature* 2002;417:867-871.

Mimeault, M. and Batra, S. K. Recent advances on multiple tumorigenic cascades involved in prostatic cancer progression and targeting therapies. *Carcinogenesis* 2006;27:1-22.

Minard, M.E., Kim, L.S., Price, J.E., and Gallick, G.E. The role of the guanine nucleotide exchange factor Tiam1 in cellular migration, invasion, adhesion and tumor progression. *Breast Cancer Research and Treatment* 2004;84:21-32.

Minard, M.E., Ellis, L.M., and Gallick, G.E. Tiam1 regulates cell adhesion, migration and apoptosis in colon tumor cells. *Clin Exp Metastasis* 2006;23:301-313.

Mundy, G. R. Metastasis to bone: causes, consequences and therapeutic opportunities. *Nat Rev Cancer* 2002;2:584-593.

Murphy, P.M. Chemokines and the molecular basis of cancer metastasis. *N Engl J Med.* 2001;345:833-835.

Nobes, C. D. and Hall, A. Rho, rac, and cdc42 GTPases regulate the assembly of multimolecular focal complexes associated with actin stress fibers, lamellipodia, and filopodia. *Cell* 1995;81:53-62.

Ridley, A. J., Schwartz, M. A., Burridge, K., Firtel, R. A., Ginsberg, M. H., Borisy, G., Parsons, J. T., and Horwitz, A. R. Cell migration: integrating signals from front to back. *Science* 2003;302:1704-1709.

Rosenfeldt, H., Vázquez-Prado, J., and Gutkind, J.S. P-REX2, a novel PI-3-kinase sensitive Rac exchange factor. *FEBS Lett.* 2004;572:167-71.

Rossman, K.L., Der, C.J., and Sondek, J. GEF means go: turning on Rho GTPases with guanine nucleotide-exchange factors. *Nature reviews: Molecular Cell Biology* 2005;6:167-180.

Singh, R. N., Nakano, T., Xuing, L., Kang, J., Nedergaard, M., and Goldman, S. A. Enhancer-specified GFP-based FACS purification of human spinal motor neurons from embryonic stem cells. *Exp Neurol* 2005;196:224-234.

Sobel, R. E. and Sadar, M. D. Cell lines used in prostate cancer research: a compendium of old and new lines--part 2. *J Urol* 2005;173:360-372.

Steeg, P.S. Metastasis suppressors alter the signal transduction of cancer cells. *Nat Rev Cancer* 2002;3:55-63.

Steeg, P.S. Tumor metastasis: mechanistic insights and clinical challenges. *Nat Med* 2006;12:895-904.

Strefford, J. C., Lillington, D. M., Young, B. D., and Oliver, R. T. The use of multicolor fluorescence technologies in the characterization of prostate carcinoma cell lines: a

comparison of multiplex fluorescence in situ hybridization and spectral karyotyping data. *Cancer Genet Cytogenet* 2001;124:112-121.

Sun, Y.X., Schneider, A., Jung, Y.H., Wang, J.H., Dai, J.L., Wang, J.C., Cook, K., Osman, N.I., Koh-Paige, A.J., Shim, H., Pienta, K.J., Keller, E.T., McCauley, L.K. and Taichman, R.S. Skeletal localization and neutralization of the SDF-1(CXCL12)/CXCR4 axis blocks prostate cancer metastasis and growth in osseous sites in vivo. *Journal of Bone and Mineral Research*. 2005;20:318-329.

Sun, D., Xu, D., and Zhang, B. Rac signaling in tumorigenesis and as target for anticancer drug development. *Drug Resist Updat* 2006;9:274-287.

Vaday, G.G., Peehl, D.M., Kadam, P.A. and Lawrence, D.M. Expression of CCL5 (RANTES) and CCR5 in prostate cancer. *The Prostate*. 2005;66:124-134.

Vivanco, I. and Sawyers, C. L. The phosphatidylinositol 3-Kinase AKT pathway in human cancer. *Nat Rev Cancer* 2002;2:489-501.

Weiner, O. D. Rac activation: P-Rex1 - a convergence point for PIP(3) and Gbetagamma? *Curr Biol* 2002;12:R429-R431.

Welch, H. C., Coadwell, W. J., Ellson, C. D., Ferguson, G. J., Andrews, S. R., Erdjument-Bromage, H., Tempst, P., Hawkins, P. T., and Stephens, L. R. P-Rex1, a PtdIns(3,4,5)P3- and Gbetagamma-regulated guanine-nucleotide exchange factor for Rac. *Cell* 2002;108:809-821.

Welch, H. C., Condliffe, A. M., Milne, L. J., Ferguson, G. J., Hill, K., Webb, L. M., Okkenhaug, K., Coadwell, W. J., Andrews, S. R., Thelen, M., Jones, G. E., Hawkins, P. T., and Stephens, L. R. P-Rex1 regulates neutrophil function. *Curr Biol* 2005;15:1867-1873.

Yamazaki, D., Kurisu, S., and Takenawa, T. Regulation of cancer cell motility through actin reorganization. *Cancer Sci* 2005;96:379-386.

Yoshizawa, M., Kawauchi, T., Sone, M., Nishimura, Y. V., Terao, M., Chihama, K., Nabeshima, Y., and Hoshino, M. Involvement of a Rac activator, P-Rex1, in neurotrophin-derived signaling and neuronal migration. *J Neurosci* 2005;25:4406-4419.

APPENDIX

X Cao, *J Qin, Y Xie, O Khan, F Dowd, M Scofield, M-F Lin, Y Tu. Regulator of G-protein Signaling 2 (RGS2) inhibits androgen-independent activation of androgen receptor in prostate cancer cell. *Oncogene* 2006; 25:3719-34. (*co-first author)

ORIGINAL ARTICLE

Regulator of G-protein signaling 2 (RGS2) inhibits androgen-independent activation of androgen receptor in prostate cancer cells

X Cao^{1,3}, J Qin^{1,3}, Y Xie¹, O Khan¹, F Dowd¹, M Scofield¹, M-F Lin² and Y Tu¹

¹Department of Pharmacology, Creighton University School of Medicine, Omaha, NE, USA and ²Department of Biochemistry and Molecular Biology, University of Nebraska Medical Center, Omaha, NE, USA

Hormones acting through G protein-coupled receptors (GPCRs) can cause androgen-independent activation of androgen receptor (AR) in prostate cancer cells. Regulators of G-protein signaling (RGS) proteins, through their GTPase activating protein (GAP) activities, inhibit GPCR-mediated signaling by inactivating G proteins. Here, we identified RGS2 as a gene specifically down-regulated in androgen-independent prostate cancer cells. Expression of RGS2, but not other RGS proteins, abolished androgen-independent AR activity in androgen-independent LNCaP cells and CWR22Rv1 cells. In LNCaP cells, RGS2 inhibited G_q-coupled GPCR signaling. Expression of exogenous wild-type RGS2, but not its GAP-deficient mutant, significantly reduced AR activation by constitutively activated G_qQ209L mutant whereas silencing endogenous RGS2 by siRNA enhanced G_qQ209L-stimulated AR activity. RGS2 had no effect on RGS-insensitive G_qQ209L/G188S-induced AR activation. Furthermore, extracellular signal-regulated kinase 1/2 (ERK1/2) was found to be involved in RGS2-mediated regulation of androgen-independent AR activity. In addition, RGS2 functioned as a growth suppressor for androgen-independent LNCaP cells whereas androgen-sensitive LNCaP cells with RGS2 silencing had a growth advantage under steroid-reduced conditions. Finally, RGS2 expression level was significantly decreased in human prostate tumor specimens. Taken together, our results suggest RGS2 as a novel regulator of AR signaling and its repression may be an important step during prostate tumorigenesis and progression.

Oncogene (2006) 25, 3719–3734. doi:10.1038/sj.onc.1209408; published online 30 January 2006

Keywords: RGS2; GPCRs; extracellular signal-regulated kinases; prostate cancer; androgen receptor; androgen independence

Introduction

Prostate cancer is the most commonly diagnosed cancer in American men and the second leading cause (after lung) of cancer mortality (Jemal *et al.*, 2005). In early stages, the growth of prostate cancer cells depends on androgens, thus hormone therapies that remove androgen and block androgen receptor (AR) cause the repression of prostate tumors. Unfortunately, the majority of prostate cancers eventually progress from being androgen-dependent to androgen-independent, making hormone therapies ineffective (Feldman and Feldman, 2001). Despite decades of intense laboratory and clinical investigations, the treatment for androgen-independent prostate cancer is still limited. The precise mechanisms underlying prostate cancer progression have remained largely unknown. It cannot be simply ascribed to the loss of AR expression since most of these prostate tumors still express the functional AR (Sadi *et al.*, 1991; Chodak *et al.*, 1992; Hobisch *et al.*, 1996). Thus, at least some hormone-refractory prostate cancers are thought to be caused by ligand-independent activation of AR (Heinlein and Chang, 2004). For example, in most androgen-independent prostate tumors, AR is activated despite the continued presence of hormonal therapies and is involved in the transition of prostate cancer from androgen dependence to androgen independence (Grossmann *et al.*, 2001). Additionally, most hormone-refractory prostate tumor cells express PSA, an androgen-regulated antigen, implying the functional activity of AR in these carcinomas (Taplin and Balk, 2004). Therefore, understanding the mechanisms of signal pathways regulating AR activation is critical for overcoming the current therapeutic limitations treating this disease. Recent works have suggested that signaling pathways triggered by G protein-coupled receptors (GPCRs) can induce androgen-independent AR activation, thus sustaining androgen-independent cell growth of prostate cancer (reviewed by Daaka, 2004).

The basic signaling unit of a GPCR signaling system contains four major components: receptor, G protein (trimeric $\alpha\beta\gamma$), effector and regulators of G-protein signaling (RGS) protein (Ross and Wilkie, 2000). G proteins, classified into G_s, G_i, G_q and G₁₂ subfamilies, stimulate intracellular signal proteins (effectors) when they bind GTP in response to ligand-activated GPCRs; signaling ends when bound GTP is hydrolysed. RGS

Correspondence: Dr Y Tu, Department of Pharmacology, Creighton University School of Medicine, 2500 California Plaza, Omaha, NE 68178, USA.

E-mail: Yat60399@creighton.edu

³These authors contributed equally to the work.

Received 19 September 2005; revised 19 December 2005; accepted 20 December 2005; published online 30 January 2006

proteins display GTPase activating protein (GAP) activity toward G proteins. They increase the rate of GTP hydrolysis of G proteins as many as 1000-fold, thus inactivating G-protein activity. Therefore, the intensity and duration of a GPCR signaling are controlled at least in part by GPCR-mediated activation of G proteins and RGS-mediated inactivation of G proteins.

Basic and clinical research results demonstrate that GPCR systems in some advanced prostate cancers may be excessively activated, due to abnormally elevated ligands of GPCRs (Nelson *et al.*, 1996; Porter and Ben-Josef, 2001; Xie *et al.*, 2002) and/or overexpression of GPCRs including endothelin A receptor (Gohji *et al.*, 2001), bradykinin 1 receptor (Taub *et al.*, 2003), follicle-stimulating hormone receptor (Ben-Josef *et al.*, 1999), thrombin receptor (Chay *et al.*, 2002) and the orphan prostate-specific GPCR (Xu *et al.*, 2000; Xia *et al.*, 2001; Weng *et al.*, 2005). In addition, advanced prostate cancers often have increased numbers of neuroendocrine cells that are known to secrete neuropeptides (Abrahamsson, 1999). These neuropeptides, exemplified by bombesin and neurotensin, acting through their GPCRs result in androgen-independent AR activation, thus promote prostate cancer cells from an androgen-dependent to androgen-independent state (Lee *et al.*, 2001; Dai *et al.*, 2002).

Since RGS proteins inhibit GPCR signaling in cells, it is reasonable to hypothesize that dysregulated RGS proteins can contribute to the aberrant GPCR signaling observed in advanced prostate cancers. Therefore, inhibiting aberrant GPCR signaling by targeting RGS gene expression in prostate cancer cells may help control prostate cancer development and/or progression. Currently, about 20 different mammalian RGS proteins that share a conservative RGS domain have been identified and classified into R4, R7, R12, RZ and RL subfamilies (Ross and Wilkie, 2000; Hollinger and Hepler, 2002). Of all the modulators involved in GPCR signaling, RGS proteins are the only ones showing dynamic changes of gene expression in response to various stimuli (Ingi *et al.*, 1998; Burchett *et al.*, 1999; Robinet *et al.*, 2001; Grillet *et al.*, 2003) and have been shown to be biologically important in neuronal, cardiovascular, and lymphocytic activities (Hollinger and Hepler, 2002; Neubig and Siderovski, 2002; Wieland and Mittmann, 2003). However, the role of RGS proteins in prostate carcinogenesis has not been explored in any depth.

The LNCaP cell line, originally established from a human prostate adenocarcinoma, is androgen sensitive and moderately differentiated. It has been used to study the regulation of AR signaling by GPCR signaling pathways. *In vitro*, stimulation of the endogenous G_q-coupled bombesin/gastrin-releasing peptide (GRP) receptor (Lee *et al.*, 2001) or the G_s-coupled β_2 -adrenergic receptor (Kasbohm *et al.*, 2005) activates AR in LNCaP cells. In addition, the neuropeptide calcitonin, activating both G_s and G_q signaling pathways, can stimulate androgen-independent growth of LNCaP cells (Shah *et al.*, 1994). Recently, Lin and his

co-workers developed a useful prostate cancer cell model including sublines of LNCaP cells (Lin *et al.*, 1998; Igawa *et al.*, 2002). The sublines express the similar level of functional AR. However, the low-passage LNCaP cells (C33) grow slowly in an androgen-sensitive manner, whereas high-passage (C81) cells grow aggressively and also become androgen-independent even though they are still androgen-responsive. This tumor cell model closely resembles the two stages of tumorigenesis with the acquisition of hormone-refractiveness as seen in prostate cancer patients (Karan *et al.*, 2001, 2002; Denmeade *et al.*, 2003) and is useful in studying the progressive changes in the primary and metastatic stages of prostate cancer (Karan *et al.*, 2001; Lee *et al.*, 2003; Lin *et al.*, 2003; Unni *et al.*, 2004).

Here we provide data showing that selective reduction of a specific type of RGS proteins, RGS2, is associated with acquisition of androgen-independence by prostate cancer cells. RGS2 is a 24-kDa protein and was originally identified as an early response gene named as GOS8 (G₀/G₁ switch regulatory gene 8) that was upregulated during the activation of T cells (Siderovski *et al.*, 1994; Wu *et al.*, 1995). Subsequent studies indicated that it has an RGS domain and can profoundly inhibit G_q-coupled GPCR signaling *in vivo*, and therefore was renamed as RGS2 (Druey *et al.*, 1996). RGS2 also functions as a GAP for G_i (Ingi *et al.*, 1998; Hains *et al.*, 2004) and may produce inhibitory effects on G_s-mediated adenylate cyclase activity via binding to adenylate cyclase (Sinnarajah *et al.*, 2001; Salim *et al.*, 2003). Functions of RGS2 in the immune, neurological and cardiovascular systems are well established utilizing RGS2-deficient mice (Oliveira-Dos-Santos *et al.*, 2000; Heximer *et al.*, 2003; Tang *et al.*, 2003). A recent study suggests that RGS2 appears to be a locus implicated in solid tumor development (Collier *et al.*, 2005). Interestingly, RGS2 maps to human chromosome 1q31 (Wu *et al.*, 1995), a region where 20–40% of allelic loss was found in clinical human prostate tumor specimens (Cunningham *et al.*, 1996; Karan *et al.*, 2001). Using a quantitative real-time PCR technique, we found that the expression level of RGS2 is significantly downregulated in human prostate tumor specimens as compared to normal prostate tissues. Expression of the wild-type RGS2 but not GAP-deficient RGS2 mutant blocks G_q-induced activation of AR in LNCaP-C33 and LNCaP-C81 cells. Moreover, our results demonstrated that RGS2 can inhibit both the constitutively activated extracellular signal-regulated kinases (ERKs) and androgen-independent AR activity in androgen-independent prostate cancer cells, thus blocking the androgen-independent prostate cancer cell growth.

Results

Androgen-independent AR activity in androgen-independent LNCaP-C81 cells

To characterize the AR activity in LNCaP cells before and after acquisition of androgen-independence, we transiently transfected LNCaP cells with an

AR-regulated luciferase reporter gene (ARE₃-tk-LUC) to detect AR-mediated gene transcription. The transfected cells were cultured in a steroid-reduced medium without or with synthetic androgen R1881. As shown in Figure 1a, in the absence of exogenous androgen, the basal relative luciferase activity in androgen-independent LNCaP-C81 cells was about seven-fold higher than that in androgen-sensitive LNCaP-C33 cells ($P < 0.01$). At the optimal concentration of R1881 (5 nM) (Sato *et al.*, 1997), additional activation of AR was observed (three-fold in LNCaP-C81 cells vs 16-fold in LNCaP-C33 cells).

Prostate-specific antigen (PSA) is an AR-regulated serine protease, secreted by the prostate. The elevated level of PSA in circulation is known as the most sensitive and reliable marker for diagnosing and monitoring the relapse of prostate cancer after hormone therapies

(Candas *et al.*, 2000). Thus, we performed Western blot analysis to examine PSA secretion from equal number of LNCaP cells using an anti-PSA antibody. Similar to previous report (Igawa *et al.*, 2002), in the steroid-reduced medium, the level of secreted PSA from androgen-independent LNCaP-C81 cells was about six-fold higher than that from androgen-sensitive LNCaP-C33 cells (Figure 1b, $P < 0.01$). Moreover, the degree of 5 nM R1881 stimulation of PSA secretion from LNCaP-C33 cells was much higher than that from LNCaP-C81 cells (12-fold vs 1.6-fold). Thus, our results strongly suggest that AR in LNCaP-C81 cells is already activated under steroid-reduced medium although androgen R1881 can still induce additional modest activation of AR, as seen in hormone-refractory clinical prostate cancers (Taplin and Balk, 2004).

Downregulation of RGS2 in androgen-independent prostate cancer cells

To address the role of RGS proteins in the regulation of androgen-responsiveness in prostate cancer cells, we performed quantitative real-time PCR to compare the mRNA expression levels of 14 RGS genes between androgen-sensitive LNCaP-C33 and androgen-independent LNCaP-C81 cells using the primer sets for human RGS genes (Table 1). These RGS genes were selected to represent five subgroups of the mammalian RGS gene family (Ross and Wilkie, 2000; Hollinger and Hepler, 2002). The housekeeping gene β -Actin was used as the normalizing gene in our experiments. While the transcripts of two RGS genes (RGS 7 and 20) were undetectable in either LNCaP-C33 or LNCaP-C81 cells, there was only a moderate difference (0.8- to 2.3-fold) in the mRNA levels of most RGS genes tested between these two sublines of LNCaP cells. However, the expression of RGS2 was decreased by more than 30-fold in LNCaP-C81 cells, compared to LNCaP-C33 cells (Figure 2a). Similar results were obtained when another housekeeping gene cyclophilin B was used as the normalizing gene (data not shown). Consistent with this result, the conventional PCR product of RGS2 was clearly detected in LNCaP-C33 cells but not in LNCaP-C81 cells (Figure 2a, inset). In support of this finding, the endogenous RGS2 protein was detected in androgen-sensitive LNCaP-C33 cells but not in androgen-independent LNCaP-C81 cells by Western blot assay while these LNCaP-C81 cells were capable of expressing exogenous RGS2 (Figure 2b). Interestingly, Western blot assays also showed that RGS2 protein could not be detected in another androgen-independent prostate cancer CWR22Rv1 cell line that was derived from a relapsed xenograft tumor and possesses features of clinically advanced disease such as AR expression and androgen-independent proliferation (Sramkoski *et al.*, 1999). The expression levels of AR are similar between LNCaP-C33 and LNCaP-C81 cells (Igawa *et al.*, 2002; Figure 2b). In contrast, the full-length AR from CWR22Rv1 cell lysates displays a consistently slower mobility compared to LNCaP cells and a prominent, truncated AR mutant with deletion of the ligand

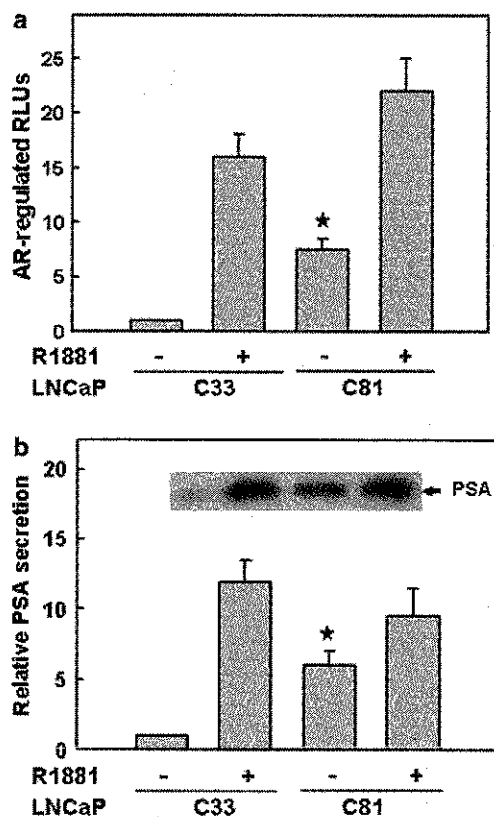


Figure 1 Androgen-independent AR activity in LNCaP cells. (a) Dual reporter genes (ARE₃-tk-LUC and pRL-tk) were transfected into LNCaP-C33 and LNCaP-C81 cells. Cells were cultured in steroid-reduced medium without or with R1881 (5 nM) treatment for 24 h. Luciferase activities of cell lysates were measured using the dual luciferase assay system (Promega). Bars show the mean \pm s.e. of the normalized luciferase activities relative to LNCaP-C33 cells in the absence of R1881 ($n = 5$) (RLUs, relative luciferase units). (b) The PSA secretion was analysed by Western blotting using the anti-PSA antibody (inset is representative of four experiments). Each lane contained 50 μ l of 1% charcoal-stripped FBS conditioned medium from LNCaP cells cultured without or with 5 nM R1881 for 48 h. Data show the mean \pm s.e. of relative PSA secretion normalized to cell numbers. * $P < 0.01$ compared to LNCaP-C33 cells in the absence of R1881.

Table 1 Quantitative real-time PCR and conventional PCR primers

RGS subgroup	Gene	Primer sequence (5' → 3')
R4	RGS2 (AF493926)	208-ATCAAGCCTTCTCCTGAGGAA-228 267-GGCTAGCAGCTCGTCAAATGC-247
	RGS3 (BC019039)	150-TCACTCGCAACGGGAACCT-168 219-CCCAGCTTGTTCTTCATGTCCTT-197
	RGS4 (AF493928)	176-GGGCTGAATCACTGGAAAAC-195 250-ATTCAGACTTCAAGAAAGCTTT-229
	RGS5 (NM_03617)	575-GCTGAGAAGGCAAAGCAA-592 646-GTGGTCAATATTCACCTCTTTAGG-623
	RGS16 (BC006243)	620-CCCACGCTTCCTGAAGTCG-638 721-GTGTGTGAGGGCTCGTCCAG-702
R7	RGS7 (AF493931)	362-GGGAGCCGAAAACACAGATT-382 424-GTGCCTTGTTTTGCATTGTTT-404
	RGS9 (AY585191)	177-CGTCCAGCGGCTTTGG-192 234-GACAATAAAGTTGCCAAGTT-214
R12	RGS10 (AF368902)	186-TTGGCTAGCATGTGAAGATTTT-207 247-TTGCCTTTTCCCTGCATCTG-229
	RGS14 (AF037195)	61-GCCCCGGCCGGACATGT-77 131-GCGCATAGCTGTGCAACTTC-112
RZ	RGS19 (CR606250)	105-GCAACCTCCTCCGCCCA-121 158-TGATCTGCTTCTCAGCCTCAT-138
	RGS20 (BC015614)	159-GCATGCTGCTTCTGCTGGT-177 216-GATCTTCTGGTTTCTAACAGTGA-193
RL	LARG (AF180681)	824-GGGGACACCCTAACAGTCACTGAGGCAGAAAC-855 914-TGGGCGGAGAAGCATCTCCACTGCTAC-888
	p115rhoGEF (NM_199002)	2423-AGTCCCTGCCCCCTGCCTC-2440 2673-CCCCATTGTCTTCTCCGCC-2654
	RGS PX1 (AF420470)	2129-TTGCAGTTACTGTTAGCTCC-2148 2197-GAAATCATAACATAGTGAGCT-2176
	β -Actin (NM_001101.2)	1403-AATGTGGCCGAGGACTTTGATTGC-1426 1495-AGGATGGCAAGGGACTTCCTGTAA-1472
	Cyclophilin B (NM_000942)	714-TGGAGAGCACCAAGACAGACA-734 779-TGCCGAGTCTGCGATGAT-761
Conventional PCR	RGS2 (AF493926)	84-GAAGCGAGAAAAGATGAAACGG-105 390-TGAGGACAGCTTTTGGGGTG-371
	β -Actin (NM_001101.2)	288-AGCACGGCATCGTCACCAACT-308 467-TGGCTGGGGTGTGAAGGTCT-447
	Cyclophilin B (NM_000942)	439-CAGCAAATCCATCGTGTAACT-460 676-AAACACCACATGCTTGCC-659

binding domain was also detected, consistent with the previous report (Tepper *et al.*, 2002). Thus, our results suggest that RGS2 was selectively silenced in AR-positive prostate cancer cells after acquisition of androgen-independence.

RGS2 inhibits the androgen-independent AR activity in androgen-independent prostate cancer cells

To investigate whether dysregulation of RGS2 is involved in the loss of androgen dependence of prostate cancer cells, we examined the effects of exogenously expressed hemagglutinin (HA)-tagged RGS proteins on the AR activity in LNCaP cells. Western blot assays using a monoclonal anti-HA antibody showed similar expression levels of these RGS proteins in LNCaP-C81 cells (Figure 3a, inset). However, expression of RGS2, but not RGS5 or RGS10, decreased the basal AR-regulated luciferase activity in androgen-independent

LNCaP-C81 cells. RGS2 reduced androgen-independent AR activity by more than 80% ($P < 0.01$); while RGS4 had only slight inhibitory effect ($< 30\%$). Similar results were observed when untagged RGS proteins were expressed in LNCaP-C81 cells (data not shown). Interestingly, neither the expression of AR (Figure 2b) nor the androgen-stimulated AR activity (Figure 3a) was affected by the expression of RGS2 in LNCaP-C81 cells. Consistent with the reporter gene assays, expression of RGS2 in LNCaP-C81 cells reduced androgen-independent PSA secretion by 90% (Figure 3b, $P < 0.01$). Interestingly, RGS4 also had an inhibitory effect about 50% ($P < 0.01$) while the effect of RGS5 or RGS10 was statistically insignificant ($P > 0.05$). In contrast, none of RGS proteins significantly impacted the basal or R1881-stimulated AR activity in androgen-sensitive LNCaP-C33 cells (data not shown).

We also tested another AR-positive, androgen-independent prostate cancer CWR22Rv1 cells. In the

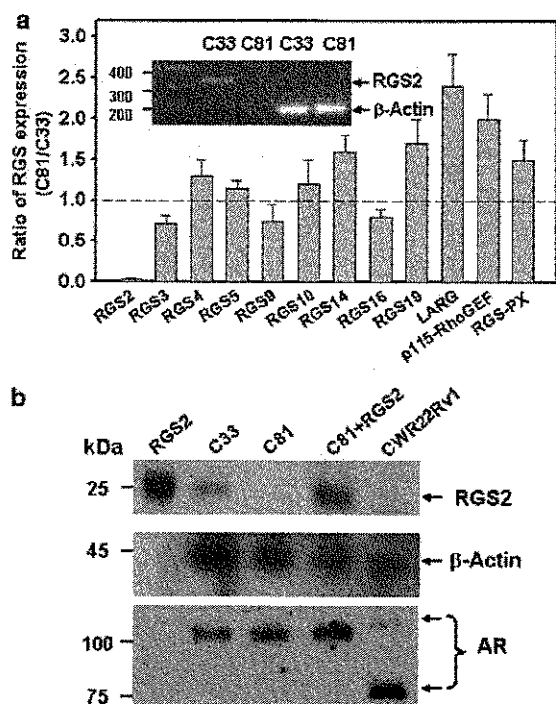


Figure 2 Selective downregulation of RGS2 expression in androgen-independent prostate cancer cells. Total RNA was prepared from cultures of androgen-sensitive LNCaP-C33 or androgen-independent LNCaP-C81 cells. (a) Quantitative real-time PCR was used to compare mRNA expression levels of RGS genes in LNCaP-C81 cells relative to LNCaP-C33 cells. Housekeeping gene β -Actin was used as an internal control. RGS7 and 20 were undetectable in both LNCaP cell lines. Inset: Conventional PCR products were subjected to 4% agarose gel electrophoresis and visualized by staining with ethidium bromide. (b) Lysates were obtained from CWR22Rv1, LNCaP-C33, LNCaP-C81 or LNCaP-C81 transfected with pcDNA3.1 encoding RGS2. Equal amount of protein (40 μ g) from each lysate was resolved by 10% SDS-PAGE and immunoblotted for RGS2, AR or β -Actin (loading control). Purified RGS2 (1 ng, lane 1) was used as a positive control. The blot shown is representative of three replicates.

absence of androgen, CWR22Rv1 cells were found to possess high basal AR activity as shown in reporter gene assays (Figure 3c), which was increased about two-fold by 5 nM R1881 but significantly inhibited by exogenous RGS2 in a dose-dependent manner with the maximum inhibition of 50%. These experiments suggest that RGS2 can inhibit androgen-independent AR activation in androgen-independent prostate cancer cell lines. Since better transfection efficiency with greater inhibitory effect of RGS2 on the androgen-independent AR activity was observed in androgen-independent LNCaP cells compared to CWR22Rv1 cells, we focused our attention on LNCaP cells that provide a model system to study the biological importance of dysregulated RGS2 in androgen-independent activation of AR.

RGS2 inhibits constitutively activated G_qQ209L mutant-induced AR activation

Data obtained from androgen-independent LNCaP-C81 and CWR22Rv1 prostate cancer cells suggest that

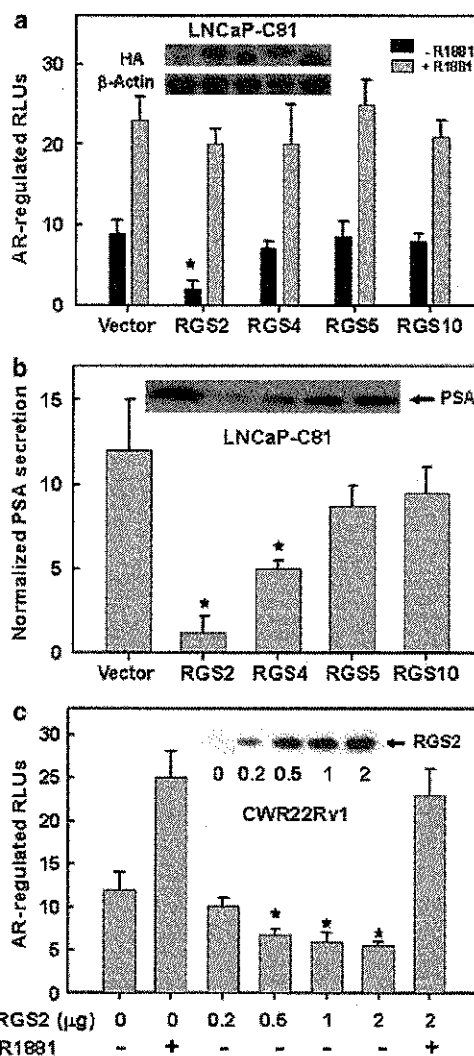


Figure 3 Inhibition of androgen-independent AR activity by RGS2 in androgen-independent prostate cancer cells. Dual reporter genes were transfected into LNCaP-C81 cells (a) or CWR22Rv1 cells (c) together with either pcDNA3.1 (vector) or pcDNA3.1 encoding different RGS genes as indicated. AR-regulated luciferase activities were measured as described in Figure 1. (b) LNCaP-C81 cells were transfected with pcDNA3.1 vector or pcDNA3.1 encoding RGS genes as indicated for 24 h prior to androgen-independent PSA secretion analysis as described in Figure 1. Data show the relative PSA secretion normalized to cell numbers. Inset: (a) Expression levels of different HA-tagged RGS proteins detected by the anti-HA antibody. (b) The PSA secretion was analysed using the anti-PSA antibody. (c) Expression of RGS2 in CWR22Rv1 cells detected by the anti-RGS2 antibody. Bars show the mean \pm s.e. ($n = 5$) with * $P < 0.01$ compared to cells transfected with pcDNA3.1 vector in the absence of R1881.

RGS2 specifically inhibits the androgen-independent activation of AR. RGS2 can inhibit both G_q-coupled and G_i-coupled signaling pathways through its GAP activity (Druey *et al.*, 1996; Ingi *et al.*, 1998; Kammermeier and Ikeda, 1999; Hains *et al.*, 2004). We found that expression of constitutively activated G_{i1}Q204L mutant in LNCaP-C33 cells had no effect on the AR-regulated luciferase activity (data not shown), consistent

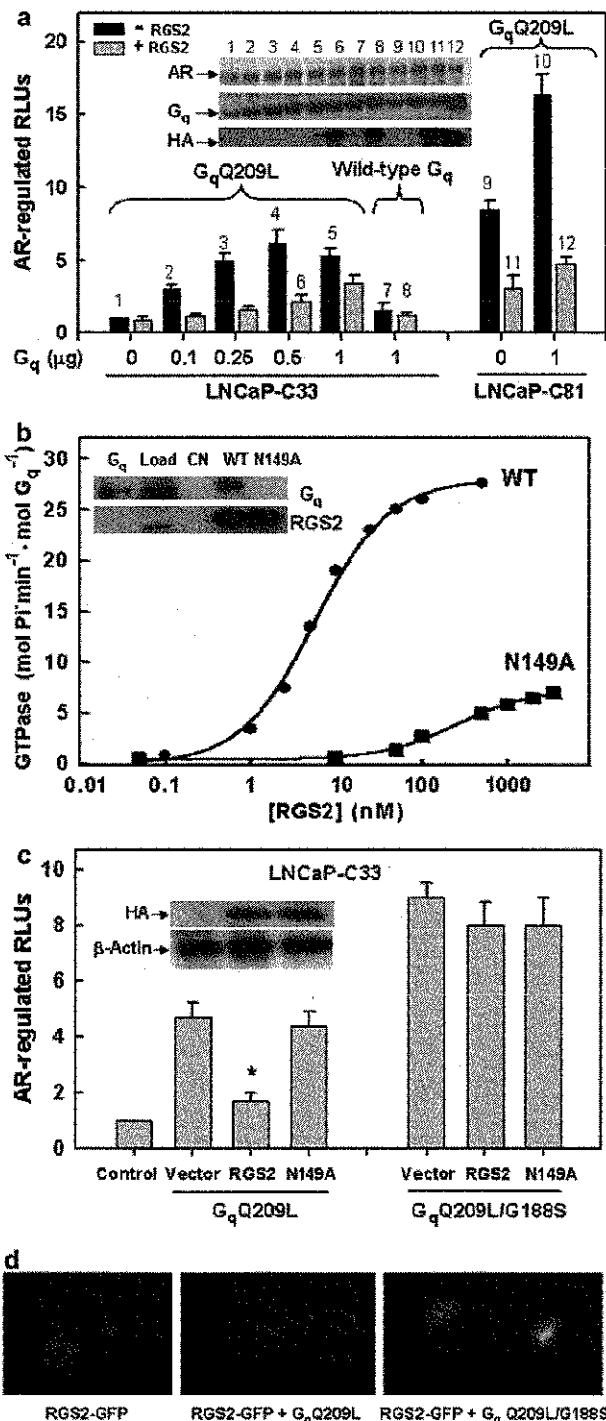
with a previous report (Kasbohm *et al.*, 2005). Therefore, we further investigated whether the modulation of G_q -coupled signaling by RGS2 would affect the AR activity in those cells.

Expression of the constitutively activated G_q Q209L mutant but not the wild-type G_q induced a dose-dependent increase in the AR-regulated luciferase activity in both LNCaP-C33 and LNCaP-C81 cells in the absence of androgen (Figure 4a) using the ARE₃-tk-LUC reporter construct. The maximal stimulation of about six-fold was achieved in androgen-sensitive LNCaP-C33 cells (bar 4 vs bar 1). Coexpression of RGS2 decreased G_q Q209L-stimulated AR activity by more than 80% (bar 6 vs bar 4). As shown in Figure 4a (inset), expression of G_q and/or RGS2 had no significant effect on the expression levels of AR in LNCaP-C33. Deletion of the ARE₃ from the ARE₃-tk-LUC vector abolished the changes of transcription in response to the expression of constitutively activated G_q Q209L or RGS2 (data not shown). In androgen-independent LNCaP-C81 cells, due to a high basal activity, maximal stimulation by G_q Q209L was about two-fold (bar 10 vs bar 9). Co-transfection of RGS2 significantly reduced both the basal and G_q Q209L-stimulated AR activity in LNCaP-C81 cells (bar 11 and 12). It should be noted that neither the expression level of AR protein nor the AR activity of LNCaP cells in the presence of androgen was affected by the expression of G_q Q209L or RGS2 (data not shown).

To test the role of RGS2 GAP activity, we generated the mutation Asn¹⁴⁹ to Ala within the highly conserved

RGS domain of RGS2. The corresponding mutation Asn¹²⁸ to Ala in RGS4 reduces its binding to G proteins by over three orders of magnitude (Posner *et al.*, 1999). We reconstituted M1 muscarinic receptors and G_q (m1AChR- G_q) into proteoliposomes as described previously (Tu *et al.*, 2001) and tested the GAP activity of wild-type RGS2 and RGS2N149A mutant in a steady-state, G_q -coupled GTPase assay (Wang *et al.*, 1998). As shown in Figure 4b, RGS2N149A mutant retained less

Figure 4 RGS2 inhibits androgen-independent, G_q -stimulated AR activity. LNCaP cells were cultured in steroid-reduced medium for 48 h and luciferase activities of cell lysates were measured. Each bar represents the mean \pm s.e. of the normalized luciferase activities ($n=4$) with $*P<0.01$ compared to cells transfected with pcDNA3.1 vector. (a) Cells were co-transfected with dual reporter genes (0.1 μ g) and the wild-type G_q or constitutively activated G_q Q209L mutant plasmid, alone or together with HA-tagged RGS2 plasmid (1 μ g). Inset: Expression levels of AR, G_q and HA-tagged RGS2 were examined by Western blot. LNCaP cells also express endogenous G_q as shown in lane 1, 9 and 11. (b) Mutation of Asn¹⁴⁹ to Ala (N149A) in RGS2 abolished both its G_q GAP activity and its ability to bind to constitutively activated G_q . Carbachol-stimulated GTPase activity in m1AChR- G_q vesicles was measured in the presence of the indicated concentrations of purified wide-type (WT) RGS2 (\bullet) or RGS2N149A mutant (\blacksquare). G_q and m1AChR were 1.3 and 0.27 nM, respectively in assays. Inset: HEK293 cells were transfected with pcDNA3.1 encoding G_q Q209L mutant. HEK293 cell extracts (50 μ g) containing expressed G_q Q209L protein (Load) were incubated without (CN) or with 20 nM purified His6-tagged RGS2 (WT) or N149A mutant. NTA-Ni²⁺ agarose (Qiagen) was used to precipitate His6-tagged RGS2 (WT or N149A) and any associated proteins. Samples were analysed by SDS-PAGE and blotted with the G_q antibody and RGS2 antibody. Purified G_q (10 ng, lane 1) was used as a positive control. (c) LNCaP-C33 cells were cotransfected with dual reporter genes (0.1 μ g), alone or together with 0.4 μ g G_q Q209L or G_q Q209L/G188S plus 1 μ g of vector, vector encoding HA-tagged wild-type RGS2 or its N149A mutant. Inset: Expression levels of HA-tagged RGS2 or its N149A mutant were examined by Western blot and β -Actin was used as loading controls. (d) The intracellular localization of C-terminal GFP-tagged RGS2 in LNCaP-C33 cells co-transfected with G_q mutants as indicated. Confocal microscopic images shown are representative of at least 50 living cells.



than 1% of the GAP activity of wild-type protein, presumably due to the loss of binding to G_q (Figure 4b, inset). As expected, RGS2N149A mutant lost its ability to inhibit the G_qQ209L-stimulated AR activity in LNCaP-C33 cells in the absence of androgen (Figure 4c) although its expression level was similar to the wild-type RGS2 (Figure 4c, Inset).

To further determine the contribution of RGS2 to the regulation of AR activity mediated by G_q in prostate cancer cells, we used a RGS-insensitive G_q mutant (Gly¹⁸⁸ to Ser) that abrogates the RGS-G_q protein interaction but does not affect other functions of the G protein such as coupling to receptors or effectors (DiBello *et al.*, 1998). We transfected G_qQ209L (RGS-sensitive) or G_qQ209L/G188S double mutant (RGS-insensitive) into androgen-sensitive LNCaP-C33 cells. As shown in Figure 4c, co-transfection of RGS2 only blocked G_qQ209L-stimulated AR activity but had no significant effect on G_qQ209L/G188S-stimulated AR activity in the absence of androgen. Moreover, G_qQ209L/G188S had stronger stimulatory effect on the androgen-independent AR activity than G_qQ209L in LNCaP-C33 cells, although their expression levels were similar (data not shown).

We also examined the intracellular localization of GFP-tagged RGS2 to assess the importance of RGS2/G_q interaction in the regulation of AR activity. In the absence of exogenous G_q, GFP-tagged RGS2 was localized predominantly in the nucleus of LNCaP-C33 cells (Figure 4d). Constitutively activated G_qQ209L caused significant amounts of GFP-RGS2 to be re-localized to the plasma membrane. In contrast, the RGS-insensitive G_qQ209L/G188S mutant did not induce GFP-RGS2 association with the plasma membrane, consistent with previous findings in HEK293 cells (Roy *et al.*, 2003).

Silencing endogenous RGS2 by siRNAs enhances G_qQ209L-induced AR activation in LNCaP-C33 cells

To test the hypothesis that endogenous RGS2 is capable of downregulating androgen-independent activation of AR, we designed and synthesized a panel of gene-specific siRNAs targeting human RGS2 gene. One siRNA (RGS2si-3, targeting RGS2 sequence: 5'-AAAGCCACAAATCACCACAGA-3', not homogenous to other RGS genes) effectively suppressed the expression of endogenous RGS2 protein, but no RGS10 protein in LNCaP-C33 cells (Figure 5a). In order to avoid the possibility of off-target effect of siRNAs (Jackson *et al.*, 2003), we also generated three psiRNA-h1zeo (G2) expression vectors that express siRNAs targeting the 3'-untranslated region (3'-UTR) of human RGS2 gene. One RGS2 siRNA expression vector (RGS2si-5, targeting RGS2 3'-UTR sequence: 5'-GGAAACATCACTCAGAACTAT-3') strongly down-regulated RGS2 expression in LNCaP-C33 cells. The knockdown effect of RGS2si-3 or RGS2si-5 was apparently achieved by a sequence-specific event because their control siRNAs with scrambled sequences had no significant effect on the expression of RGS2

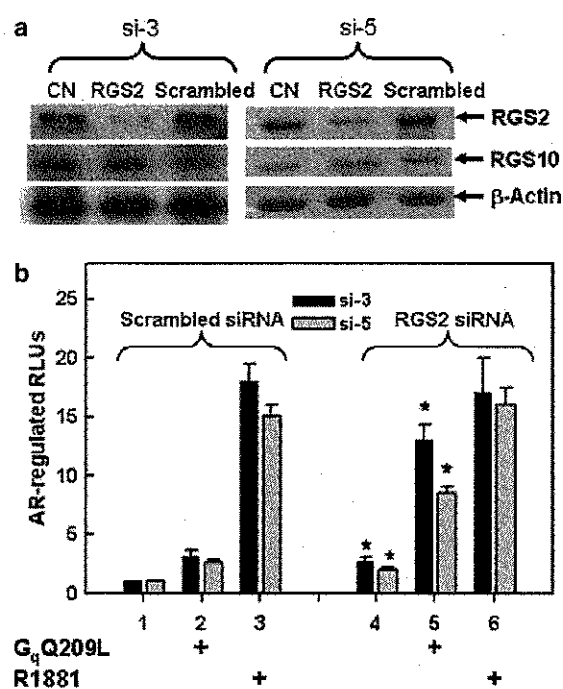


Figure 5 Effects of RGS2 siRNAs on G_qQ209L- or R1881-stimulated AR activity in androgen-sensitive LNCaP-C33 cells. LNCaP-C33 cells (1×10^6) were either untransfected (CN) or transfected with RGS2si-5 expression vector (2 μ g), RGS2si-3 (1.5 μ g) or their corresponding control siRNAs with scrambled sequences as described in 'Materials and methods'. Transfected cells were harvested and subjected to Western blot analysis (a) or were reseeded on 24-well plates for luciferase reporter assays (b). (a) Western blot analysis with RGS2 antibody or RGS10 antibody (β -Actin as loading controls). (b) LNCaP-C33 cells were transfected with dual reporter genes plus control vector or G_qQ209L plasmid (0.25 μ g) using LipofectamineTM 2000 (Invitrogen). AR-regulated luciferase activities were measured as described in Figure 1. Data shown are means \pm s.e. of three independent experiments each conducted in triplicates. * $P < 0.01$ compared to cells transfected with scrambled siRNAs, respectively.

protein. Under steroid-reduced medium culture conditions, introduction of RGS2si-3 or RGS2si-5 expression vector into LNCaP-C33 cells resulted in an increased basal AR activity (lane 1 vs 4) and enhanced the AR activity induced by G_qQ209L mutant by over three-fold (lane 2 vs 5) as demonstrated in an AR-regulated luciferase reporter assay (Figure 5b). However, the AR activity in the presence of R1881 (5 nM) was not affected (lane 3 vs 6).

ERK1/2 mediate the inhibition of androgen-independent AR activity by RGS2 in LNCaP cells

Since the mitogen-activated protein kinase (MAPK), particularly the ERK signaling pathway, plays an important role in prostate cancer progression (Gioeli *et al.*, 1999; Bakin *et al.*, 2003) and ERK1/2 are constitutively activated in high-passage androgen-independent LNCaP cells (Lee *et al.*, 2003; Unni *et al.*, 2004), we investigated the role of ERK signaling pathway in G_q-mediated activation of AR. G_qQ209L

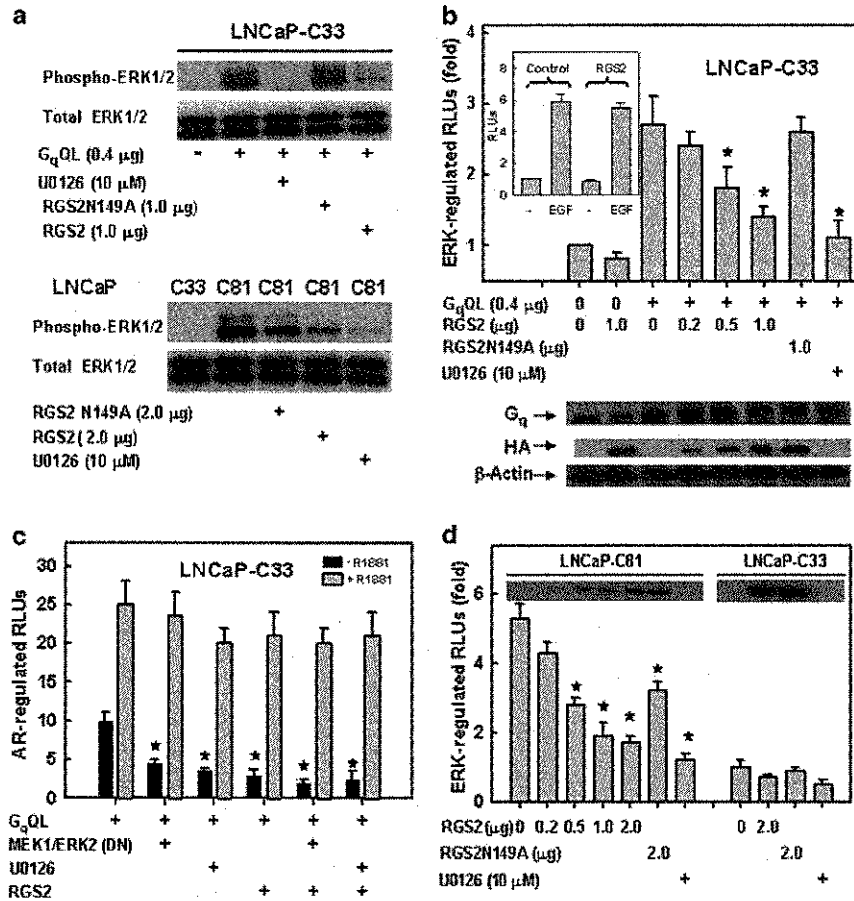


Figure 6 ERKs are involved in RGS2-mediated regulation of AR in LNCaP cells. A Cell Line Nucleofector Kit V (Amaxa) was used for cell transfection. As a control, cells were incubated with U0126 (10 μM) for 30 min prior to transfection. (a) Upper panel: LNCaP-C33 cells were transfected with pcDNA3.1 encoding different genes as indicated. Lower panel: LNCaP-C33 cells transfected with pcDNA3.1 vector whereas LNCaP-C81 cells were transfected with pcDNA3.1 vector or pcDNA3.1 encoding RGS2 or RGS2N149A. Cell lysates were analysed by 10% SDS-PAGE and immunoblotting with antiphosphorylated ERK1/2 (active) antibody or anti-ERK1/2 (total) antibody. (b) LNCaP-C33 cells were transfected with ERK reporter plasmids (pGAL4-LUC and pGAL4-Elk-1-TA) along with either pcDNA3.1 or pcDNA3.1 encoding different genes as indicated for 30 h. Expression levels of G_q and HA-tagged RGS2 or its mutant were shown at the bottom of Figure 2b. Inset: In a separate experiment, transfected cells were treated without or with EGF (25 ng/ml) for 6 h. (c) LNCaP-C33 cells were transfected with G_qQ209L (0.4 μg) and dual reporter genes of AR (ARE₃-tk-LUC and pRL-tk) along with control vector, dominant-negative MEK1/ERK2 (DN) mutants or RGS2 plasmid for 16 h and then treated without or with R1881 (5 nM) for 24 h. AR-regulated luciferase activities were measured as described in Figure 1. Data (mean ± s.e.) are shown for three independent experiments. *P < 0.01 compared to cells transfected with control vector. (d) RGS2 inhibits constitutively activated ERK activity in androgen-independent LNCaP-C81 cells. LNCaP-C81 cells or LNCaP-C33 were transfected with pGAL4-LUC and pGAL4-Elk-1-TA along with control vector, RGS2 or its N149A mutant plasmid. Inset: Expression levels of HA-tagged RGS2 or RGS2N149N mutant. ERK-stimulated luciferase activities of different cells in (b) and (d) are expressed as fold increase as compared to LNCaP-C33 cells transfected with control vector. Data (mean ± s.e.) are shown in four independent experiments. *P < 0.01 compared to either LNCaP-C33 cells transfected with G_qQ209L (b) or LNCaP-C81 cells transfected with control vector (d).

plasmid was transfected into LNCaP-C33 cells without or with RGS2 or RGS2N149A plasmids and the level of active ERK1/2 (phosphorylated) in cell lysates was determined by Western blot assay using antiphosphorylated ERK1/2 antibody. As shown in Figure 6a (upper panel), transfection of G_qQ209L was associated with an induction of ERK1/2 phosphorylation that was blocked by co-transfected RGS2 but not RGS2N149A. As a control, MEK inhibitor U0126 (10 μM) completely diminished G_qQ209L-stimulated ERK1/2 phosphorylation.

Activated ERKs can phosphorylate transcription factors such as Elk-1, thus ERK activity in LNCaP cells can be estimated through the measurement of ERK-activated, Elk-1-dependent expression of a luciferase reporter gene (Guha *et al.*, 2001). As shown in Figure 6b, transfection of G_qQ209L gene into LNCaP-C33 cells stimulated the Elk-1-dependent luciferase activity by about three-fold. Co-transfection with plasmid expressing the wild-type RGS2 blocked the G_q-stimulated, Elk-1-dependent luciferase activity in a dose-dependent manner with at least a 70% inhibition.

In contrast, the GAP-deficient RGS2N149A mutant had no inhibitory effect. As a control, the G_qQ209L-stimulated, Elk-1-dependent luciferase activity was abolished in LNCaP-C33 cells pretreated with the MEK inhibitor U0126 (10 μ M). We also examined the effect of RGS2 on epidermal growth factor (EGF)-induced ERK activity. As shown in Figure 6b (inset), treatment with EGF (25 ng/ml) increased Elk-1-dependent luciferase activity in LNCaP-C33 cells by six-fold, which was not affected by the expression of RGS2.

We next assessed the effects of inhibition of endogenous ERK1/2 activity on G_qQ209L-induced AR activation using MEK1-K97M and ERK2-K52R dominant-negative mutants (DN) (Frost *et al.*, 1994). As shown in Figure 6c, the G_qQ209L-stimulated AR-regulated luciferase activity was inhibited over 60% in LNCaP-C33 cells transfected with MEK1/ERK2 (DN). In contrast, expression of these mutants had a minimal effect on the R1881-stimulated AR activity, suggesting that ERK1/2 signaling pathway is responsible for androgen-independent, but not androgen-dependent activation of AR in G_qQ209L-transfected LNCaP-C33 cells. This conclusion was further supported by the result that LNCaP-C33 cells treated with the MEK inhibitor U0126 (10 μ M) for 30 min prior to transfection had significant lower androgen-independent AR activity but only a slight reduction in androgen-dependent AR activity (Figure 6c). In addition, the inhibition of G_qQ209L-stimulated AR activity by exogenous RGS2 plus MEK1/ERK2 (DN) was only slightly greater than RGS2 or MEK1/ERK2 (DN) alone.

We further investigated whether downregulation of RGS2 expression contributes to constitutively activated ERK activity in LNCaP-C81 cells. As shown in Figure 6a (lower panel), the level of active ERK1/2 (phosphorylated) in LNCaP-C81 cells was significantly higher compared to LNCaP-C33 cells, consistent with the previous reports that ERKs were activated in androgen-independent LNCaP cells in the absence of exogenous androgen (Lee *et al.*, 2003; Unni *et al.*, 2004). Expression of RGS2 or treatment of MEK inhibitor U0126 strongly decreased the level of active ERK1/2 (phosphorylated) in LNCaP-C81 cells. We then examined the exogenous expression of RGS2 on ERK activities in LNCaP-C81 cells. As shown in Figure 6d, under steroid-reduced medium, ERK-activated, Elk-1-dependent luciferase activity in androgen-independent LNCaP-C81 cells was five-fold higher than that in androgen-sensitive LNCaP-C33 cells. Transfection with plasmid encoding the wild-type RGS2 into LNCaP-C81 cells reduced the Elk-1-dependent luciferase activity in a dose-dependent manner with a maximum inhibition of over 80%. Interestingly, the GAP-deficient mutant RGS2N149A had a modest inhibitory effect (~40%, $P < 0.01$) in LNCaP-C81. This result was supported by the data that RGS2N149A also partially reduced the level of active ERK1/2 in LNCaP-C81 cells (Figure 6a, lower panel). Thus, our results suggest that RGS2 can inhibit ERK activity independently of its GAP activity in LNCaP-C81 cells. This is consistent with the fact that GAP activity is not the only activity ascribed to RGS2

(Kehrl and Sinnarajah, 2002) (see Discussion). In contrast, due to low basal ERK activity in LNCaP-C33 cells, neither the wild-type RGS2 nor RGS2N149A had a significant effect. Thus, RGS2 selectively inhibits constitutively activated ERK activity in androgen-independent LNCaP-C81 cells. As a control, Elk-1-dependent luciferase was strongly reduced in LNCaP-C81 and LNCaP-C33 cells pretreated with the MEK inhibitor U0126 (10 μ M).

RGS2 modulates androgen-independent growth of LNCaP cells

We next performed colony formation assays to test the growth-inhibitory effect of RGS2. We transfected vectors encoding GFP, GFP-fused RGS2, or GFP-fused RGS2N149A mutant into androgen-independent LNCaP-C81 cells, selected the transfected cells with G418 in steroid-reduced medium for 3 weeks, then counted the surviving colonies. In steroid-reduced medium, GFP-fused RGS2 strongly suppressed both the number of colonies by about 70% and size of colonies relative to GFP control (Figure 7a). GFP-fused RGS2N149A mutant also showed a modest inhibitory effect with a reduction of 40%. These results suggest that in LNCaP cells, RGS2 functions as a potent cell growth inhibitor and the mutation created in RGS2 that disrupts GAP activity only partially limits its ability to inhibit the androgen-independent LNCaP cell growth.

The correlation of hormone refractoriness with downregulated RGS2 expression in androgen-independent prostate cancer cells also prompted us to investigate whether downregulation of RGS2 expression in prostate cancer cells would have a growth advantage under steroid-reduced culture conditions. As shown in Figure 7b, in steroid-reduced medium, androgen-independent LNCaP-C81 cells retained the rapid growth ability, which was independent of androgen R1881 (lane 1 vs 2) but was suppressed about 50% by the expression of exogenous RGS2 (lane 1 vs 3). In contrast, LNCaP-C33 cells grew very slowly in steroid-reduced medium. However, 5 nM R1881 stimulated LNCaP-C33 cell growth by more than six-fold (lane 5 vs 6). Silencing RGS2 in LNCaP-C33 cells by transiently transfected RGS2-specific siRNA (RGS2si-3) enhanced androgen-independent cell growth by about 2.5-fold (lane 5 vs 7) but did not affect R1881-stimulated cell growth (lane 6 vs 8). Thus, downregulation of RGS2 expression facilitates androgen-independent cell proliferation.

Reduction of RGS2 expression in prostate tumors

To further explore the clinical relevance of dysregulation of RGS2 in prostate cancer development and progression, we first used the semiquantitative PCR technique to examine the expression level of RGS2 mRNA in Matched Tumor/Normal prostate tissue RNA pairs (Ambion, Austin, TX, USA). As shown in Figure 8a, the PCR product derived from RGS2 was clearly detected in the normal sample but was decreased by over 70% in the matched tumor whereas expression levels of housekeeping gene β -Actin or cyclophilin B

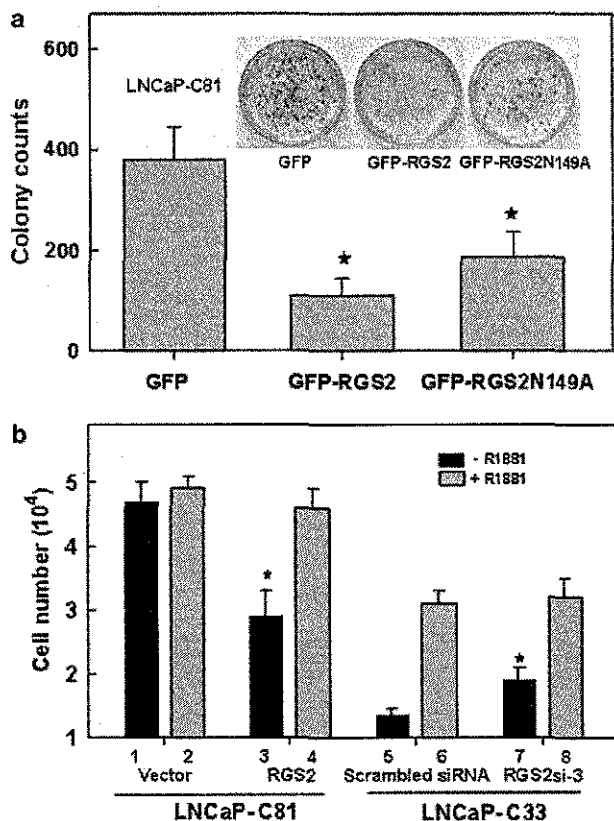


Figure 7 RGS2 inhibits androgen-independent growth of LNCaP cells. (a) Inhibition of colony formation of androgen-independent LNCaP-C81 cells by RGS2. The indicated constructs were transfected into LNCaP-C81 cells, and the cells were grown under steroid-reduced medium in the presence of the selection agent G418 for 3 weeks. The colonies were stained with Giemsa solution, and counted. The results are representative of six experiments. Data show the mean \pm s.e. with * $P < 0.01$ compared to cells transfected with GFP. (b) Altering RGS2 expression modulates the growth of LNCaP cells. Androgen-independent LNCaP-C81 cells were transfected with pcDNA3.1 vector (lane 1 and 2) or pcDNA3.1 encoding RGS2 (lane 3 and 4) whereas androgen-sensitive LNCaP-C33 cells were transfected with RGS2si-3 (lane 7 and 8) or its scrambled siRNA (lane 5 and 6). Transfected cells were seeded on six-well plates and cultured for 24 h in steroid-reduced medium. Cells were harvested and reseeded on 12-well plates (10^4 /well) and were grown for 4 days in the steroid-reduced medium without or with R1881 (5 nM). Total cell numbers in each well were counted. Data shown are means \pm s.e. of triplicates and these experiments were repeated twice. Student's *t*-test indicates significant difference between lane 3 and 1, lane 7 and 5 (* $P < 0.01$).

were similar between normal and tumor samples. Since RGS2 and RGS5 are the most related genes in the RGS family (Ross and Wilkie, 2000), we further examined the expression levels of these two RGS genes in five pairs of prostate tumors and their paired normal tissues using quantitative real-time PCR. The data were shown as the copy number of RGS2 or RGS5 per 1000 copies of β -Actin. All the samples examined showed lower levels of RGS2 mRNA in the tumors as compared to the corresponding normal tissues (Figure 8b). The mean ratio of amounts of RGS2 mRNA in prostate tumors to those in corresponding normal prostate tissues was 1:6.5

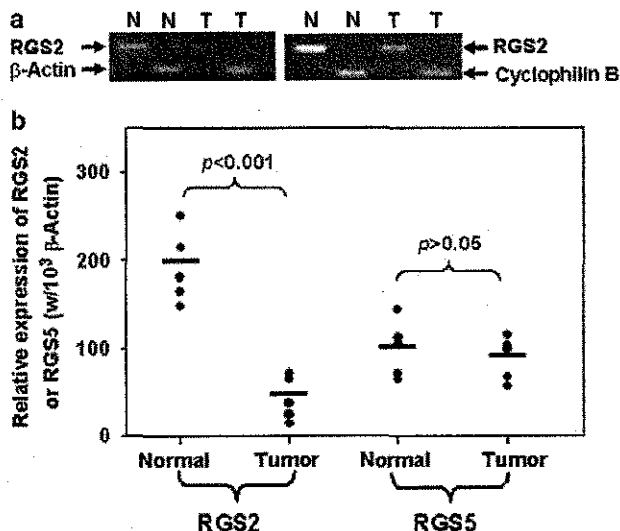


Figure 8 Analysis of RGS genes expression in human prostate cancer specimens. T = tumor; N = corresponding normal tissue. (a) Conventional PCR was performed using one matched human prostate tumor/normal RNA sample (Ambion). β -Actin or cyclophilin B was used as a control in two separate experiments. PCR products were subjected to 4% agarose gel electrophoresis and visualized by staining with ethidium bromide. (b) RGS2 and RGS5 mRNA levels (copies/10³ β -Actin) in human prostate tumors and corresponding normal prostate tissues ($n = 5$) determined by quantitative real-time PCR method. '—' shows the mean of RGS mRNA in tumor or normal samples.

(± 2.3) ($P < 0.001$, $n = 5$). When cyclophilin B was used as the normalizing gene, the mean ratio was 1:8 (± 4) ($P < 0.001$, $n = 5$) (data not shown). In contrast, no significant difference was observed for the expression level of RGS5 ($P > 0.05$, $n = 5$).

Discussion

One of major challenges for treating advanced prostate cancer is the acquisition of androgen-independence by prostate cancer cells that causes the failure of hormone ablation therapies. At least a subpopulation of hormone-refractory prostate cancer is thought to be apparently caused by androgen-independent activation of AR. Therefore, a full understanding of the mechanism underlying androgen-independent activation of AR will lead to improved therapies. Recent studies have shown that aberrant GPCR signaling, due to over-expression of GPCRs and/or elevated ligands, can promote androgen-independent prostate cancer cell growth. In the present study, we investigated a possible role of RGS proteins, negative regulators of GPCR signaling, in prostate cancer cells during the transition from an androgen-sensitive to androgen-independent state. Our study presents the first evidence suggesting that the decrease of a RGS protein may play an important role in androgen-independent prostate cancer progression.

First, we showed that the expression level of RGS2 is selectively reduced in androgen-independent prostate cancer LNCaP-C81 and CWR22Rv1 cells as compared to androgen-sensitive LNCaP-C33 cells. Conversely, the expression of RGS2, but not other RGS proteins, is able to significantly inhibit androgen-independent, but not androgen-stimulated, AR activity in androgen-independent LNCaP-C81 and CWR22Rv1 cells. These results support the concept that loss of RGS2 expression contributes to the androgen-independent activation of AR in androgen-independent prostate cancer cells.

G proteins are classified into four subfamilies, G_s , G_i , G_q and G_{12} (Wilkie *et al.*, 1992). Since RGS2 inhibits G_q -coupled signaling *in vivo* (Druey *et al.*, 1996; Kammermeier and Ikeda, 1999), we examined the effect of regulation of G_q -signaling by RGS2 on the AR activity using the constitutively activated G_q Q209L mutant that mimics the activation of G_q signaling pathways by GPCRs. Interestingly, co-expression of wild-type RGS2 but not GAP-deficient RGS2N149A mutant blocked G_q Q209L-stimulated AR activity in LNCaP-C33 cells. Since constitutively activated G_q Q209L mutant does not hydrolyse its bound GTP even in the presence of RGS proteins (Berman *et al.*, 1996), the RGS2-mediated inhibitory effect is presumably due to occlusion of the binding site on G_q Q209L for its primary effector phospholipase C by RGS2 (Hepler *et al.*, 1997). This is consistent with the result that G_q Q209L can recruit RGS2 to the plasma membrane, which is crucial for the regulation of G protein-coupled signaling by RGS proteins. Thus, our data support the concept that RGS2 inhibits G_q -mediated stimulation of AR activity through its interaction with G_q . This is further supported by the result that RGS2 is unable to suppress RGS-insensitive G_q Q209L/G188S-stimulated AR activity in prostate cancer cells, presumably due to loss of interaction between G_q Q209L/G188S and RGS2 since G_q Q209L/G188S is unable to recruit RGS2 to plasma membrane.

It should be noted that G_q Q209L/G188S has a stronger stimulatory effect on the AR activity than RGS2-sensitive G_q Q209L in LNCaP-C33 cells. This result may suggest a possible contribution of endogenous RGS2 in the downregulation of AR activity in LNCaP-C33 cells. Indeed, silencing of endogenous RGS2 in LNCaP-C33 cells by RGS2-specific siRNA activates AR under steroid-reduced medium conditions without any significant effect on androgen-dependent AR activity. Moreover, silencing of endogenous RGS2 further enhances constitutively activated G_q Q209L-stimulated AR activity. These results further implicate the involvement of dysregulated RGS2 in the transition of prostate cancer cells from an androgen-sensitive to independent state.

Our data collectively suggest that RGS2 inhibits androgen-independent AR activation by inactivating G_q -coupled signaling pathway in prostate cancer cells. Thus, reduced expression of RGS2 can lead to androgen-independent proliferation. However, the mechanism underlying androgen-independent, G_q -coupled signaling-stimulated AR activity is still unknown. One possible

mediator in this pathway is ERK, which has been shown to play an important role in clinical prostate cancer progression (Gioeli *et al.*, 1999; Bakin *et al.*, 2003). In fact, activation of phospholipase C through G_q -coupled receptors, with subsequently increased levels of inositol-1,4,5-trisphosphate, diacylglycerol and free intracellular Ca^{2+} can activate ERK via both Ras-dependent and Ras-independent pathways (reviewed by Gutkind, 2000). Interestingly, in the presence of U0126, a specific inhibitor of MEK, both ERK activity and AR activity were blocked in LNCaP cells. Since dominant-negative mutants of MEK1 and ERK2 also blocked G_q Q209L-stimulated AR activity, our data suggest that ERK1/2 are implicated in the transmission of signal from G_q to androgen-independent AR activation in prostate cancer cells. Furthermore, co-expression of RGS2 but not its GAP-deficient mutant inhibited G_q Q209L-stimulated ERK activity and AR activity in androgen-sensitive LNCaP-C33 cells under steroid-reduced conditions. In addition, the inhibitory effect by exogenous RGS2 plus dominant-negative mutants of MEK1 and ERK2 was only slightly greater than RGS2 alone, suggesting that RGS2 and dominant-negative mutants of MEK1 and ERK2 block the same G protein-coupled signaling pathway that stimulates the androgen-independent but not androgen-dependent AR activity. In fact, ERKs can directly phosphorylate AR *in vitro*, and inhibition of ERK activity attenuates the human epidermal receptor 2 (HER2)-mediated activation of AR signaling (Yeh *et al.*, 1999; Lee *et al.*, 2003). It is possible that RGS2 suppresses androgen-independent AR activity by inhibiting ERK activity in prostate cancer cells. Indeed, the expression of exogenous RGS2 inhibits the constitutively activated ERK activity that only affects androgen-independent AR activity in LNCaP-C81 cells. Our data are consistent with the model depicted in Figure 9 that GPCRs induce androgen-independent AR activation via a signal relay from G_q (inactivated by RGS2), MEK1/2 (inhibited by U0126), and ERK1/2 in prostate cancer cells. RGS4, a known GAP toward G_i and G_q (Hains *et al.*, 2004), also can inhibit intracellular G_q signaling but is less potent compared to RGS2 (Tovey and Willars, 2004). This is consistent with our observation that at equivalent levels of expression, RGS2 reduced

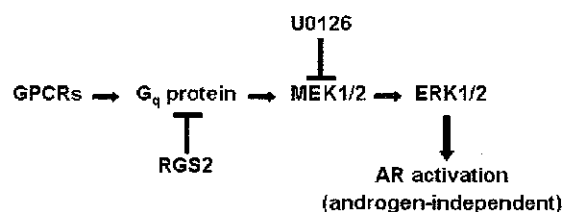


Figure 9 A model for the regulation of androgen-independent AR activation by RGS2 through G_q -coupled receptor signaling pathway. Various G protein-coupled receptors (GPCRs) induce androgen-independent AR activation via signaling relay from G_q to ERK1/2 in prostate cancer cells. RGS2 inactivates G_q , whereas U0126 inhibits MEK1/2. Both inhibit androgen-independent AR activation.

AR-regulated PSA secretion by 90% in LNCaP-C81 cells whereas RGS4 had only a moderate inhibitory effect (about 50%).

Interestingly, the GAP-deficient mutant RGS2N149A also has an inhibitory effect by about 40% on the constitutively activated ERK activity in LNCaP-C81 cells. Such an effect is probably not due to the residual GAP activity of the mutant (<1% of that of the wild-type RGS2). Since RGS2N149A showed no effect on G_q -stimulated ERK activity in androgen-sensitive LNCaP-C33 cells, it is likely that signaling pathways other than G_q -coupled signaling also contribute to the constitutively activated ERK activity in androgen-independent LNCaP cells, which can be inhibited by GAP-deficient RGS2N149A mutant. In fact, expression of RGS2N149A mutant also showed a partial inhibitory effect on the high basal AR activity in androgen-independent LNCaP-C81 cells (unpublished data). It has been shown recently that G_s activates AR in LNCaP cells by stimulating the adenylylate cyclase/PKA pathway (Kasbohm *et al.*, 2005) that can activate ERKs via the small G protein Rap1 (Schmitt and Stork, 2000). Since RGS2 can also directly suppress the adenylylate cyclase activity independent of its GAP activity (Sinnarajah *et al.*, 2001; Salim *et al.*, 2003). It is possible that aberrant activation of the G_s /adenylylate cyclase/PKA pathway contributes in part to both the constitutively activated ERK activity and high basal androgen-independent AR activity in androgen-independent LNCaP cells, which can be inhibited by the GAP-deficient RGS2N149A mutant. This is further supported by the results that the RGS2N149A mutant could partially inhibit androgen-independent growth of androgen-independent LNCaP-C81 cells. The mechanism underlying the regulation of G_s -stimulated AR activity by RGS2 is currently under investigation.

Regulation of the G_q -coupled signaling pathway by RGS2 may be physiologically important in the regulation of prostate cancer cell growth. It has been reported that activation of G_q -coupled α_1 -adrenergic receptor by its agonist can stimulate LNCaP cell proliferation in the absence of androgen (Thebault *et al.*, 2003). Neuropeptides such as neurotensin and bombesin, acting through G_q -coupled receptors, also activate AR and enhance the androgen-independent growth of prostate cancer cells (Lee *et al.*, 2001; Dai *et al.*, 2002). Our data support the notion that RGS2 can inhibit several G_q -coupled GPCRs that stimulate the androgen-independent AR signaling pathway, thus attenuating androgen-independent prostate cancer cell growth. Indeed, our colony formation assays demonstrate that RGS2 can inhibit androgen-independent growth of prostate cancer cells. This is further supported by the result that androgen-sensitive LNCaP cells with silencing RGS2 expression have a growth advantage under steroid-reduced culture conditions, presumably due to the androgen-independent activation of AR. Our findings may have important clinical implications since many patients that become refractory to the hormone therapy still express normal levels of AR-regulated genes (Grossmann *et al.*, 2001), suggesting that AR is fully functional. Our results

therefore predict that prostate cancer cells in which RGS2 is downregulated would be resistant to hormone therapy. In fact, all five prostate cancer specimens tested in our studies have lower levels of RGS2 expression as compared to their noncancerous prostate tissues. Interestingly, a recent study by Hubert Serve's group showed that RGS2 protein was suppressed by fetal liver tyrosine kinase 3 mutants (Flt3-ITD) in the majority of acute myeloid leukemia cases and co-expression of RGS2 with Flt3-ITD inhibited Flt3-ITD-induced autonomous proliferation and clonal growth of myeloid cells (Schwable *et al.*, 2005). This finding is consistent with our results, suggesting that repression of RGS2 is an important event in the development of different cancers and upregulation of RGS2 can potentially suppress the proliferative signaling in cancer cells. Since expression of RGS2 in androgen-independent prostate cancer cells significantly decreased both the androgen-independent AR activity and cell growth, targeting the RGS2 expression level in prostate cancer cells, in combination with hormone therapy, should significantly improve the treatment of advanced prostate cancer patients.

Early prediction of androgen-independence of prostate cancer is crucial to the treatment of advanced prostate cancer. Since RGS2 expression levels are reduced in androgen-independent prostate cancer cells and in prostate cancer specimens we analysed, the expression levels of RGS2 could potentially be used as a novel marker for predicting the clinical efficacy of antiandrogen therapy. Thus, future studies will be necessary to correlate RGS2 expression levels in clinical prostate cancer samples with tumor progression stages and therapeutic responsiveness to anti-androgen treatment.

Materials and methods

Materials

$G\alpha_q$, $G\beta_1\gamma_2$ and m1AChR were purified from Sf9 cells whereas His6 tagged RGS2 protein, wild-type and mutant, were purified from *E. coli* as described (Tu *et al.*, 2001). Phenol red-free RPMI-1640 cell media were purchased from Invitrogen. FBS and charcoal-treated certified FBS were from Hyclone (Logan, UT, USA). Rabbit poly-clonal anti-RGS2 C-terminal peptide (KKPQITTEPHAT) antibody was a kind gift from Dr D Siderovski (University of North Carolina at Chapel Hill). The polyclonal rabbit G_q antibody (W082-14), a gift from Paul C Sternweis (UT Southwestern Medical Center), was raised against a peptide representing an internal sequence in G_q (Gutowski *et al.*, 1991). Monoclonal mouse anti-human AR antibody, rabbit anti-human PSA antibody, rat anti-HA antibody and rabbit anti-RGS10 antibody were purchased from Santa Cruz. Anti-phosphorylated p44/42 MAP kinases (active ERK1 and 2) antibody (10E) and anti-ERK1/2 total protein antibody were from Cell Signaling Technology. An enhanced chemiluminescence (ECL) reagent kit was purchased from Pierce (Rockford, IL, USA). Nonmetabolizable androgen R1881 was obtained from NEN Life Science Products (Boston, MA, USA). MAPK kinase (MEK) inhibitor U0126 was from Calbiochem. ARE₃-tk-LUC was a gift from Dr Li-Hua Wang (National Cancer Institute-Frederick Cancer Research and Development Center). It contains three tandem copies of androgen-response element

(ARE) from the androgen-responsive, prostate-specific antigen promoter upstream of the tk-LUC reporter. *Renilla* luciferase expression plasmid, pRL-tk plasmid was a gift from Dr Zhaoyi Wang (Cancer Center, Creighton University). The pFA2-Elk-1 (pGAL4-Elk-1TA) expresses the GAL4 DNA-binding domain fused with the transactivation domain of Elk-1. The reporter plasmid pFR-LUC (pGAL4-LUC) contains 5 copies of the GAL4 binding site upstream of a minimal promoter that drives expression of the firefly luciferase reporter gene. Both were purchased from Stratagene. All pcDNA3.1 plasmids encoding different HA-tagged or un-tagged RGS proteins or constitutively activated G_qQ209L were obtained from UMR cDNA Resource Center (Rolla, MO, USA). G_qQ209L/G188S was generated from G_qQ209L using a QuikChange mutagenesis kit (Stratagene). Gly at position 188 of G_q was mutated to Ser using the oligonucleotides 5'-GTATTCGATGATCGA TGTGGTGGGGACTC-3' and 5'-GAGTCCCCACCACAT CGATCATCGAATAC-3'. Asn at position 149 of RGS2 was mutated to Ala (N149A) as described previously (Salim et al., 2003). Green fluorescent protein (GFP)-fused RGS2 or its GAP-deficient N149A mutant was generated by ligating RGS2 or RGS2N149A into pEGFP-N1 (Clontech). Catalytically defective MEK1 mutant (K97M) and ERK2 mutant (K52) were kind gifts from Dr M Cobb (University of Texas Southwestern Medical Center, Dallas, TX, USA). The MEK1-K97M cDNA construct was subcloned into vector pRSET (Invitrogen), and the ERK2-K52R cDNA was subcloned into vector pCMV5M. All plasmids were verified by DNA sequencing. Matched Tumor/Normal prostate tissue RNA pairs were purchased from Ambion (Austin, TX, USA). Prostate tumors and their adjacent normal tissues were obtained from the National Cancer Institute (NCI) Cooperative Prostate Cancer Tissue Resource.

Receptor-G protein vesicles and steady-state GAP assays

Unilamellar m1AChR-G_q protein vesicles were reconstituted as described previously (Tu et al., 2001). Steady-state GAP activity was determined according to the increase in agonist-stimulated GTPase activity in phospholipid vesicles that contained trimeric G protein and receptor (Wang et al., 1998).

Cells and cell culture

Low-passage androgen-sensitive LNCaP-C33 (passage <33) was purchased from the American Type Culture Collection (ATCC). They are routinely maintained in RPMI-1640 medium supplemented with 5% FBS at 37°C in a humidified atmosphere of 5% CO₂ in air. An androgen-independent high-passage LNCaP-C81 (passage >81) cell line has been established by more than 12-month continuous culture of low-passage LNCaP-C33 cells as described previously (Igawa et al., 2002). CWR22Rv1 cells (ATCC, CRL-2505), derived from the relapsed xenograft, were grown in RPMI-1640 medium supplemented with 10% FBS, and 10 mM HEPES.

Transfection and luciferase reporter assays

LNCaP cells were transiently transfected using Lipofectamine™ 2000 (Invitrogen) in serum-free medium, according to the manufacturer's instructions. Briefly, 0.1 μg of dual luciferase reporter constructs (ARE₃-tk-LUC and pRL-tk) were co-transfected with pcDNA3.1 empty vector or expression vectors as indicated into 2 × 10⁵ of LNCaP cells in 24-well plates for 16 h followed by incubation in steroid-reduced medium (phenol red-free RPMI 1640 plus 5% charcoal-stripped FBS) with or without R1881 for 24 h. The total amount of plasmid DNA used was normalized to 2 μg/well by the addition of empty plasmid. *Renilla* luciferase expression plasmid, pRL-tk

(10 ng), was used as an internal control for transfection efficiency. Luciferase activities in cell lysates were measured with a Sirius luminometer (Berthold, Germany) using the dual luciferase assay system (Promega) and were normalized by the *Renilla* activities and protein concentrations of the samples. The results are presented as fold induction, which is the relative luciferase activity (RLUs, ratio of reporter luciferases/*Renilla* luciferases) of the treated cells over that of the control cells.

Detection of ERK activity

To monitor ERK activities, we used a reporter system (Stratagene) based on the use of fusion proteins that are comprised of a GAL4 DNA binding domain fused to the activation domain of specific transcription factors that, in turn, drive the expression of the luciferase reporter gene (pGAL4-LUC). An expression plasmid (pFA-Elk) expresses a chimeric protein GAL4-Elk1, the phosphorylation target of activated ERKs. Routinely, 2 × 10⁵ of LNCaP cells were co-transfected with pGAL4-LUC (8 ng), pGAL4-Elk-1-TA (8 ng) and either pcDNA3.1 or pcDNA3.1 encoding different genes as indicated (total 2 μg) using Lipofectamine™ 2000 (Invitrogen) for 30 h. Luciferase activity was measured using the dual luciferase assay system from Promega.

PSA secretion

LNCaP cells were cultured in phenol-free RPMI 1640 plus 1% charcoal-stripped FBS conditioned medium without or with 5 nM R1881 for 48 h. PSA in 50 μl of collected medium was analysed by Western blotting with the anti-PSA antibody as described below. PSA levels were quantified by densitometry and were corrected for LNCaP cell numbers.

Protein extraction, electrophoresis and Western blot analysis

Protein was extracted from exponentially growing cells using 1 × RIPA complete lysis buffer (Santa Cruz). Protein samples (40 μg) and prestained protein standards were loaded on 10% SDS polyacrylamide gels, electrophoresed and transferred onto a PVDF membrane (Immobilon, pore size 0.45 μm). Immunoblots were probed with antibodies against AR, RGS2, RGS10, G_q or anti-HA in a 10% blocking solution and developed according to instructions in the ECL kit (Amersham Biosciences). Anti-β-Actin antibody was used to detect Actin in lysates as loading controls. Cell lysates transfected with different plasmids were also analysed by 10% SDS-PAGE and immunoblotting with a monoclonal antibody specific against the phosphorylated ERK1/2. Total ERK1/2 protein was blotted as a control (Lee et al., 2002).

RNA interference experiments

Four RGS2 siRNAs were designed according to different regions of RGS2 gene that are unique to RGS2 using siRNA Wizard software on the website of InvivoGen Inc. One relatively potent siRNA (RGS2si-3, targeting RGS2 sequence: 5'-AAAGCCACAAATCACCACAGA-3') was identified by its ability to knockdown RGS2 expression in androgen-sensitive LNCaP-C33 cells that expresses endogenous RGS2 protein. RGS2 siRNA (1.5 μg) or its scrambled siRNA was transfected into LNCaP-C33 cells (1 × 10⁶) with a Cell Line Nucleofector Kit V (Amaxa), and transfected LNCaP-C33 cells were seeded on six-well plates. After 48 h of incubation at 37°C, cells were harvested and subjected to luciferase reporter assays and cell growth analysis. We also designed three other RGS2 siRNAs according to different regions of the 3'-untranslated region (3'-UTR) of RGS2 gene (GenBank Accession No. NM-002923). The short-hairpin-RNA-encoding complementary single-stranded oligonucleotides, which hybridized to give overhangs compatible with *BbsI/BbsI*, were

synthesized and cloned into the expression vector psiRNA-hH1zeo (G2) (Invivogen Inc.) that carries an SV40 promoter and a Zeocin resistant gene as a selection marker. The three siRNA expression vectors (2 μ g) were transfected into LNCaP-C33 cells as described above. One of them (RGS2si-5, targeting RGS2 3'-UTR sequence: 5'-GGAAACATCACT CAG AACTAT-3') strongly downregulated RGS2 expression in LNCaP-C33 cells. Cells transfected with the RGS2si-5 expression vector were harvested 72 h post-transfection and subjected to luciferase reporter assays and cell growth analysis.

Growth assays

Approximately 1×10^4 transfected cells/well were plated in 12-well tissue culture plates (Becton Dickinson) in steroid-reduced medium for 24 h, and then the medium was replaced with fresh steroid-reduced medium without or with 5 nM R1881 for 4 days. Cells were counted using a Coulter Counter ZM (Coulter Electronics). Results represent an average of two independent experiments performed in triplicates.

Colony formation assay

Androgen-independent LNCaP-C81 cells were transfected with a vector encoding GFP, or a vector encoding GFP-fused RGS2 or RGS2N149A mutant. After 24 h, the cells were replated into 60-mm dishes with 3×10^4 cells/dish and the cells were cultured in steroid-reduced medium plus 500 μ g/ml G418 for 3 weeks. The colonies were fixed with formalin, stained with Giemsa, and counted. All assays were carried out in triplicates, and the results are expressed as the number of colonies obtained.

Confocal microscopy

GFP-tagged RGS proteins were visualized in live LNCaP cells. Microscopy was performed using a Zeiss LSM 510 confocal microscope equipped with three lasers (Argon, Green HeNe and Red HeNe). Enhanced GFP fluorescence was examined under a fluorescein isothiocyanate filter. For each experimental condition, fluorescence distribution patterns similar to the image shown were observed in the majority (>70%) of cells inspected.

Total RNA isolation and reverse transcription

Total RNA was isolated from cells or tissues using Trizol Reagent (Life Technologies), according to the manufacturer's protocol. The quality of the RNA was confirmed by visualization of the integrity of the 18S and 28S RNA bands on agarose gel. The concentration of the total RNA was determined by measuring the absorbance at 260 nm with an ultraviolet spectrophotometer. All the RNA samples used for assay were treated with DNase I (Life Technologies) to remove contaminating genomic DNA prior to experiments. The reverse transcription reaction was performed by incubating a reaction mixture containing 0.5 μ g RNA, 100 pmol of random hexamer primer (Applied Biosystems), 50 U of reverse transcriptase (Applied Biosystems), 20 U of RNase inhibitor (Promega), and 1 mM dNTP (Life Technologies) in a total of 20 μ l reaction buffer at 42 °C for 50 min, followed by 95 °C for 5 min. The cDNA samples were then stored at -20 °C until use.

Conventional PCR and quantitative real-time PCR

Primers for each gene were chosen with the assistance of the computer program Primer Express (Applied Biosystems). The

primers and probes used for conventional PCR and quantitative real-time PCR of RGS genes are listed in Table 1. The housekeeping genes β -Actin and cyclophilin B were used as control genes.

The conventional PCR cycling conditions were 1 cycle at 94 °C for 3 min; 30 cycles of 94 °C - 1 min, 55 °C - 1 min, 72 °C - 1 min, followed by 1 cycle of 72 °C for 7 min. The PCR products were separated by a 4% agarose gel electrophoresis and stained with ethidium bromide, then photographed under UV light. The predicted size of the PCR product was 238-bp for cyclophilin B, 180-bp for β -Actin and 307-bp for RGS2, and confirmed by DNA sequencing analysis.

All real-time PCR reactions were performed using an ABI Prism 5700 Sequence Detection System (Applied Biosystems). For each PCR run, a master mix was prepared on ice with $1 \times$ TaqMan buffer, 5 mM MgCl₂, 200 μ M dNTP, 300 nM of each primer, 150 nM probe, and 1 U of AmpliTaq Gold DNA Polymerase (Applied Biosystems), and 3 μ l of cDNA solution in a total of 30 μ l. The thermal cycling conditions were an initial denaturation step at 95 °C for 10 min, followed by 40 cycles at 95 °C for 15 s and 60 °C for 1 min.

Human β -Actin plasmid was purchased from ATCC (MGC-10559). Human RGS2, RGS5 or cyclophilin B was constructed into pcDNA3.1 (Invitrogen). All plasmids were prepared by using the Qiagen Spin Mini-Prep Kit. Quantification of plasmid was performed by using UV/visible spectrophotometer (Beckman). The plasmid concentration was converted into copy number; a dilution series of each plasmid from 10^7 to 10^2 were used as DNA standard for real-time PCR. All real-time PCR efficiencies were controlled in the range of $100 \pm 10\%$. Standard curves were drawn by plotting the threshold cycle (C_T) against the natural log of the copy number of plasmid molecules. The C_T was defined as the cycle at which a statistically significant increase in the magnitude of the signal generated by the PCR reaction was first detected. The equations drawn from the graphs were used to calculate the copy numbers of cDNA molecules present in the unknown samples based on the corresponding C_T values.

Statistical analysis

Results are expressed as the mean \pm s.e. of at least three determinations and statistical comparisons are based on the Student's *t*-test. A probability (*P*), value of <0.05 was considered to be significant.

Acknowledgements

We thank Dr David Siderovski, University of North Carolina at Chapel Hill for providing anti-RGS2 antibody, Dr Paul C Sternweis (UT Southwestern Medical Center) for the polyclonal rabbit G_q antibody and Dr Melanin Cobb (UT Southwestern Medical Center) for providing dominant-negative MEK1 and ERK2 mutants. We also thank Dr Zafar Nawaz for critical reading of the manuscript. This work was supported in part by NIH Grant number P20 RR018759 from the National Center for Research Resource (YT and MFL), CA88184 (MFL), Creighton Health Future Foundation (YT), Nebraska State LB692 (YT) and National Scientist Development Grant from American Heart Association (YT).

References

Abrahamsson PA. (1999). *Endocr Relat Cancer* **6**: 503-519.

Bakin RE, Gioeli D, Sikes RA, Bissonette EA, Weber MJ. (2003). *Cancer Res* **63**: 1981-1989.

- Ben-Josef E, Yang SY, Ji TH, Bidart JM, Garde SV, Chopra DP et al. (1999). *J Urol* **161**: 970–976.
- Berman DM, Wilkie TM, Gilman AG. (1996). *Cell* **86**: 445–452.
- Burchett SA, Bannon MJ, Granneman JG. (1999). *J Neurochem* **72**: 1529–1533.
- Candas B, Cusan L, Gomez JL, Diamond P, Suburu RE, Levesque J et al. (2000). *Prostate* **45**: 19–35.
- Chay CH, Cooper CR, Gendernalik JD, Dhanasekaran SM, Chinnaiyan AM, Rubin MA et al. (2002). *Urology* **60**: 760–765.
- Chodak GW, Kranc DM, Puy LA, Takeda H, Johnson K, Chang C. (1992). *J Urol* **147**: 798–803.
- Collier LS, Carlson CM, Ravimohan S, Dupuy AJ, Largaespada DA. (2005). *Nature* **436**: 272–276.
- Cunningham JM, Shan A, Wick MJ, McDonnell SK, Schaid DJ, Tester DJ et al. (1996). *Cancer Res* **56**: 4475–4482.
- Daaka Y. (2004). *Sci STKE* **216**: 2–20.
- Dai J, Shen R, Sumitomo M, Stahl R, Navarro D, Gershengorn MC et al. (2002). *Clin Cancer Res* **8**: 2399–2405.
- Denmeade SR, Sokoll LJ, Dalrymple S, Rosen DM, Gady AM, Bruzek D et al. (2003). *Prostate* **54**: 249–257.
- DiBello PR, Garrison TR, Apanovitch DM, Hoffman G, Shuey DJ, Mason K et al. (1998). *J Biol Chem* **273**: 5780–5784.
- Druey KM, Blumer KJ, Kang VH, Kehrl JH. (1996). *Nature* **379**: 742–746.
- Feldman BJ, Feldman D. (2001). *Nat Rev Cancer* **1**: 34–45.
- Frost JA, Geppert TD, Cobb MH, Feramisco JR. (1994). *Proc Natl Acad Sci USA* **91**: 3844–3848.
- Gioeli D, Mandell JW, Petroni GR, Frierson Jr HF, Weber MJ. (1999). *Cancer Res* **59**: 279–284.
- Gohji K, Kitazawa S, Tamada H, Katsuoka Y, Nakajima M. (2001). *J Urol* **165**: 1033–1036.
- Grillet N, Dubreuil V, Dufour HD, Brunet JF. (2003). *J Neurosci* **23**: 10613–10621.
- Grossmann ME, Huang H, Tindall DJ. (2001). *J Natl Cancer Inst* **93**: 1687–1697.
- Guha M, O'Connell MA, Pawlinski R, Hollis A, McGovern P, Yan SF et al. (2001). *Blood* **98**: 1429–1439.
- Gutkind JS. (2000). *Sci STKE* **40**: RE1.
- Gutowski S, Smrcka A, Nowak L, Wu DG, Simon M, Sternweis PC. (1991). *J Biol Chem* **266**: 20519–20524.
- Hains MD, Siderovski DP, Harden TK. (2004). *Methods Enzymol* **389**: 71–88.
- Heinlein CA, Chang C. (2004). *Endocr Rev* **25**: 276–308.
- Hepler JR, Berman DM, Gilman AG, Kozasa T. (1997). *Proc Natl Acad Sci USA* **94**: 428–432.
- Heximer SP, Knutsen RH, Sun X, Kaltenbronn KM, Rhee MH, Peng N et al. (2003). *J Clin Invest* **111**: 445–452.
- Hobisch A, Culig Z, Radmayr C, Bartsch G, Klocker H, Hittmair A. (1996). *Prostate* **28**: 129–135.
- Hollinger S, Hepler JR. (2002). *Pharmacol Rev* **54**: 527–559.
- Igawa T, Lin FF, Lee MS, Karan D, Batra SK, Lin MF. (2002). *Prostate* **50**: 222–235.
- Ingi T, Krumins AM, Chidiac P, Brothers GM, Chung S, Snow BE et al. (1998). *J Neurosci* **18**: 7178–7188.
- Jackson AL, Bartz SR, Schelter J, Kobayashi SV, Burchard J, Mao M et al. (2003). *Nat Biotechnol* **21**: 635–637.
- Jemal A, Murray T, Ward E, Samuels A, Tiwari RC, Ghafoor A et al. (2005). *CA Cancer J Clin* **55**: 10–30.
- Kammermeier PJ, Ikeda SR. (1999). *Neuron* **22**: 819–829.
- Karan D, Kelly DL, Rizzino A, Lin MF, Batra SK. (2002). *Carcinogenesis* **23**: 967–975.
- Karan D, Schmied BM, Dave BJ, Wittel UA, Lin MF, Batra SK. (2001). *Clin Cancer Res* **7**: 3472–3480.
- Kasbohm EA, Guo R, Yowell CW, Bagchi G, Kelly P, Arora P et al. (2005). *J Biol Chem* **280**: 11583–11589.
- Kehrl JH, Sinnarajah S. (2002). *Int J Biochem Cell Biol* **34**: 432–438.
- Lee LF, Guan J, Qiu Y, Kung HJ. (2001). *MolCell Biol* **21**: 8385–8397.
- Lee MS, Igawa T, Yuan TC, Zhang XQ, Lin FF, Lin MF. (2003). *Oncogene* **22**: 781–796.
- Lee YF, Lin WJ, Huang J, Messing EM, Chan FL, Wilding G et al. (2002). *Cancer Res* **62**: 6039–6044.
- Lin HK, Hu YC, Yang L, Altuwajri S, Chen YT, Kang HY et al. (2003). *J Biol Chem* **278**: 50902–50907.
- Lin MF, Meng TC, Rao PS, Chang C, Schonthal AH, Lin FF. (1998). *J Biol Chem* **273**: 5939–5947.
- Nelson JB, Chan-Tack K, Hedican SP, Magnuson SR, Opgenorth TJ, Bova GS et al. (1996). *Cancer Res* **56**: 663–668.
- Neubig RR, Siderovski DP. (2002). *Nat Rev Drug Discov* **1**: 187–197.
- Oliveira-Dos-Santos AJ, Matsumoto G, Snow BE, Bai D, Houston FP, Whishaw IQ et al. (2000). *Proc Natl Acad Sci USA* **97**: 12272–12277.
- Porter AT, Ben-Josef E. (2001). *Urol Oncol* **6**: 131–138.
- Posner BA, Mukhopadhyay S, Tesmer JJ, Gilman AG, Ross EM. (1999). *Biochemistry* **38**: 7773–7779.
- Robinet EA, Wurch T, Pauwels PJ. (2001). *Neuroreport* **12**: 1731–1735.
- Ross EM, Wilkie TM. (2000). *Annu Rev Biochem* **69**: 795–827.
- Roy AA, Lemberg KE, Chidiac P. (2003). *Mol Pharmacol* **64**: 587–593.
- Sadi MV, Walsh PC, Barrack ER. (1991). *Cancer* **67**: 3057–3064.
- Salim S, Sinnarajah S, Kehrl JH, Dessauer CW. (2003). *J Biol Chem* **278**: 15842–15849.
- Sato N, Sadar MD, Bruchovsky N, Saatcioglu F, Rennie PS, Sato S et al. (1997). *J Biol Chem* **272**: 17485–17494.
- Schmitt JM, Stork PJ. (2000). *J Biol Chem* **275**: 25342–25350.
- Schwable J, Choudhary C, Thiede C, Tickenbrock L, Sargin B, Steur C et al. (2005). *Blood* **105**: 2107–2114.
- Shah GV, Rayford W, Noble MJ, Austenfeld M, Weigel J, Vamos S et al. (1994). *Endocrinology* **134**: 596–602.
- Siderovski DP, Heximer SP, Forsdyke DR. (1994). *DNA Cell Biol* **13**: 125–147.
- Sinnarajah S, Dessauer CW, Srikumar D, Chen J, Yuen J, Yilma S et al. (2001). *Nature* **409**: 1051–1055.
- Sramkoski RM, Pretlow TG, Giaconia JM, Pretlow TP, Schwartz S, Sy MS et al. (1999). *In vitro Cell Dev Biol Anim* **35**: 403–409.
- Tang KM, Wang GR, Lu P, Karas RH, Aronovitz M, Heximer SP et al. (2003). *Nat Med* **9**: 1506–1512.
- Taplin ME, Balk SP. (2004). *J Cell Biochem* **91**: 483–490.
- Taub JS, Guo R, Leeb-Lundberg LM, Madden JF, Daaka Y. (2003). *Cancer Res* **63**: 2037–2041.
- Tepper CG, Boucher DL, Ryan PE, Ma AH, Xia L, Lee LF et al. (2002). *Cancer Res* **62**: 6606–6614.
- Thebault S, Roudbaraki M, Sydorenko V, Shuba Y, Lemonnier L, Slomianny C et al. (2003). *J Clin Invest* **111**: 1691–1701.
- Tovey SC, Willars GB. (2004). *Mol Pharmacol* **66**: 1453–1464.
- Tu Y, Woodson J, Ross EM. (2001). *J Biol Chem* **276**: 20160–20166.
- Unni E, Sun S, Nan B, McPhaul MJ, Cheskis B, Mancini MA et al. (2004). *Cancer Res* **64**: 7156–7168.

- Wang J, Tu Y, Mukhopadhyay S, Chidiac P, Biddlecome GH, Ross EM. (1998) In: Manning DR (ed). *G Proteins: Techniques of Analysis*. CRC Press: Boca Raton, pp 123–151.
- Weng J, Wang J, Cai Y, Stafford LJ, Mitchell D, Ittmann M *et al.* (2005). *Int J Cancer* **113**: 811–818.
- Wieland T, Mittmann C. (2003). *Pharmacol Ther* **97**: 95–115.
- Wilkie TM, Gilbert DJ, Olsen AS, Chen XN, Amatruda TT, Korenberg JR *et al.* (1992). *Nat Genet* **1**: 85–91.
- Wu HK, Heng HH, Shi XM, Forsdyke DR, Tsui LC, Mak TW *et al.* (1995). *Leukemia* **9**: 1291–1298.
- Xia C, Ma W, Wang F, Hua SB, Liu M. (2001). *Oncogene* **20**: 5903–5907.
- Xie Y, Gibbs TC, Mukhin YV, Meier KE. (2002). *J Biol Chem* **277**: 32516–32526.
- Xu LL, Stackhouse BG, Florence K, Zhang W, Shanmugam N, Sesterhenn IA *et al.* (2000). *Cancer Res* **60**: 6568–6572.
- Yeh S, Lin HK, Kang HY, Thin TH, Lin MF, Chang C. (1999). *Proc Natl Acad Sci USA* **96**: 5458–5463.